

Cirrus Technologies  
Presents  
**Cirrus Eco-Strut**



Response to the 2008-2009 AIAA Foundation  
Undergraduate Team Aircraft Design Competition

May 7, 2009

Virginia Polytechnic Institute and State University  
Department of Aerospace and Ocean Engineering  
Blacksburg, Virginia

# Cirrus Technologies



**Brian Smith**  
Team Leader, Systems  
AIAA Member # 261437

**Josh Shiben**  
Flight Controls, Cost  
AIAA Member # 266222

**Christian Rupnarine**  
Aerodynamics  
AIAA Member # 301044

**Hazima Javaid**  
Weights  
AIAA Member # 275323

**Melea McDonald**  
Structures  
AIAA Member # 303834

**Dylan Scott**  
Configuration  
AIAA Member # 260884

**Jason McZara**  
Propulsion  
AIAA Member # 303937

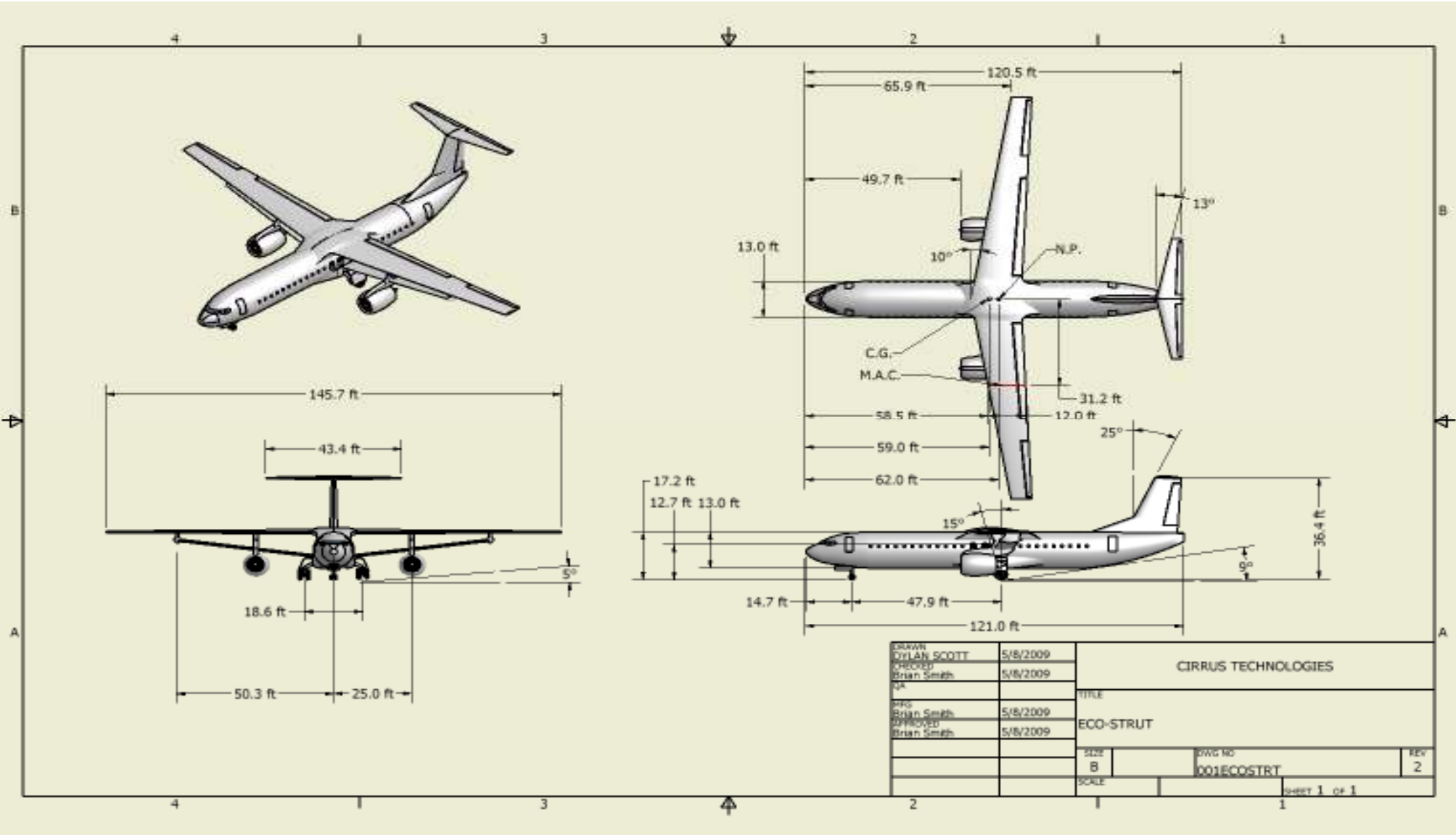
**Daniel Shin**  
Performance  
AIAA Member # 303967

**Dr. William H. Mason**  
Faculty Advisor

## Executive Summary

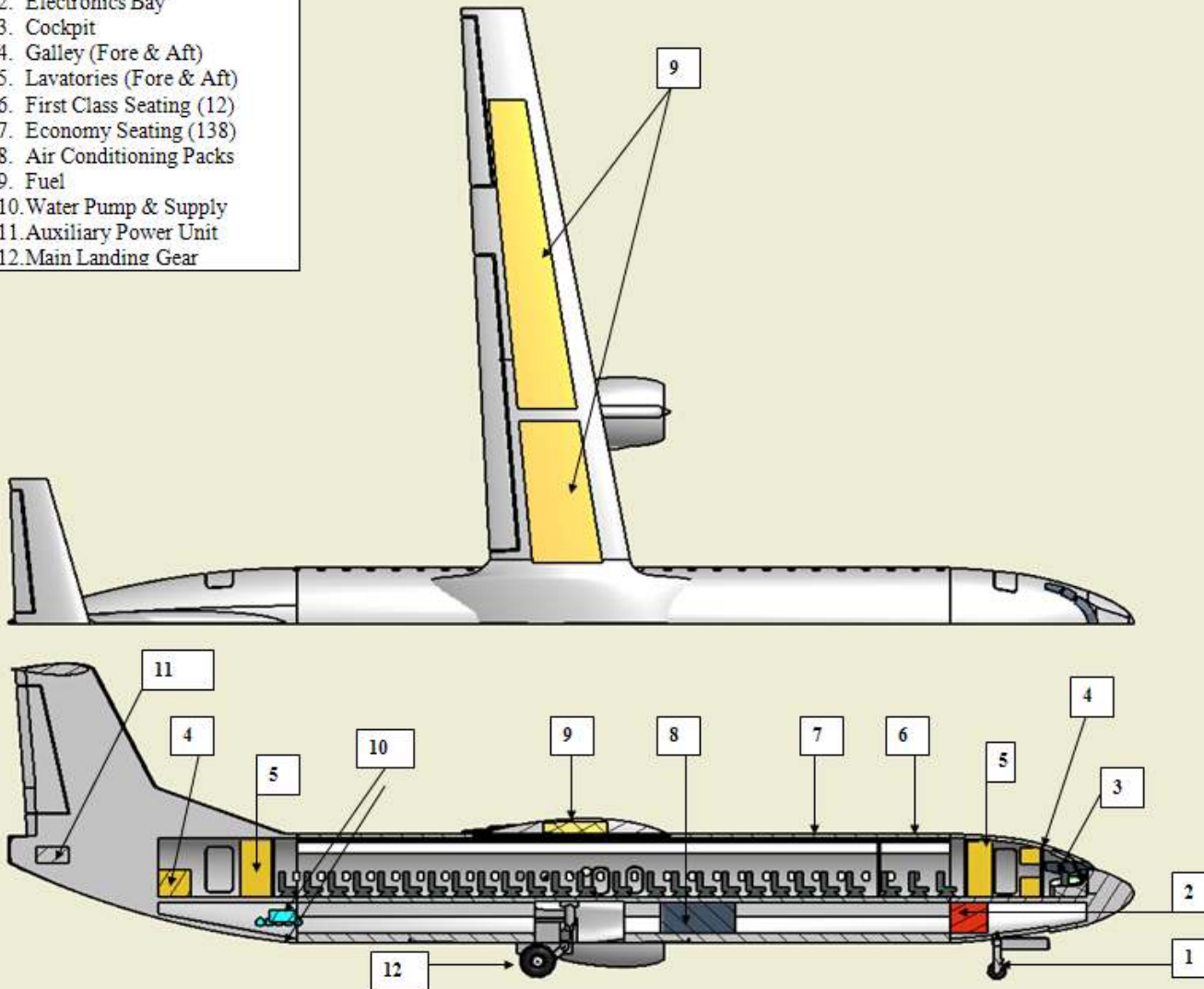
In September 2008, Cirrus Technologies was presented with a request for proposal (RFP) for the 2008-2009 America Institute of Aeronautics and Astronautics Foundation Undergraduate Team Aircraft Design Competition. This year's competition required the development of a new commercial transport designed to accommodate approximately 150 passengers in a dual class configuration. The new aircraft is to be designed for introduction into service in 2018 and must operate within the current aviation infrastructure. Significant improvements are required to be made in reduced fuel burn and decreased community noise while ensuring the aircraft remains financially competitive. The new commercial transport design must also adhere to a variety of technical requirements outlined in the RFP. Taking these requirements and any more into consideration, a new design, the Cirrus Eco-Strut, is proposed which meets and/or exceeds the requirements set forth by the competition committee.

The Cirrus Eco-Strut employs a strut-braced wing design currently being researched by numerous academic institutions and private companies around the world. A strut connecting the side of the fuselage to the wing allows for reduced sizing of the cantilever wing spar. The smaller spar permits a reduced wing thickness to chord ratio and decreased sweep angle. The decreased sweep angle promotes laminar flow thus decreasing drag. Weight is reduced due to the strut-braced design, resulting in decreased fuel burn and reduced operational costs. The Cirrus Eco-Strut benefits from all of these improvements which results in a competitive design capable of transforming the future of aviation.



# Cirrus Technologies

1. Nose Landing Gear
2. Electronics Bay
3. Cockpit
4. Galley (Fore & Aft)
5. Lavatories (Fore & Aft)
6. First Class Seating (12)
7. Economy Seating (138)
8. Air Conditioning Packs
9. Fuel
10. Water Pump & Supply
11. Auxiliary Power Unit
12. Main Landing Gear



## CIRRUS TECHNOLOGIES ECO-STRUT

### INBOARD PROFILE:

**Wings:** Aluminum, interior, carbon laminate skin, strut braced high cantilever design

**Fuselage:** Carbon laminate

**Powerplant:** 2 Pratt & Whitney PW1000G Geared Turbofan

**Landing Gear:** Tricycle, Goodyear Flight Leader series tires, nose gear steering, main landing gear modeled after BAE 146

**Tail Unit:** T-tail design, aluminum/ composite mixed internal, carbon laminate skin

**Accommodations:** Seats 150, 12 first class (36" seat pitch), 138 economy (32" seat pitch), 4 crew, also able to fit high density 30" seat pitch, 9000+ lbs of cargo

### Performance:

- Max Range: 2800 nm
- Rate of Climb: 2353 ft/min
- Cruise Speed: 0.8 Mach
- Fuel Capacity: 6396 US-gal
- Balanced T/O Field Length: 3930 ft
- Balanced Landing Field Length: 2964 ft

### Dimensions External:

- Wing Span: 145.7 ft
- Length Overall: 121 ft
- Overall Height: 36.4 ft
- Wheel Base: 47.9 ft
- Wheel Track: 18.6 ft

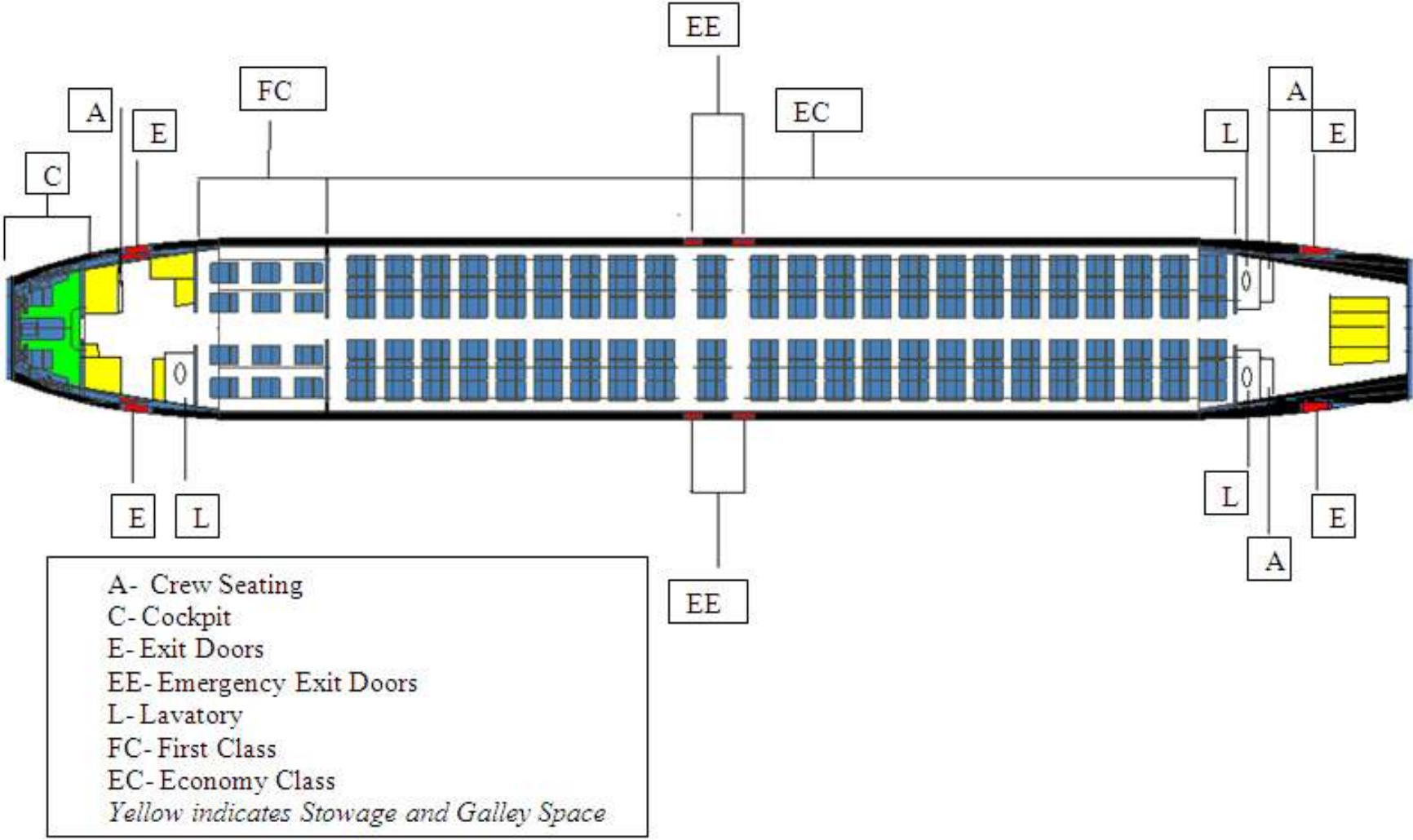


# Table of Contents

<b>Executive Summary .....</b>	<b>iii</b>
<b>List of Symbols .....</b>	<b>3</b>
<b>List of Figures .....</b>	<b>5</b>
<b>List of Tables .....</b>	<b>7</b>
<b>1 Introduction and Request for Proposal.....</b>	<b>8</b>
1.1 Introduction	8
1.2 Background Information	8
1.3 RFP Requirements	9
1.3.1 Capacity Requirement.....	9
1.3.2 Performance Requirement.....	10
1.3.3 Economic Requirement.....	11
1.3.4 Environmental Requirements.....	11
1.4 Design Drivers	11
1.4.1 Community Noise .....	11
1.4.2 Fuel Consumption .....	12
1.4.3 Operating Costs.....	12
1.5 Advanced Technologies of Eco-Strut	12
1.5.1 Use of Struts.....	12
1.5.2 Advanced Turbofan.....	13
1.5.3 No Bleed System.....	13
1.5.4 Use of Composites Materials .....	13
<b>2 Design Evolution.....</b>	<b>14</b>
2.1 Configuration Concepts	14
2.1.1 Tube and Wing.....	14
2.1.2 Strut-Braced Wing .....	15
2.1.3 Blended Wing Body.....	17
2.2 Sizing	18
2.3 Concept Decision Matrix and Final Decision	20
2.4 Final Sizing	21
<b>3 Weights, Moments and Center of Gravity.....</b>	<b>23</b>
3.1 Weight Statement	23
3.2 Center of Gravity Travel	24
<b>4 Propulsion Systems.....</b>	<b>26</b>
4.1 Engine Selection and Thrust Requirements	26
4.2 Engine Specifications and Placement	28
4.3 APU	30
<b>5 Noise Analysis.....</b>	<b>30</b>
<b>6 Aerodynamics .....</b>	<b>32</b>
6.1 Wing Design	32
6.2 Laminar Flow	34
6.3 High Lift System	34
6.4 Wing Lift Distribution	35
6.5 Drag Analysis	35
<b>7 Stability and Control.....</b>	<b>37</b>
7.1 Control Requirements	37
7.2 Control Surface Configuration	37
7.3 Horizontal Tail Sizing	38
7.4 Vertical Tail Sizing	40
7.5 Ailerons	41
7.6 Static Margin	41
7.7 Aircraft Modeling and Stability Derivatives	42

7.8	Longitudinal Maneuvering	44
7.9	Departure Criteria	47
<b>8</b>	<b>Performance</b> .....	<b>49</b>
8.1	Requirements	49
8.2	Takeoff Performance	49
8.3	Range	50
8.4	Landing Performance	50
8.5	Cruise and Fuel Consumption	51
<b>9</b>	<b>Materials and Structure</b> .....	<b>54</b>
9.1	Materials	54
9.2	Structural Analysis	57
<b>10</b>	<b>Systems</b> .....	<b>66</b>
10.1	Landing Gear Kinematics	66
10.2	No-Bleed System Architecture	70
10.3	Electrical System	70
10.4	Hydraulic System	72
10.5	Avionics	74
10.6	Cockpit	75
10.7	Wing Ice Protection	77
10.8	Environmental Control System	77
10.9	Emergency Systems	78
10.10	Fire Prevention	79
10.11	Lighting	79
10.12	Water, Galley, and Lavatory Systems	80
<b>11</b>	<b>Cost Analysis</b> .....	<b>80</b>
11.1	Cost Reduction Methods	80
11.2	Cost Analysis Assumptions	81
11.3	Life Cycle Costs	82
11.4	Research, Development, Testing and Evaluation	82
11.5	Acquisition Cost	83
11.6	Operational Cost	84
11.7	Disposal Phase	85
11.8	Total Life Cycle Costs	85
<b>12</b>	<b>Conclusion</b> .....	<b>86</b>
	<b>References</b> .....	<b>87</b>

## List of Symbols

<i>Symbol</i>	<i>Definition</i>	<i>Units</i>
<i>English</i>		
AFIS	Airborne Flight Information System	-
AIAA	American Institute of Aeronautics and Astronautics	-
APU	Auxiliary Power Unit	-
AR	Aspect Ratio	-
$b$	Wing Span	ft
BWB	Blended-Wing Body	-
$c$	Chord Length	ft, in
CAD	Computer-Aided Design	-
$C_D$	Airplane Drag Coefficient	-
$C_{Dde}$	Derivative of Drag Force Coefficient with Respect to Elevator Deflection	-
$C_{Do}$	Airplane Zero-Lift Drag Coefficient	-
CG	Center of Gravity	-
$C_L$	Airplane Lift Coefficient	-
$C_{L\alpha}$	Lift Curve Slope	1/rad
$C_{l\beta}$	Dihedral Effect	1/rad
$C_{l\delta a}$	Rolling Moment Gradient due to Aileron	1/rad
$C_{l\delta e}$	Rolling Moment Gradient due to Elevator	1/rad
$C_{l\delta r}$	Rolling Moment Gradient due to Rudder	1/rad
$C_{Lmax}$	Maximum Airplane Lift Coefficient	-
$C_{lp}$	Roll Damping	1/(rad/s)
$C_{Lq}$	Lifting Force Gradient due to Pitch Rate	1/(rad/s)
$C_{nr}$	Yaw Damping	1/(rad/s)
$C_{m\alpha}$	Gradient of $C_m$ with respect to Angle of Attack	1/rad
$C_{m\delta e}$	Pitching Moment Gradient due to Elevator	1/rad
$C_{mq}$	Pitch Damping	1/(rad/s)
$C_{n\beta}$	Weathercock Stability	1/rad
$C_{n\delta a}$	Yawing Moment Gradient due to Aileron Deflection	1/rad
$C_{n\delta e}$	Yawing Moment Gradient due to Elevator Deflection	1/rad
$C_{n\delta r}$	Yawing Moment Gradient due to Rudder Deflection	1/rad
$C_{np}$	Yawing Moment Gradient due to Roll Rate	1/(rad/s)
$C_{nr}$	Yaw Rate Damping	1/(rad/s)
$C_{y\beta}$	Side Force Gradient due to Sideslip	1/rad
$C_{y\delta a}$	Side Force Gradient due to Aileron Deflection	1/rad
$C_{y\delta e}$	Side Force Gradient due to Elevator Deflection	1/rad
$C_{y\delta r}$	Side Force Gradient due to Rudder Deflection	1/rad
$C_{yp}$	Side Force Gradient due to Roll Rate	1/rad
$C_{yr}$	Side Force Gradient due to Yaw Rate	1/(rad/s)
$D$	Drag	-
dB	Decibels	-
deg	Degrees	-

<i>DME</i>	Distance Measuring Equipment	-
<i>EGPWS</i>	Enhanced Ground Proximity Warning System	-
<i>FAR</i>	Federal Aviation Regulations	-
<i>ft</i>	Feet	-
<i>gpm</i>	Gallons per minute	g/min
<i>GPS</i>	Global Positioning System	-
<i>GPU</i>	Ground Power Unit	-
<i>HF</i>	High Frequency	-
<i>HUD</i>	Heads Up Display	-
<i>hrs</i>	Hours	-
<i>ILS</i>	Instrument Landing System	-
<i>kts</i>	Knots	-
<i>lb</i>	Pounds	-
<i>L</i>	Lift	-
<i>L/D</i>	Lift Over Drag	-
<i>LCD</i>	Liquid Crystal Display	-
<i>LRC</i>	Long Range Cruise	nmi
<i>mac</i>	Mean Aerodynamic Chord	ft
<i>MLW</i>	Maximum Landing Weight	lb
<i>MTOW</i>	Maximum Takeoff Weight	lb
<i>nm</i>	Nautical Miles	-
<i>psi</i>	Pounds per Square Inch	psi/in
<i>rad</i>	Radians	-
<i>RFP</i>	Request for Proposal	-
<i>S</i>	Seconds	-
<i>S</i>	Airplane Wing Planform Area	ft <sup>2</sup>
<i>SFC</i>	Specific Fuel Consumption	lb/hp/hr
<i>SBW</i>	Strut-Braced Wing	-
<i>T</i>	Thrust	lb
<i>t/c</i>	Thickness to Chord Ratio	-
<i>TCAS</i>	Traffic Collision Avoidance System	-
<i>TOFL</i>	Takeoff Field Length	nm
<i>TOGW</i>	Takeoff Gross Weight	lb
<i>V</i>	Velocity	ft/s, kts
<i>VHF</i>	Very High Frequency	-
<i>VoIP</i>	Voice Over Internet Protocol	-
<i>VOR</i>	VHF Omni-Directional Radio Range	-
<i>V<sub>stall</sub></i>	Stall Velocity	ft/s, kts
<i>V<sub>TO</sub></i>	Takeoff Velocity	ft/s, kts
<i>W</i>	Weight	lb
<i>W/S</i>	Wing Loading	lb/ft <sup>2</sup>
<i>W<sub>e</sub></i>	Empty Weight	lb
<i>W<sub>nsp</sub></i>	Undamped Short Period Frequency	sec <sup>-1</sup>
Greek		
$\alpha$	Angle of Attack	deg
$\rho$	Density	lb/ft <sup>3</sup>
$\delta_e$	Elevator Deflection	deg

## List of Figures

Figure 1 Cirrus Eco-Strut Mission Profile .....	10
Figure 2 Four Tube and Wing Concepts.....	14
Figure 3 CAD Illustration of Tube and Wing Design.....	15
Figure 4 Strut-Braced Wing Concept .....	16
Figure 5 CAD Illustration of Strut-Braced Wing Design .....	16
Figure 6 Blended Wing Body Concepts .....	17
Figure 7 CAD Illustration of Blended-Wing Body Design .....	18
Figure 8 Flowchart of Weight Calculations.....	19
Figure 10 Strut-Braced Wing Aircraft Sizing I.....	22
Figure 11 Strut-Braced Wing Aircraft Sizing II .....	22
Figure 12 Center of Gravity Range.....	25
Figure 13 Engine SFC Values over Various Engine Thrust Levels [15].....	27
Figure 14 Maximum Thrust Provided for Each Engine.....	27
Figure 15 Thrust Available vs. Altitude for PW1000G Engine used on Eco-Strut.....	28
Figure 16 Pratt Whitney 1000G Engine Cross Sectional View [16]. .....	29
Figure 17 The installation of the PW1000G engine on Eco-Strut .....	29
Figure 18 Trajectory and Aircraft Noise Certification Measurement Points for Sideline (Lateral), Approach and Flyover (Takeoff) [17] .....	30
Figure 19 Approach and Sideline Noise Requirements set for Stage 3 .....	31
Figure 20 Takeoff Noise Certification Requirements for Stage 3 .....	31
Figure 21 Thickness-to-Chord Ratio: Leading Edge Sweep Angle Optimization .....	33
Figure 22 Cross-Section of the chosen SC(2)-0410 Airfoil.....	34
Figure 23 The High-Lift System.....	34
Figure 24 Wing Lift Distribution at Cruise.....	35
Figure 25 Take-off, Cruise and Approach Parasitic Drag Build Ups .....	36
Figure 26 Take-off, Cruise, and Approach Drag Polars .....	36
Figure 27 Required Horizontal Tail Aspect Ratio vs. Horizontal Tail Area .....	38
Figure 28 Required Tail Aspect Ratio versus Root-Chord and Semi-Span of the Horizontal Tail .....	39
Figure 29 Elevator Effectiveness in Trim over Various Cls.....	39
Figure 30 Vertical Tail Sizing.....	40
Figure 31 Flight Envelope CG Travel in relation to the Neutral Point.....	42
Figure 32 Steady, Vortex-Lattice Method Eco-Strut Model Produced in Tornado.....	43
Figure 33 The Short Period Mode over Time.....	45
Figure 34 The Uncontrolled Phugoid Mode Over Time.....	46
Figure 35 The Phugoid Mode Over Time When Thrust is Controlled by a Proportional Feedback Control Loop.....	46
Figure 36 The Eco-Strut location on the Bihrl-Weissman Chart – see below for a description of the 8 regions .....	47
Figure 37 Cirrus Eco-Strut Range versus Weights .....	50
Figure 38 Specific Range including Drag Rise at an Altitude of 40,000 ft.....	52
Figure 39 Eco-Strut 850 nm Mission.....	52
Figure 40 Eco-Strut Fuel Tanks.....	54
Figure 41 Specific Strength for Aerospace Materials.....	55
Figure 42 Specific Strength for Aerospace Materials.....	55
Figure 43 Materials Distribution for Boeing 787 & Airbus A350.....	56
Figure 44 Materials Breakdown Drawing of Strut Braced Wing .....	57

Figure 45 V-n Diagram for Maneuver and Gust Loads.....	58
Figure 46 Outline of Structural Analysis Code.....	58
Figure 47 Wing Loading at Steady, Level Flight for Structural Analysis.....	59
Figure 48 Wing Loading at $n = 2.5$ for Structural Analysis .....	60
Figure 49 Nodes of the Wing Structure .....	60
Figure 50 Structural Type of Each Element .....	61
Figure 51 Degrees of Freedom at Each Node of the Structure .....	61
Figure 52 The Flange Width and Web Height as a Function of Span .....	62
Figure 53 Shear as a Function of Span .....	63
Figure 54 Bending Moment as a Function of Span .....	64
Figure 55 Eco-Strut Landing Gear Location .....	68
Figure 56 Eco-Strut Landing Gear Kinematics .....	69
Figure 57 Cirrus Eco-Strut Electrical System Schematic.....	72
Figure 58 Cirrus Eco-Strut Hydraulic System.....	74
Figure 59 Cirrus Eco-Strut Cockpit Layout.....	76
Figure 60 Leading Edge Heater Mat [11].....	77
Figure 61 Eco-Strut Emergency Exit Locations .....	78
Figure 62 Cirrus Eco-Strut Exterior Lighting Configuration .....	79
Figure 63 General Trends for Aircraft Pricing [4].....	81

## List of Tables

Table 1 Conceptual Designs' Sizing I & II Results .....	20
Table 2 Concept Decision Matrix .....	21
Table 3 Cirrus Eco-Strut Weight Statement .....	23
Table 4 Eco-Strut Weights at Mission Segments .....	24
Table 5 Engine Data for Engines Considered During Design Process [15] .....	26
Table 6 Take-off, Cruise and Approach Parasitic Drag Build Ups .....	35
Table 7 Requirements for Level 1 Flight Rating in Roll .....	41
Table 8 Longitudinal Stability Derivatives.....	43
Table 9 Lateral-Directional Stability Derivatives.....	44
Table 10 The Short Period Mode Requirements for Level 1 Flight Conditions.....	44
Table 11 The Phugoid Mode Requirements for Level 1 Flight Conditions .....	45
Table 12 The Eco-Strut LCDP and $Cn\beta_{dynamic}$ Values Over Angles of Attack.....	47
Table 13 Cirrus Eco-Strut RFP Requirements.....	49
Table 14 Cirrus Eco-Strut Parameters .....	49
Table 15 Cirrus Eco-Strut Maximum Performance Characteristics .....	51
Table 17 Eco-Strut Fuel Burn .....	53
Table 18 Cirrus Eco-Strut Landing Gear Load Analysis Summary .....	66
Table 19 Cirrus Eco-Strut Selected Tire Data (Design Point Bolded) .....	67
Table 20 Hybrid Electrical System Voltages and Supplied Services .....	71
Table 21 Hydraulic System Summary .....	73
Table 22 Design and Testing Cost of Eco-Strut (in 2009 U.S. Dollars).....	82
Table 23 Average RDTE Aircraft Cost .....	83
Table 24 Cost to Requisition 500 or 1500 Eco-Strut Aircrafts (in U.S. Dollars).....	83
Table 25 Cirrus Eco-Strut Price (in U.S. Dollars) .....	83
Table 26 Cost of Operating Eco-Strut with 30 year Lifespan (in U.S. Dollars).....	84
Table 27 Operational Costs Comparison (in U.S. Dollars) [14].....	84
Table 28 Disposal Cost of all Requisitioned Aircraft (in U.S. Dollars) .....	85
Table 29 Total Cost to Design, Test, and Manufacture, Utilize and Dispose of the Cirrus Eco-Strut (in U.S. Dollars) .....	85
Table 30 RFP Compliance Summary .....	86

# 1 Introduction and Request for Proposal

## 1.1 Introduction

Cirrus Technologies is pleased to respond to request for proposal (RFP) for the 2008-2009 AIAA Foundation Undergraduate Team Aircraft Design Competition. Cirrus Technologies proposes a new aircraft design-The Cirrus Eco-Strut. It seats 150 passengers (dual class) and has improvements in fuel burn, reduced community noise, and competitive acquisition and operational costs. The aircraft must also be certificated for entry into service in 2018. Numerous other requirements are spelled out in the RFP which pertain to specific weight, performance, propulsion, and/or cost. All requirements are to be met or exceeded. It is the objective of Cirrus Technologies to design the Eco-Strut to be not only competitive to current commercial aircraft such as the Boeing 737 and Airbus A320 but also provide a significant advantage in efficiency, cost, and environmental efficiency.

## 1.2 Background Information

As the world's airline companies continue to fly aircraft that exceed 20 years of service, there is a need for a new, reduced cost, innovative aircraft. The Boeing 737 and Airbus A320 have become increasingly more popular, however as the price of gas continues to rise and becomes a monetary burden for all airline companies even more fuel efficient aircraft are desired. With an even more efficient aircraft, airline companies can save significant amounts of money.

As stated in the RFP, a new environmentally friendly, fuel efficient, cost effective, and low noise aircraft must be developed. At Cirrus Technologies, this problem was approached from different technological and engineering prospective. The major issues were identified and design drivers were defined. Each team member created their own concept using their own ideas. In the end, eight different concepts were created. The concepts ranged from conventional tube and wing designs to strut-braced wing designs to blended-wing bodies. Each concept exhibited different pros and cons. Three concepts—the tube and wing, the strut-braced wing, and the blended wing body—were selected as potential candidates using a design matrix. Sizing, performance, and cost data were found and one

favorable concept emerged. In the end, the strut-braced wing design was chosen as the concept of choice. It is named the Cirrus Eco-Strut because of the designs environmental friendliness and use of struts to support wings.

### **1.3 RFP Requirements**

The Request for Proposal (RFP) of the American Institute for Aeronautics and Astronautics (AIAA) directly reflects the requirements that are expected from future commercial aircraft. The RFP requirements can be divided into the following categories: capacity, performance, economic, and environmental friendliness. The RFP asked for an aircraft with significantly lower fuel burn and emissions, while the aircraft should have a competitive acquisition cost, and a significantly lower operating cost. The aircraft should be able to at least match most of the current performance levels, operate within the current infrastructure, and be able to be certified and entered into service by 2018. While each requirement needs to be met, originality of the design consists of 20 percent of the evaluation weight, and the practical application and feasibility is one quarter of the weight for evaluation. Keeping in mind that technical content, organization and presentation, originality, and practical application and feasibility are important factors, the following requirements should be observed.

#### **1.3.1 Capacity Requirement**

As non-stop flights continue to be desirable by passengers, there is a growing demand for smaller commercial aircraft which are able to fly to many destinations non-stop. This will eliminate the process of passenger transfer at hubs which proves to be difficult and inefficient at times. The RFP states the aircraft should have a 150 passenger seating capacity. The RFP places great importance to the comfort of the passenger. Therefore it is important that the aircraft has dual class seating with about 12 first class seats having 36 inch of pitch, and about 138 economy seats having 32 inch of pitch. Along with the seating capacity a 7.5 cubic feet cargo capacity should accompany each

passenger. The passenger weight estimated to be 185 lbs with a personal cargo allotment of 8 lb/ft<sup>3</sup>. The estimated total weight per passenger is 225 lbs.

### 1.3.2 Performance Requirement

The RFP sets the speed requirements at 0.78 Mach, with an objective of 0.80 Mach. With the speed requirements set at the transonic region, the aircraft should have a maximum range of 2800 nm with the assumption of full dual class passenger load and 225 lbs per passenger. The aircraft should be able to fly from any point on the continental U.S. to any destination in the continental U.S. Based on current aircraft in service, average missions are described as 500 nm for 50% of the missions, and 1000 nm for 40% of the missions, and only 10% of the missions will have an average range of 2000 nm. As the requirements are set, it can be seen that on average 90% of the missions have a range of less than 1000 nm. This designed aircraft should have a takeoff distance of 7000 ft at sea level at 86 degrees Fahrenheit. Therefore, a large thrust to weight ratio is required. The aircraft climb rate with or without one engine out should meet or exceed the FAA requirements. The aircraft should operate at the minimum altitude of 35000 ft at 15 degrees Centigrade. Figure 1 outlines the mission profile.

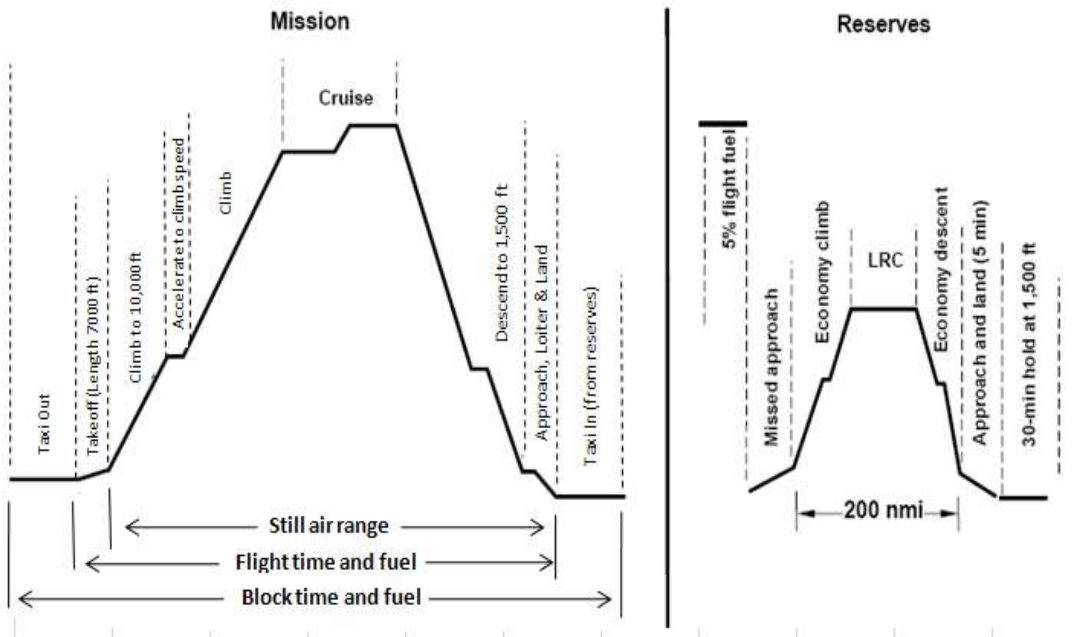


Figure 1 Cirrus Eco-Strut Mission Profile

### **1.3.3 Economic Requirement**

Most of the capacity and performance requirements are met with current commercial passenger aircraft. However, the limiting factor for the RFP is the limit set on the operating costs. It is required that the proposed aircraft have 8% or better operating cost, although a reduction of 10% in the operating cost is the objective. With the assumption of a constant 2.50 U.S. dollars per gallon for fuel consumed, the reduction in the operating cost should be achieved in comparison to the current, comparably-sized commercial transports in typical U.S. major airline type operation. The airplane acquisition cost shall be commensurate with current 150 seat category transports. Hence, in order to achieve lower commensurate cost, lower weight and lower cost parts is a major factor. For calculation purposes it can be assumed 500 to 1500 of the designed aircraft will be produced.

### **1.3.4 Environmental Requirements**

With increased awareness of the environment, the preference for environmentally friendlier airplanes exists. It is required that the aircraft fuel burn block per seat at a 500 nm mission is less than or equal to 41 pounds per seat. Cirrus Technologies' objective is for 38 pounds per seat. This objective can be obtained by using advanced technologies and reduced drag methods. The lower level of fuel consumption also accompanies lower emission levels by the aircraft. The aircraft should also be quieter than current aircraft. The community noise shall be ICAO Chapter 4 level, minus 20 dB cumulative. For a quieter aircraft not only the engine noise levels but also the aircraft fuselage and wing integration should be carefully evaluated.

## **1.4 Design Drivers**

### **1.4.1 Community Noise**

Noise has and still remains to be an issue within the aviation industry. To reduce noise, several new propulsion systems which claim to be quieter and more fuel efficient are being introduced within the next few years. Using a propulsion system that operates at a quieter level can greatly reduce the overall noise output of the aircraft. Also, airframe noise is a major contributor to the noise

created by today's commercial airliners. Cirrus Technologies will eliminate 20 dB or more cumulative noise by choosing appropriate propulsion systems and refining the airframe geometry.

### **1.4.2 Fuel Consumption**

Currently airline companies are attempting everything in their power to save money. One of the biggest ways to save money is to use an aircraft which is more fuel efficient and has a low operating cost. The choice of a propulsion system is once again crucial to this design concern. As previously mentioned, engine manufacturers are developing engines that are extremely fuel efficient and extremely quiet. Implementing these types of engines on a strut-braced wing design would lead to performance that exceeds any current aircraft in production today. Cirrus Technologies will reduce fuel burn to less than 38 pounds per seat. The reduced drag of the Eco-Strut will lead to reduced required thrust and ultimately reduced fuel consumption.

### **1.4.3 Operating Costs**

Airline companies have cut numerous routes since a lot of the aircraft currently in service are not very efficient and very costly to operate. With the strut-braced wing design, airline companies could return to profitability due to more fuel efficient engines, lower net weight, and increased lift due to higher wing span with reduced induced drag. The combination of these things would be very attractive to airline companies looking to increase efficiency. Cirrus Technologies will improve operational cost.

## **1.5 Advanced Technologies of Eco-Strut**

With the high standards set by the RFP requirements the use of advanced technologies and ideas were key points in Cirrus Technologies design of Eco-Strut. The design drivers were addresses in the use of various technologies.

### **1.5.1 Use of Struts**

The Eco-Strut uses a key idea for reducing drag, using struts to support the weight and load of on most of the wings. The Eco-Strut effectively implemented the use of struts to support the high

aspect ratio wings which allowed the aircraft to have thinner wings with substantially less sweep and a higher span. Eco-Strut is capable of operating at 0.8 Mach while maintaining laminar flow over the wings. The wings with high aspect ratio and low thickness to chord ratio have been extremely effective. The reduced drag and weight directly allows the plane to consume less fuel while serving its missions.

### **1.5.2 Advanced Turbofan**

The Eco-Strut is designed to use the Pratt and Whitney 1000G geared turbofan (PW1000G). This engine, currently under testing, has a high bypass ratio turbofan that uses a state of the art gearbox. The gearbox allows the fan and the compressor each to operate at their own most efficient speed. The PW1000G has a lower weight while have an increased efficiency of 12%. This efficiency contributes to the fuel consumption design driver. The PW1000G is also environmentally friendly. Together with low levels of fuel consumption the PW1000G also generates substantially less CO<sub>2</sub> and NO<sub>x</sub> emissions. A lower level of noise generation is also key to the success of Eco-Strut, and PW1000G promises a 20dB cumulative reduction in noise level from stage 4.

### **1.5.3 No Bleed System**

With the use of advanced heating systems and the “Hamilton Sundstrand” Auxiliary Power Unit, the Eco-Strut will be one of the first in its kinds to implement such advanced systems and eliminate bleed air. The use of bleed air requires greater trust from the engines. The Eco-Strut will not use any bleed air from the engines, and all the systems will be operated using electricity energy. The use of electricity energy and elimination of bleeding systems allows the Eco-Strut to once again meet the stringent requirements of efficiency and low cost.

### **1.5.4 Use of Composites Materials**

Similar to the Boeing 787 the Eco-Strut will heavily rely on composite materials for the structure of the aircraft. Using composite materials will allow the Eco-Strut to obtain even lower dry weight while maintaining strength of the structure. The use of composite materials results in lower

production, operation, and maintenance costs, addressing the cost aspects of the design drivers, while promising a longer lifecycle for the aircraft.

## 2 Design Evolution

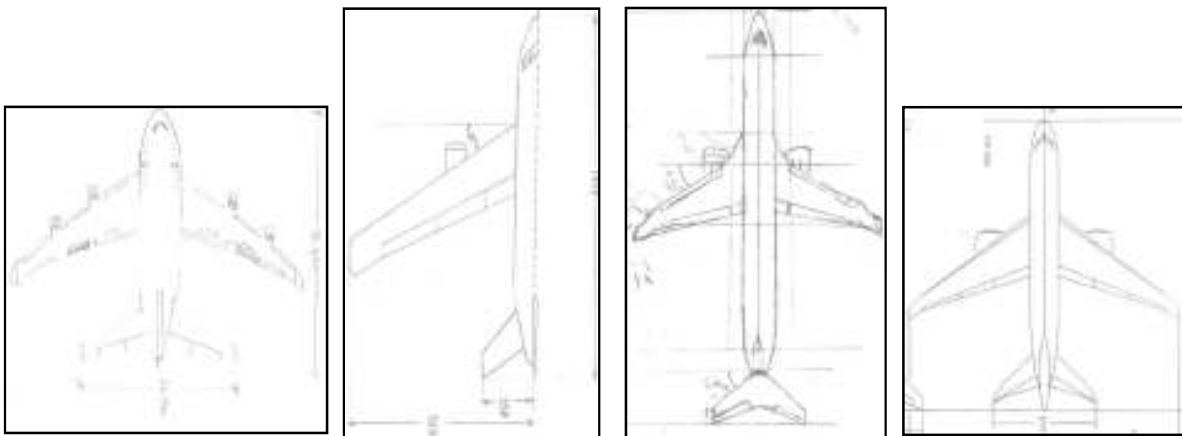
### 2.1 Configuration Concepts

After studying the design requirements, existing aircraft in its class are investigated. Each team member is tasked with developing a conceptual design. Due to similarities among members' ideas, concepts are categorized according to their design type. The concepts are then rated in a concept matrix to determine how well they meet design objectives. Each design type and concept decision matrix category is discussed below.

#### 2.1.1 Tube and Wing

Four tube and wing concepts developed by members of Cirrus Technologies are presented in Figure 2.

**Figure 2** Four Tube and Wing Concepts



The tube and wing design is a proven success for existing commercial transport aircraft. A benefit of considering this design type is its research and development cost savings. Application of

technological advancements in individual design areas can be more easily analyzed and evaluated than when applied to nonconventional concepts. Improvements in efficiency and noise can be achieved through the use of advanced winglets and engines, among other factors. This design also serves as a baseline for comparison of other concepts. A representative drawing is presented in Figure 3.



**Figure 3** CAD Illustration of Tube and Wing Design

An advantage of the conventional tube and wing is that it is a proven concept. Being around for over half a century in the commercial market, improvements have been continually made to this design. As a result acquisition costs would be lower than nonconventional designs. It is possible that the law of diminishing returns becomes more apparent in attempting to meet RFP requirements, as efficiency limits of the tube and wing are approached.

### **2.1.2 Strut-Braced Wing**

One strut-braced wing concept is developed by a member of Cirrus Technologies is shown in Figure 4.

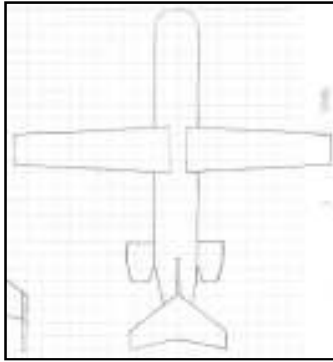


**Figure 4** Strut-Braced Wing Concept

The strut-braced wing is much like a conventional tube and wing, with the exception of a strut extending from the fuselage to each wing. This strut serves to relieve bending moments when the wing is under loading. As a result of decreased moments, there are less structural demands on the wing and the wing thickness can be reduced. A thinner wing reduces wave drag which allows the wing sweep to be lowered. As the wings are unswept, natural laminar flow is promoted. The strut also allows for a higher wing span which makes increases efficiency [1]. Improved aerodynamic performance and weight savings are highlights of this design.

A challenge of the strut-braced wing concept which must be considered is possible buckling of the strut under heavy loading conditions [2]. Analysis of the strut must be performed to ensure structural integrity. An illustration of the strut-braced design is shown in Figure 5.



**Figure 5** CAD Illustration of Strut-Braced Wing Design

The strengths of strut-braced wing are the possibility for a laminar wing boundary layer, its low weight, high efficiency, and practicality. Innovative solutions are needed to address potential strut buckling, and interference drag.

### 2.1.3 Blended Wing Body

Three blended wing body concepts developed by members of Cirrus Technologies are presented in Figure 6.

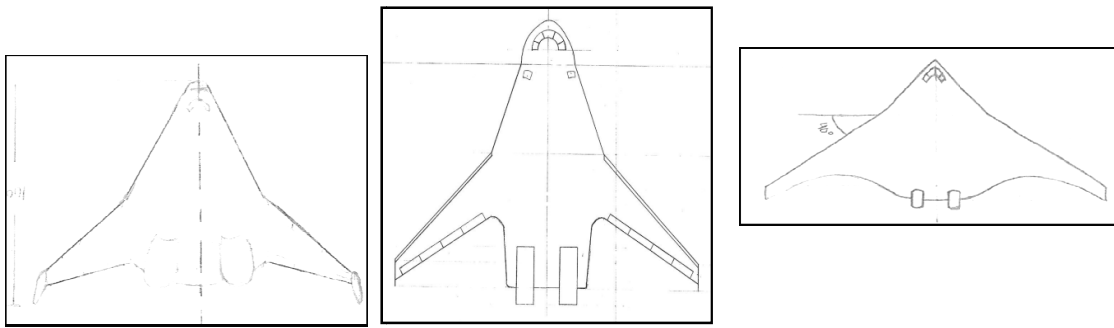


**Figure 6** Blended Wing Body Concepts

The blended wing body has a flying-wing shape which incorporates the fuselage and lifting surfaces. Engines can also be integrated into the body for reduced drag and improved efficiency. Its shape makes mounting a high efficiency distributed propulsion system feasible. In addition to meeting the passenger capacity, the blended provides sufficient room for luggage and cargo [3].

A possible issue that may arise is operation of the cabin pressurization system in blended wing body aircraft, since more empirical data exists for cylindrical cabins for commercial aircraft [3]. A blended wing-body aircraft is depicted in Figure 7.

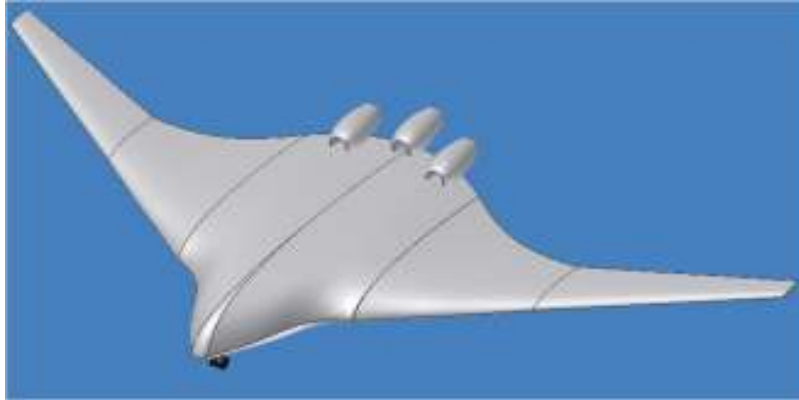


**Figure 7** CAD Illustration of Blended-Wing Body Design

The pros of the blended wing body are its low drag, high efficiency, and low noise pollution. Limitations of this concept are its high acquisition and operation costs, and suitability to larger passenger capacity. Considering design and certification time, its unconventional design may have difficulty meeting the entry into service requirement.

## 2.2 Sizing

The sizing of an aircraft provides specific ranges of weight that an aircraft must have total in order to operate an intended mission with an intended payload. Typical calculations are obtained by gaining initial requirements for the aircraft such as the design, the range, and the payload along with other parameters which are outlined in detail in the AIAA RFP. The aircraft sizing procedure is performed by adopting values from past historical aircraft and/or researched and proposed aircraft designs. Consequently choosing the right candidate for this project's design depended on the sizing, which produces the minimum weight in order to perform the required range mission of 2800 nm.

Initially the weight estimations were made by comparing each conceptual design to an historical one. For this case, this was the Boeing 737-800 and Airbus 320 aircraft for the conventional tube and wing, comparatively sized BWB, and strut-braced wing aircraft. The typical mission profile predicted for each aircraft's operation is illustrated in Figure 1. This is essential to outline since an aircraft experiences differences in its weights according to each segment of its mission.

The takeoff gross weight, TOGW, is the total weight of the conceptually designed aircraft as it commences its mission. It may be broken down into payload or passenger weight, crew weight, fuel

weight and other remaining empty weight of the plane. The empty weight specifically only carries the structure, landing gear, fixed equipment and systems, and engines. During the segments in Figure 1, the aircraft decreases in weight caused by the burning of fuel. In order to account for these losses in weight, sizing was performed which utilizes historical mission segment weight fractions [4]. In turn these weight fractions and other RFP parameters were employed into a sizing computer program to produce the required and available weights over a range of the takeoff gross weight. From that point the ideal  $TOGW$  and  $W_e$  were chosen for analysis of all three conceptual aircraft designs.

After obtaining the  $TOGW$  and  $W_e$  values, a second type of sizing was performed. This was done by taking into account more aerodynamic parameters of each aircraft as well as the engine parameters. Briefly, the engine chosen in order to evaluate the wing loadings was the Pratt & Whitney 1000G geared turbofan. The complete first and second order sizing process is diagrammed in Figure 8.

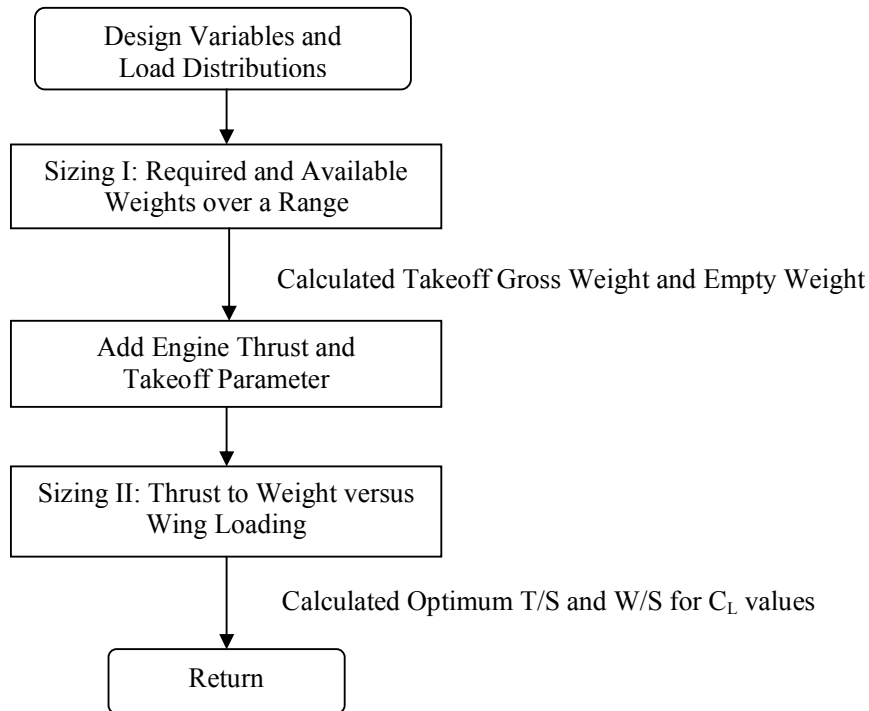


**Figure 8** Flowchart of Weight Calculations

The second sizing of each conceptual aircraft design, the thrust to weight ratio and wing loading were determined by taking the values obtained from the first sizing procedure,  $TOGW$  and  $W_e$ ,

and adding Pratt & Whitney 1000G engine data. References for the engine and aerodynamic data may be found in the Propulsions and Aerodynamics section of this report, respectively.

Wing loading is essentially the loaded weight of the aircraft divided by the area of its wing. Typical aircraft wing loadings may range from 20 lb/ft<sup>2</sup> up to about 120 lb/ft<sup>2</sup>. This is a useful measurement in that it illustrates the maneuvering performance of an aircraft traveling through the air as a result of the lift generated by the wings. Consequently aircraft with larger wetted areas relative to its mass have a lower wing loading, and a higher lift at any given traveling speed. The results of sizing one and two for each aircraft are combined in Table 1.

**Table 1** Conceptual Designs' Sizing I & II Results

	Conventional Tube & Wing	BWB	Strut-Braced Wing
Empty Weight (lb)	112,200	75,380	71,970
TOGW (lb)	227,029	155,268	148,500
Wing Loading (lb/ft <sup>2</sup> )	120	121	115
Thrust/Weight	0.2309	0.2289	0.2199

### 2.3 Concept Decision Matrix and Final Decision

Each design type is given a rating that corresponds to a concept matrix category. Feasibility accounts for whether a 2018 entry into service is possible. The noise and fuel burn ratings indicate how well the concept is expected to meet noise reduction and fuel burn objectives, respectively. Being major deciding factors of customers, acquisition cost and operational cost are also rated. The overall marketability of each concept is then rated to examine the potential success of each concept. Each concept is rated out of the respective maximum value for each category. The maximum total rating is 100 points, with higher ratings being more favorable. Independent ratings by each team member are averaged. The concept matrix is tabulated in Table 2.

**Table 2** Concept Decision Matrix

	Maximum Value	Tube & Wing	Strut-braced	BWB
Meets RFP	20	16	18	16
Feasibility	12	11	10	6
Noise	17	11	13	16
Fuel Burn	16	11	14	13
Operational Cost	15	11	13	9
Acquisition Cost	10	8	8	3
Marketability	10	9	8	6
Totals:	100	76	84	70

As shown in Table 2, the concept matrix results in descending order are strut-braced wing with 84 points, tube and wing with 76 points, and blended wing body with 70 points. Therefore, the strut-braced wing aircraft was the highest preferred concept.

There were also many other reasons for selecting the strut-braced wing concept over the others. This design is well-rounded to reduce community noise, have weight and cost savings, while meeting the 2018 entry into service. Along with these benefits, the strut-braced wing concept is capable of providing stability during all segments of its mission as depicted in Figure 1. Comparing the different types of aircraft altogether, the design drivers seemed to best fit and could be most accommodated by choice of a strut-braced wing.

## 2.4 Final Sizing

The strut-braced aircraft is a highly integrated technology concept in which many critical reductions of the aircraft’s parameters maximize its cruise performance. In comparison to the conventional tube and wing and BWB, its operational benefits include a higher aspect ratio, lower thickness ratio and therefore lower wing weight. The reduction in wing weight is correlated with the reduction in thickness allowing the wing sweep to be minimized to lower drag losses [1]. This advantage in reduction of the wing sweep permits a larger percentage of the wing area that in turn produces natural laminar flow and lower drag. Figures 9 and 10 illustrate the optimized values for the design obtained through sizing as was depicted in Figure 8.

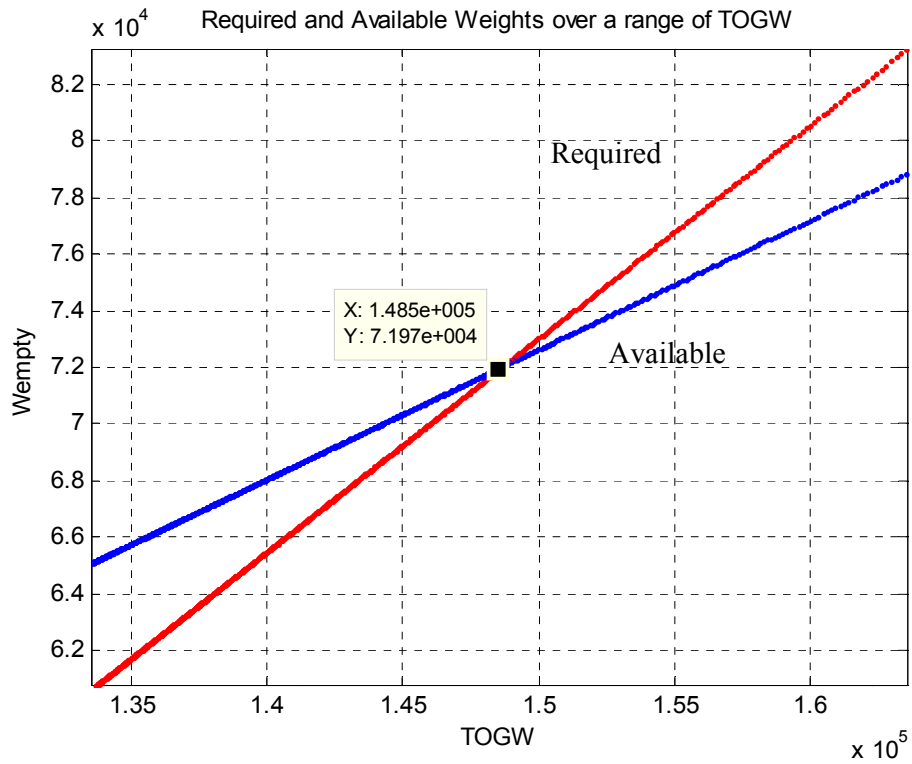


Figure 9 Strut-Braced Wing Aircraft Sizing I

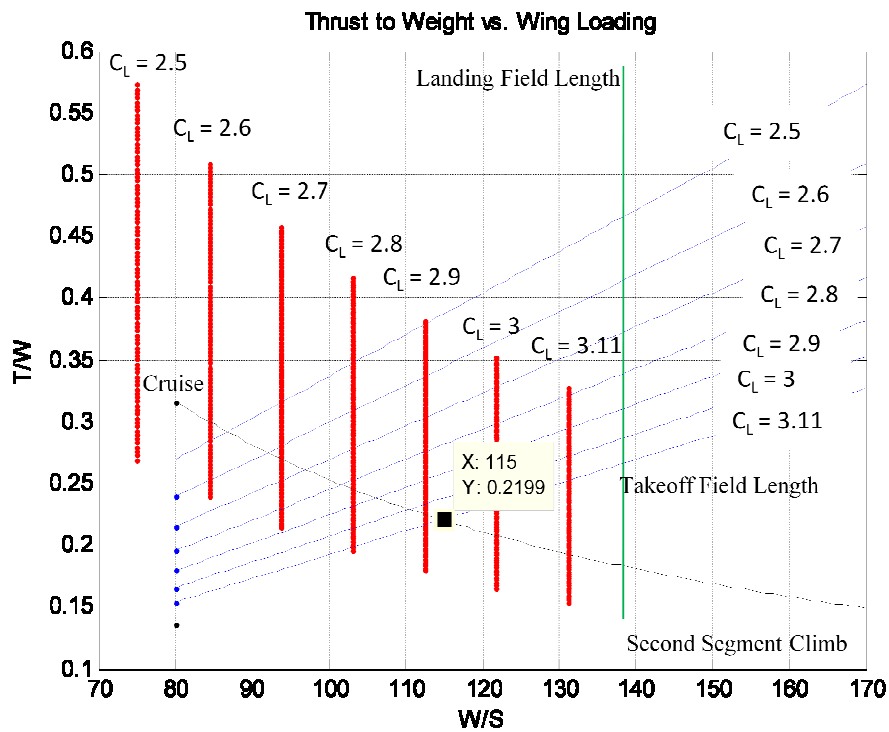


Figure 10 Strut-Braced Wing Aircraft Sizing II

### 3 Weights, Moments and Center of Gravity

The weight of the Cirrus Eco-Strut was estimated using a component method [4], which takes into consideration all of the materials used to compile the aircraft, as well as all of the system weights. Other components such as fuel weights throughout the mission were computed using fuel fractions weight methods presented in *Raymer* [4] and *Roskams'* [6] aircraft design books. In order to maintain as much accuracy as possible, the component weights of the Cirrus Eco-Strut were sized closely with the Boeing 737-800 and the Airbus 320. Both of these aircraft carry the same amount of capacity as described in the RFP being 150 passengers, and are valuable comparers for this design. As a result of the high-wing placement on the Eco-Strut, and the reduction in its sweep, the Eco-Strut is meant to produce 25% in weight reduction as compared to Boeing 737-800 and Airbus 320.

#### 3.1 Weight Statement

The weights summaries as well as each component's center of gravity location on the Eco-Strut and related moments of inertia are listed in Table 3. The weight of each component was obtained by calculations detailed in *Raymer* [4] and was then placed in the aircraft to obtain the design center of gravity location.

**Table 3** Cirrus Eco-Strut Weight Statement

Eco-Strut Component	Weight	$X_{cg}$	$Z_{cg}$	$I_x$	$I_y$	$I_z$
	lbs.	ft.	ft.	lbs·ft <sup>2</sup>	lbs·ft <sup>2</sup>	lbs·ft <sup>2</sup>
Fuselage	12877	54	7	398375	692378	294003
Wing	17897	66	14	54054	961779	907725
Empennage	3856	111	29	1054625	11570367	10515742
Engine	11600	58	3	952610	959636	7026
Landing Gear Forward	700	16	1	85659	1372640	1286981
Landing Gear Aft	5600	66	1	685272	938291	253019
Fixed Equipment	7000	25	8	101725	8159606	8057881
<b>Empty Weight</b>	<b>59530</b>	<b>61</b>	<b>9</b>	<b>558179</b>	<b>852030</b>	<b>293851</b>
Trapped Fuel and Oil	3800	58	4	246990	249292	2302
Fuel	35740	58	16	641884	663531	21647
<b>Operating Weight</b>	<b>63330</b>	<b>60</b>	<b>9</b>	<b>593809</b>	<b>688341</b>	<b>94532</b>
Crew in Cabin	820	11	9	7689	1879553	1871864
Cargo	8000	58	16	143679	148524	4845
Passengers	27750	61	13	24411	106674	82263
<b>Take Off Weight</b>	<b>135640</b>	<b>59</b>	<b>12</b>	<b>523</b>	<b>7193</b>	<b>6670</b>

The takeoff gross weight of the Eco-Strut is the total weight of the aircraft at the beginning of the mission and can be broken down into payload or passenger weight, crew weight, fuel weight and remaining empty weight. The empty weight carries the structure, landing gear, engines and fixed equipment and systems. During each segment of the mission profile as illustrated in Figure 1, the Eco-Strut decreases in its weight. The result of the reduction in weight for the 2300 nm mission with full payload is depicted in Table 4. It should be noted that these weight values are obtained at the end of each segment listed.

**Table 4** Eco-Strut Weights at Mission Segments

<b>Mission Segment</b>	<b>Weight at Segment</b>
Take off	135640
Climb	133605
Cruise	115128
Loiter	113781
Landing	113212

### 3.2 Center of Gravity Travel

The Cirrus Eco-Strut has a gross takeoff weight of 135,640 lbs. carrying 150 passengers, four crew members and approximately 36,000 lbs of fuel. This makes the Eco-Strut produce approximately more than 20% of weight savings as compared to the Boeing 737-800. The center of gravity of the entire aircraft component ranges from 25%-40% of the MAC chord. The travel of the center of gravity location throughout its mission profile is represented in Figure 11. This graphical representation satisfies the Cirrus Eco-Strut's stability and control requirements, as well as the total aircraft weight related to those constraints. As a result of fuel burn throughout the mission, this causes the forward movement of the CG location on the aircraft. Consequently, the payload expenditure in return causes an aft movement of the CG location. The forward and aft limits of the CG are discussed further in the Stability section of this report.

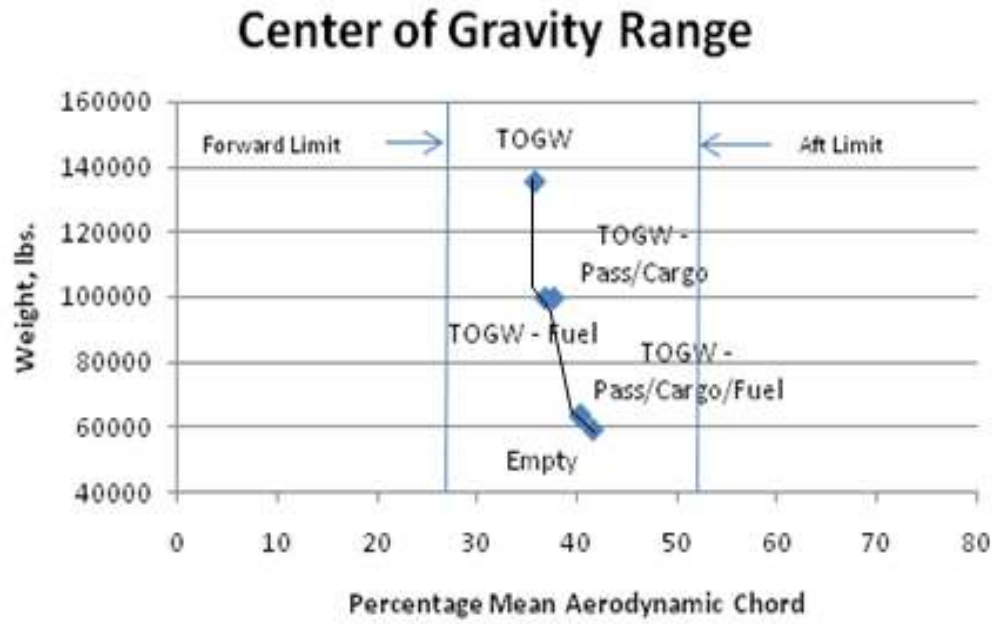


**Figure 11** Center of Gravity Range

## 4 Propulsion Systems

### 4.1 Engine Selection and Thrust Requirements

Considering the thrust and fuel use, selection of the proper engine is critical. For the RFP requirements for this aircraft (low fuel consumption, low cost, low noise, and low emissions), an engine which burns a low amount of fuel (thereby saving money on fuel, and reducing emissions), is quiet, and lightweight is important. Three engines were compared with respect to these categories to determine which engine would fit the design criteria best. The three engines were the CFM 56-3B-2, the CFM 56-7B27 (currently used on the Boeing 737-800), and the PW1000G (currently under development by Pratt and Whitney). With engine out requirements, it is required that each of the two engines produce 19,500 lbs of thrust. Each of these engines is a turbofan and produces sufficient thrust to perform takeoff maneuvers for aircraft of this size.

The Pratt and Whitney PW1000G is different from the other two engines, in that it has a significantly higher bypass ratio, and a state-of-the-art gear system allowing the engine fan to operate at a different speed than the compressor and turbine [16]. These two improvements are expected to increase the fuel efficiency of the engine significantly, and drop the noise output by 20dB when compared to the other competitor engines. This engine is expected to be available midway through the next decade, making it a feasible candidate for the Eco-Strut. In order to properly compare the three engines fuel consumption Figure 12 displays the SFC values of the three engines displayed in Table 5.

**Table 5** Engine Data for Engines Considered During Design Process [15]

Engine	Thrust (lb)	SFC (lb/(lbf-hr))			
		100% Thrust	85%Thrust	30%Thrust	7%Thrust
Pratt & Whitney 1000G	23,000	3.207	3.137	3.179	5.163
CFM 56-3B-2	22,100	3.793	3.710	3.760	6.106
CFM 56-7B27	27,300	3.733	3.567	3.382	4.817

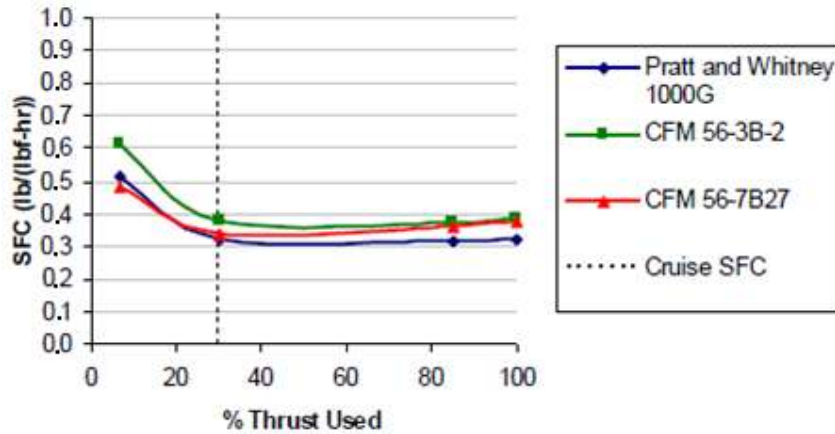


**Figure 12** Engine SFC Values over Various Engine Thrust Levels [15].

It can be seen in Figure 12 that the PW1000G outperforms the other two engines in efficiency in takeoff, climb, and cruise, but it falls behind the CFM 56-7B27 in loiter. The bulk of the fuel in any transport mission like this is used primarily in the cruise phase. It is for this reason, along with the expected drop in both sound and weight, that the PW1000G is the more desirable engine for this design. Figure 13 compares the thrust produced for the three different types of engines.

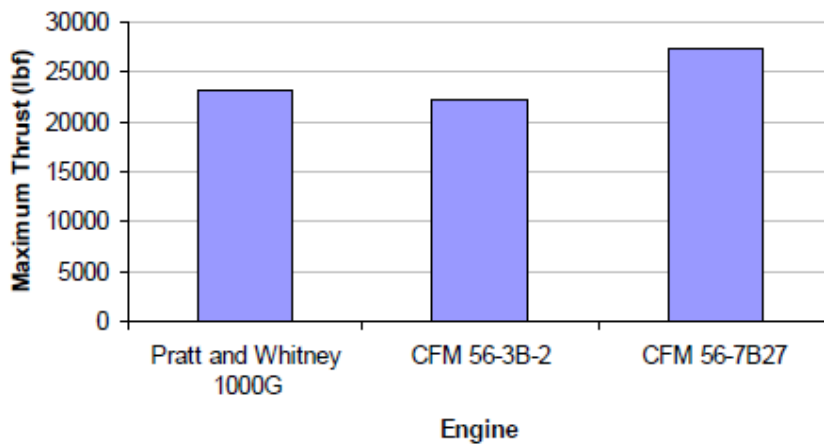


**Figure 13** Maximum Thrust Provided for Each Engine

The maximum thrust provided by the Pratt and Whitney 1000G engine meets the engine out requirements set by the FAA for the Eco-Strut. As the operating altitude of the Eco-Strut increases the density of the air decreases hence decreasing the available thrust of the engine. The available thrust of

the Pratt and Whitney 1000G engine is plotted as a function of altitude in Figure 14 based on the decrease in density.

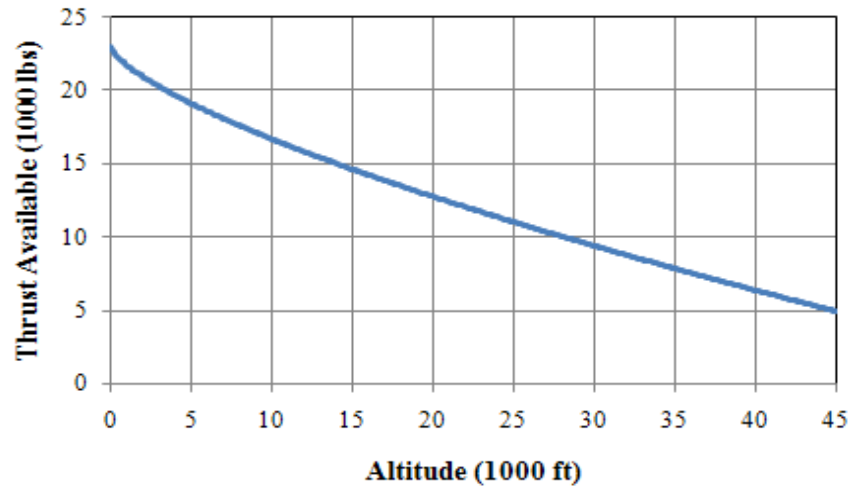


**Figure 14** Thrust Available vs. Altitude for PW1000G Engine used on Eco-Strut

## 4.2 Engine Specifications and Placement

The Pratt and Whitney 1000G engine (Figure 15) with 23,000 lbs of thrust is promised to have a 12% reduction in fuel consumption. The PW1000G has a 20dB noise reduction compared from stage 4, 3000tonnes reduction in CO<sub>2</sub> emissions annually, and 55% reduction in NO<sub>x</sub> [16]. These factors are important given the strong emphasis on environmental friendliness of the Eco-Strut. With a fan diameter of 73 inches the PW1000G has a greater bypass ratio which is a key factor in the design of the engine. However the main revolutionary technology that is used in the PW1000G is the implementation of a gear system which allows the fan and the compressor each to rotate at their optimal condition [16].

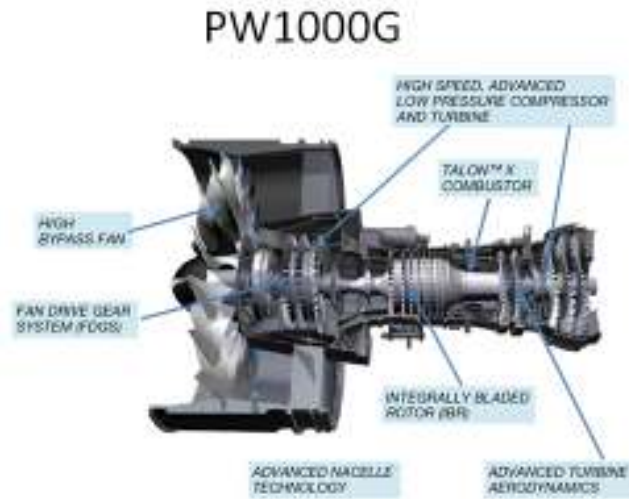


**Figure 15** Pratt & Whitney 1000G Engine Cross Sectional View [16].

Although Eco-Strut will use the revolutionary design of strut braced wing, the engine will be placed in a conventional manner under the wing and the strut as displayed in Figure 16.

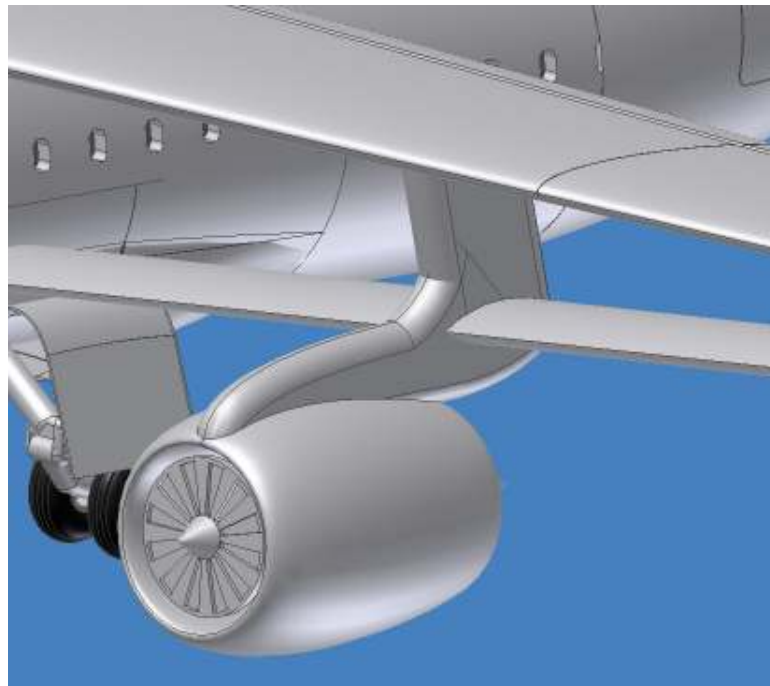


**Figure 16** The installation of the PW1000G engine on Eco-Strut.

This configuration allows for easy maintenance and repair of the engine. Loadings on the engine is carefully examined to make sure that the forces acting on the engine are balance and do not damage

the engine. The structural integrity of the concept has been thoroughly analyzed and the mounting is designed in a safe and conventionally adequate manner.

### 4.3 APU

The Eco-Strut will need an auxiliary power unit (APU) to start the engine. The Eco-Strut does not require any bleed air due to its simplicity and efficiency, therefore. The sole use of the APU will be to start the engine. The Eco-Strut will use the technologically advanced, low cost, Hamilton Sundstrand APS 5000 Auxiliary Power Unit. The Hamilton Sundstrand APS 5000 APU was designed for the Boeing 787 with the no-bleed system architecture. This APU has a 1,100 shaft hp, 1.4 MW of electrical power, and is capable of starting and operating up to an altitude of 43,000 ft. Due to FAA regulations an on-board inert gas generation system is to be used.

## 5 Noise Analysis

The Eco-Strut is designed to be a quieter aircraft compared to current commercial aircrafts. The Eco-Strut is designed to meet the RFP requirement of 20dB lower than the ICAO stage 4 requirements. The ICAO stage 4 requirements are defined by a cumulative 10dB noise reduction with respect to stage 3. Based on the three locations of Sideline, Approach and Takeoff as seen in Figure 17, the noise requirements are set.

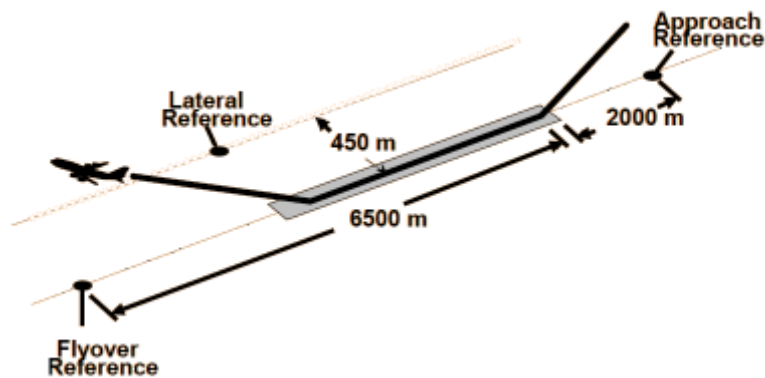


**Figure 17** Trajectory and Aircraft Noise Certification Measurement Points for Sideline (Lateral), Approach and Flyover (Takeoff) [17]

The noise level at each of these locations is measured based on the Effective Perceived Noise (EPNdB) which is based on expressed human response to either loudness or annoyance. Based on Figure 18 and Figure 19, the stage 3 requirements are set.

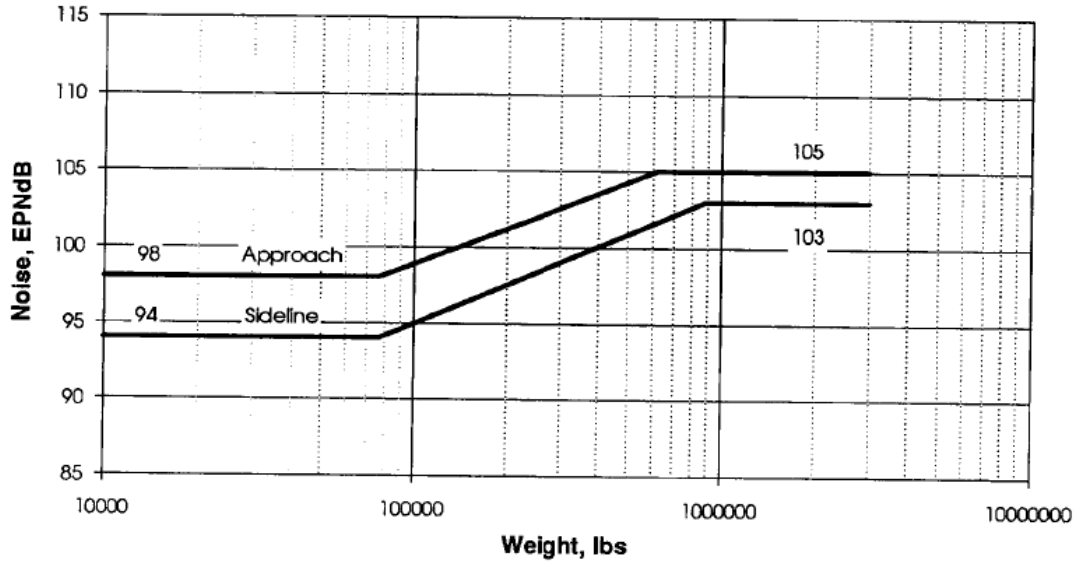


Figure 18 Approach and Sideline Noise Requirements set for Stage 3

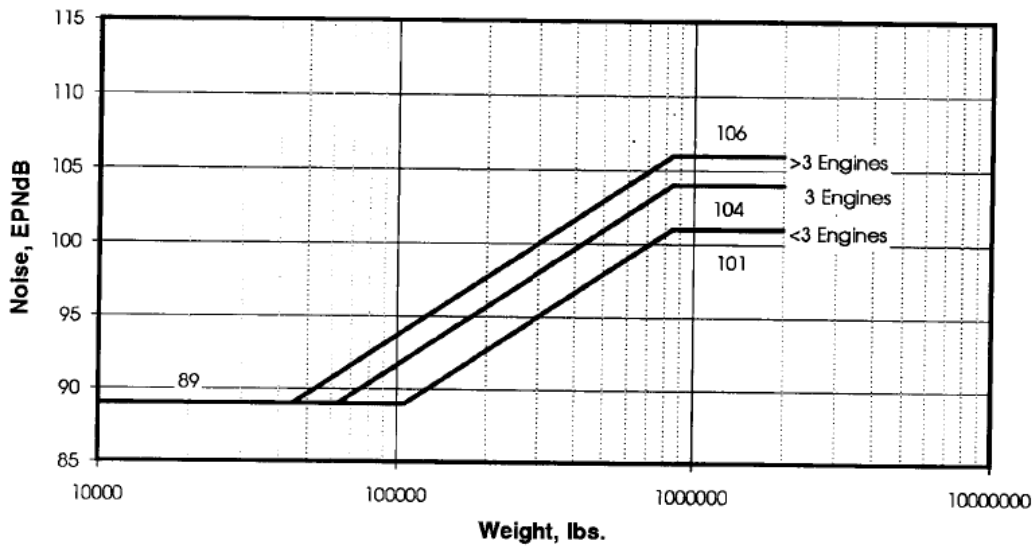


Figure 19 Takeoff Noise Certification Requirements for Stage 3

It is determined that for stage 3 the Eco-Strut should have a noise level below 100EPNdB for Approach, 96EPNdB for Sideline, and 89EPNdB for Takeoff. Based on the RFP requirement the Eco-

Strut should have 20dB cumulative decrease compared with Stage 4, and the Stage 4 requirement is 10dB cumulative decrease compared with Stage 3. The main sources of noise generation for the aircraft are the engines, creation of turbulent flow over the wing and high lift systems, and the landing gear system. The PW1000G engine chosen for Eco-Strut has a 20dB noise reduction. The Eco-Strut is using low sweep and low thickness to chord ratio wings, this is particularly important in maintaining laminar flow and reducing the noise generated by the wings. The landing gear of Eco-Strut is substantially shorter than the landing gear for conventional commercial airplanes. The implementation of the short landing gear assists in a 3EPNdB reduction of noise compared to conventional aircrafts. The implementation of a low noise landing gear system which eliminates spaces between the parts of the landing gear is proven to reduce the noise generated by the landing gears [18]. The Eco-Strut has a lower TOGW compared to the Boeing 737 which allows the Eco-Strut to easily takeoff and land without the implementation of slats on the wing. The elimination of slats not only creates simplification for the production of the aircraft, but it also substantially reduces the noise create by the wing. Although the strut used for the Eco-Strut will create 67.16 EPNdB of noise by itself, it will have negligible contribution to the overall noise of the aircraft at the current noise levels [19]. Another method of noise reduction is covering the cavities of the landing gears; however this is not implemented for the Eco-Strut due to complexity of the system. After the combination of noise reduction techniques were incorporated in the design of the Eco-Strut, it could be said that the Eco-Strut should be able to easily meet and even exceed the noise requirements set by the RFP.

## **6 Aerodynamics**

### **6.1 Wing Design**

Advanced aerodynamic design is crucial in meeting and exceeding requirement objectives, with emphasis on improved aircraft efficiency and noise reduction. The wing is designed for performance during cruise, together with capability in the take-off and approach/landing regimes.

The synergistic nature of strut braced wing aircraft enables superior aerodynamic performance over conventional designs. The strut serves to relieve bending moments when the wing is under loading. As a result of decreased moments, there are less structural demands on the wing and the wing thickness can be reduced. A thinner wing reduces wave drag, which allows the wing sweep to be lowered. As the wings are unswept natural laminar flow is facilitated, which results in reduced parasitic drag. Further drag reduction is achieved through the use of supercritical airfoils. Its larger wing span than that of comparable aircraft also makes this design more efficient [1].

The Korn equation, together with the use of simple sweep theory optimizes the wing geometry parameters [28]. The goal to cruise at a Mach number of 0.8 introduces transonic compressibility effects. To avoid drag penalties, the aircraft is operated at the drag divergence Mach number. Figure 20 shows the selected thickness-to-chord ratio and leading edge sweep angle of 10% and 10° respectively, at the cruise lift coefficient of 0.47.

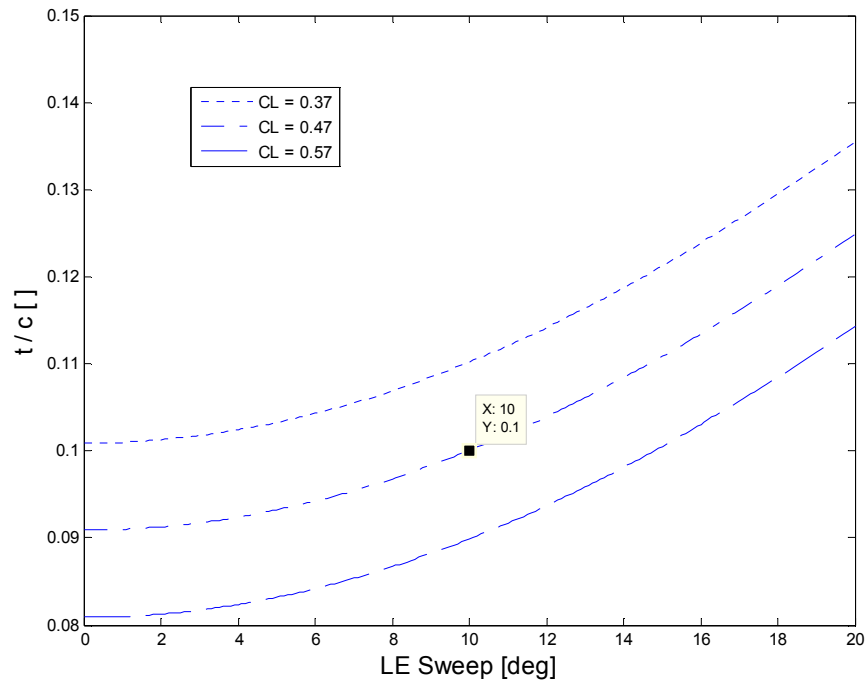


**Figure 20** Thickness-to-Chord Ratio: Leading Edge Sweep Angle Optimization

With the lift coefficient and thickness-to-chord ratio known, the supercritical SC(2)-0410 airfoil is chosen. The airfoil geometry is shown in Figure 23.

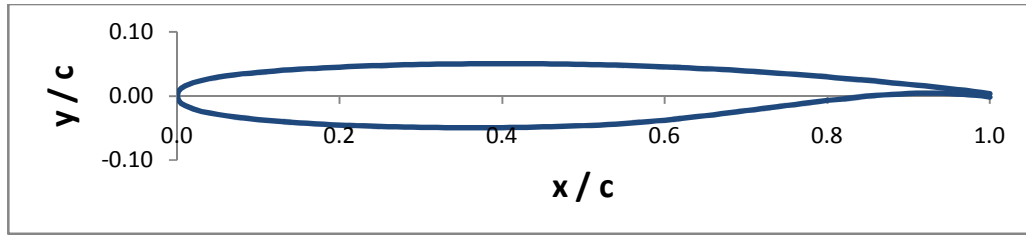


**Figure 21** Cross-Section of the chosen SC(2)-0410 Airfoil

## 6.2 Laminar Flow

The ability to maintain natural laminar flow along the wing reduces drag. The extent of laminar flow is based on a transition Reynolds number of  $12 \times 10^6$  [29]. Values at four span wise stations are averaged, equally spaced between the aircraft centerline and wing tip, are averaged. It is determined that laminar flow is achieved along an average of 74% of the wing, in the chord-wise direction.

## 6.3 High Lift System

The landing approach speed restriction of 135 knots largely dictates the maximum lift coefficient required for the Eco Strut. Based on methods in Raymer [4] the “clean wing” contributes 1.41 out of the required 1.95 maximum lift coefficient. A supplementary high lift system is needed. Compared to the Boeing 737 and Airbus 320, less-complicated single slotted fowler flaps are allowed to be employed [29]. The flaps occupy 20% of the wing chord length, which offers adequate room for fuel. Figure 22 shows the high-lift system [29]. Weight and noise level targets are easier to achieve since leading edge slats are not needed.



**Figure 22** The High-Lift System

### 6.4 Wing Lift Distribution

A vortex lattice method program, “VLMpc.exe” [31] is used to determine the wing lift distribution. Among its inputs are the planform geometry coordinates, and flight condition parameters. Figure 23 shows the wing lift distribution at cruise.

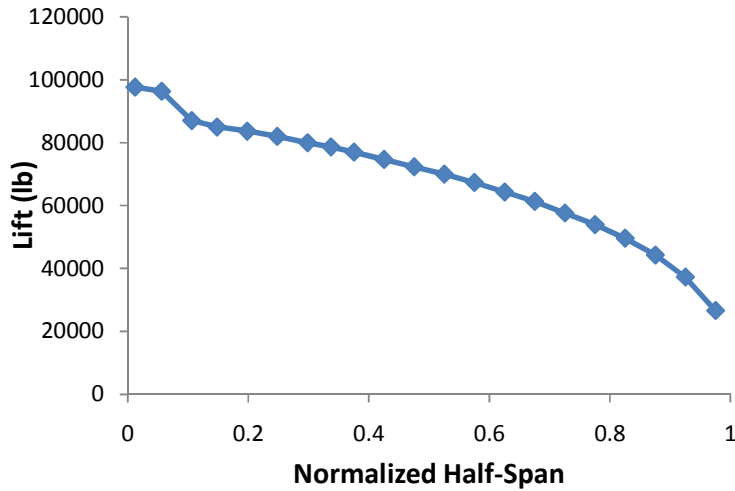


Figure 23 Wing Lift Distribution at Cruise

### 6.5 Drag Analysis

The drag produced by components depends on the flight regime. Laminar and turbulent parasitic drag build ups are obtained through the use of a program, “friction.exe” [31], as well as methods in Roskam [32]. Skin friction and form drag is output from friction.exe. The parasitic drag during cruise, take-off, and approach are listed and shown in Table 6 and Figure 24 respectively.

Table 6 Take-off, Cruise and Approach Parasitic Drag Build Ups

COMPONENT	Cruise	Take-Off	Approach
FUSELAGE	0.0053	0.0057	0.0058
WING	0.0023	0.0021	0.0021
HORIZ. TAIL	0.0012	0.0017	0.0013
VERT TAIL	0.0012	0.0016	0.0012
STRUT AND PYLON	0.0021	0.0023	0.0023
NACELLE	0.0017	0.0018	0.0019
LANDING GEAR HOUSING	0.0003	0.0003	0.0003
TRIM DRAG	0.0005	0.0005	0.0005
WINDSHIELD	0.0002	0.0002	0.0002
FLAPS	0.0000	0.0083	0.0182
LANDING GEAR	0.0000	0.0213	0.0213
<b>TOTAL</b>	<b>0.0148</b>	<b>0.0457</b>	<b>0.0551</b>

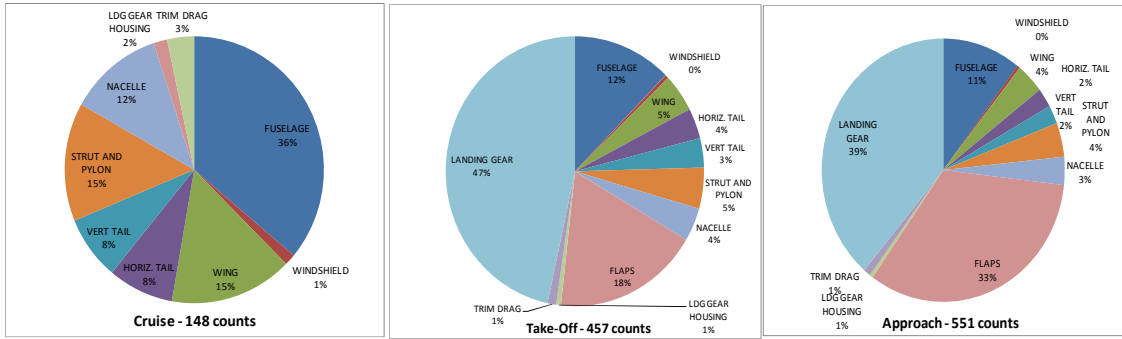


Figure 24 Take-off, Cruise and Approach Parasitic Drag Build Ups

Wave drag contributes 26 drag counts, using the method in Mason [28]. The drag polar equation in Mason [28] is used to plot the drag during take-off, cruise, and approach regimes. These are displayed in Figure 25.

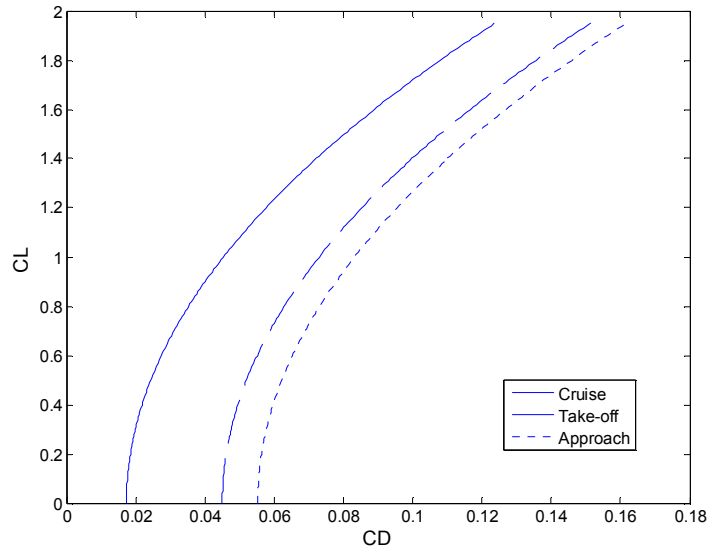


Figure 25 Take-off, Cruise, and Approach Drag Polars

## 7 Stability and Control

An important aspect of the Cirrus Eco-Strut's mission is its need to carry passengers in large numbers regularly. This means that the aircraft does not need to be as maneuverable as fighters or military aircraft, but it must be safe, stable, and have good ride qualities. A passenger aircraft that does not have these qualities is not acceptable for an airliner. For this reason, great measure has been taken to ensure that the Cirrus Eco-Strut is a very comfortable and stable aircraft.

### 7.1 Control Requirements

The Cirrus Eco-Strut is a class 3 aircraft, which must meet several requirements in order to have a Level 1 flight rating. It is extremely important for the aircraft to have such a rating, as it will ensure the Eco-Strut will have both good ride qualities, and will be safe to operate. These specific requirements and the Eco-Strut's ability to meet them are discussed later in this section.

### 7.2 Control Surface Configuration

There are many potential configurations for control surfaces on an aircraft. It was decided that in order to maintain low mechanical complexity, the control surfaces should be as simple as possible. For this reason a standard configuration, with horizontal and vertical tails, each mounted with elevators and rudders (respectively), along with ailerons mounted on the outboard wings was selected. Although canards often prove to be effective lifting surfaces that also aid in moment control, they were not considered, as their wakes could potentially disturb the laminar flow over wings. There were many configurations available for the horizontal and vertical tails, including the standard, low-tail configuration utilized in most common passenger airliners today, and the vertical T-tail, which is utilized in the Eco-Strut. The conventional low-tail configuration is not feasible for a strut-braced wing design like the Eco-Strut, because the tail will be directly in wake from the strut, causing a loss of tail elevator effectiveness. The T-tail was selected in order to allow for a shorter vertical tail, as the horizontal tail actually increases the effectiveness of the vertical tail, allow for a more efficient and smaller horizontal tail, as the tail is high above any wake or flow distortions caused by other parts of the aircraft, and to reduce buffeting on the horizontal tail, resulting in less fatigue in

both the structure of the aircraft, and the pilot. It was for these reasons that the T-tail was selected for the Cirrus Eco-Strut.

### 7.3 Horizontal Tail Sizing

The horizontal tail of the Cirrus Eco-Strut provides the aircraft with pitch stability and control. Using elevators to increase the lift on this surface, the horizontal tail is capable of creating large controlling moments about the CG of the aircraft. As the horizontal tail provides a downwards lift, it is important to keep the size of the horizontal tail relatively small, so as to minimize the downward lift it produces. The horizontal tail’s critical condition which dictates its necessary size is takeoff, as it must be large enough to create enough rotation for the aircraft to takeoff. A pitch angular acceleration at the instant that rotation begins of  $7^\circ/s^2$  is commonly used on Class 3 aircraft, and will ensure the Eco-Strut meets all Level 1 flight requirements. The horizontal tail was sized using an iterative approach with the methods found in *Roskam* [20] to ensure that the aircraft was capable of reaching this pitch angular acceleration. See Figure 26 for a plot of the required size of the horizontal tail determined using the method in Roskam [20], plotted against the aspect ratio of the tail. See Figure 27 for a plot of the root chord and the semi-span of the horizontal tail plotted against the aspect ratio.

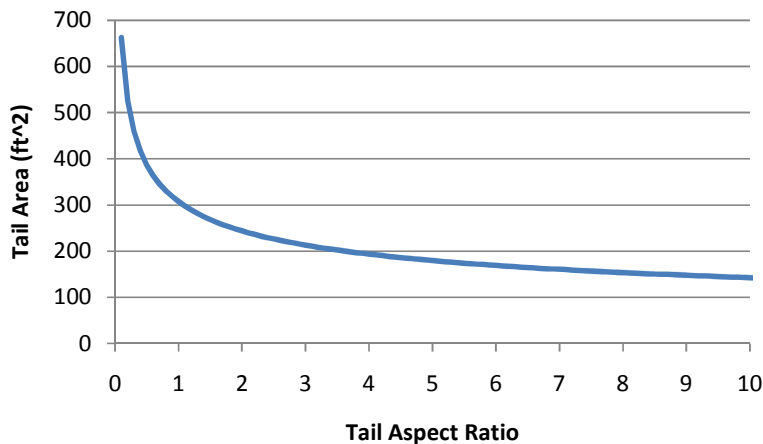


**Figure 26** Required Horizontal Tail Aspect Ratio vs. Horizontal Tail Area

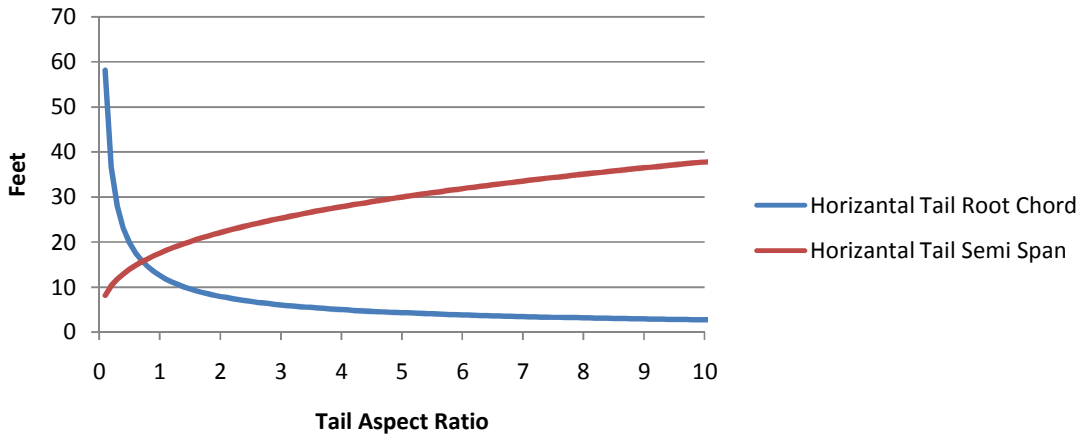


**Figure 27** Required Tail Aspect Ratio versus Root-Chord and Semi-Span of the Horizontal Tail

Using the plots in Figure 26 and Figure 27, a vertical tail with a root chord of 8.16', and a semi-span of 21.7' was selected. This tail has a surface area of 248 square feet, and is pitched downwards 5 degrees in order to improve its effectiveness. Elevators are on the rear of the tail, and take up 25% of the chord. See Figure 28 for a plot of the moment coefficient against the aircraft coefficient of lift for a variety of elevator deflection angles.

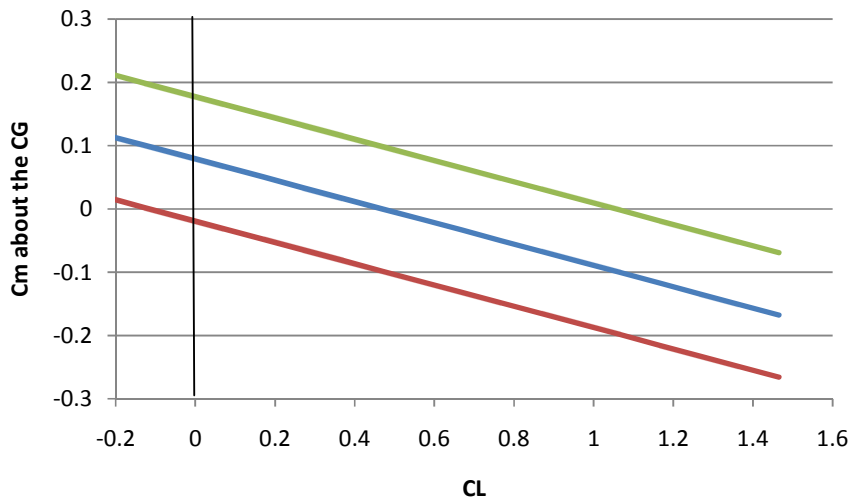


**Figure 28** Elevator Effectiveness in Trim over Various CLs

Figure 28 shows that across a large range of angles of attack, small elevator deflections can effectively trim the aircraft. The elevators on the Eco-Strut are capable of deflecting up to 25 degrees, which is more than sufficient to trim the aircraft in all regimes of flight. The Eco-Strut will be equipped with an alpha-limiter, to prevent the accidental stalling of the aircraft. This limiter will not allow the pilot to pull up any further than 10 degrees, which is more than enough for takeoff and climb conditions.

### 7.4 Vertical Tail Sizing

The vertical tail is necessary for preventing unwanted aircraft yaw. It is particularly important in takeoff and landing scenarios as it must be large enough to continue straight even in the event of an engine out or strong crosswind. The further out on a wing the engine of an aircraft is the larger the yawing moment from that engine due to asymmetric thrust in the event of an engine failure. Because of the jury strut placed on the wing to support the engine on the Eco-Strut, the engines were able to be placed closer to the center body of the aircraft, thereby reducing the size needed in the vertical tail to control the aircraft. See Figure 29 for a comparison of the required vertical tail size for the two configurations, the first without the jury strut, and the second with.

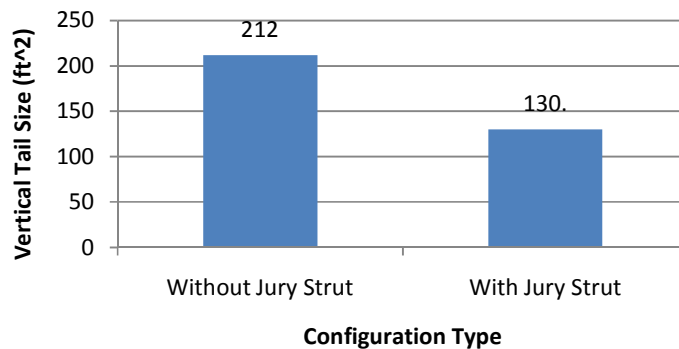


**Figure 29** Vertical Tail Sizing

A smaller vertical tail is desirable, as it weighs less, and is less costly to produce. The vertical tail of the Eco-Strut will be complete with a rudder capable of deflecting 15 degrees, making up 32% of its chord. It will be in the shape of a NACA 0012 airfoil to reduce the drag in steady level flight.

## 7.5 Ailerons

The ailerons are placed on the outside of the wings taking up 37% of the span, and 25% of the wing chord. These are placed on the outside so as to provide the largest moment arm possible for large rolling moments. Using the methods in Roskam [20], the ailerons were sized so as to be of sufficient size to be able to roll the Eco-Strut quickly enough to meet all control criteria necessary for a Level 1 flight rating. See Table 7 for the specific requirements and Eco-Strut values for Level 1 flight rating in roll.

**Table 7** Requirements for Level 1 Flight Rating in Roll

	<b>Level 1 Requirement</b>	<b>Eco-Strut</b>
<b>Maximum Roll Time Constant (s)</b>	1.4	0.8467
<b>Time to Roll 30 degrees (s)</b>	1.5	1.2903

## 7.6 Static Margin

One of the most important attributes to an aircraft's stability is its static margin. The Eco-Strut has a positive static margin that varies between 11.6% and 17.5%. This positive static margin ensures that the aircraft is statically stable, and will fly properly, regardless of the loading of passengers and luggage, or fuel consumption. The CG range varies from locations between 58.5 feet from the aircraft nose in a fully unloaded position to 59.1 feet from the nose for a fully loaded position. This amounts to a shift of slightly over 5% of the mean aerodynamic chord. See Figure 30 for a plot of this CG data.

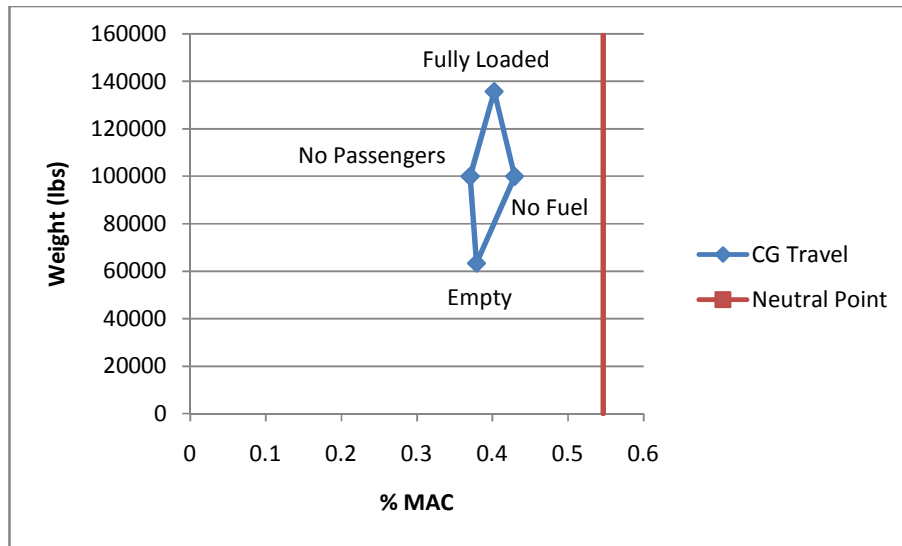


**Figure 30** Flight Envelope CG Travel in relation to the Neutral Point

A static margin this high is often avoided, as it generally creates a very high trim drag, however, as was shown above in section 7.3, very small deflections of the elevators are needed to trim this aircraft.

## 7.7 Aircraft Modeling and Stability Derivatives

The Eco-Strut control surfaces were simulated and tested through multiple different flight regimes using the inviscid vortex lattice method code Tornado. The model with control surfaces on it can be seen in Figure 31. This allowed for the preliminary testing and evaluation of control surface effectiveness, and for the calculation of stability derivatives. These derivatives can be seen in Table 8 and Table 9.

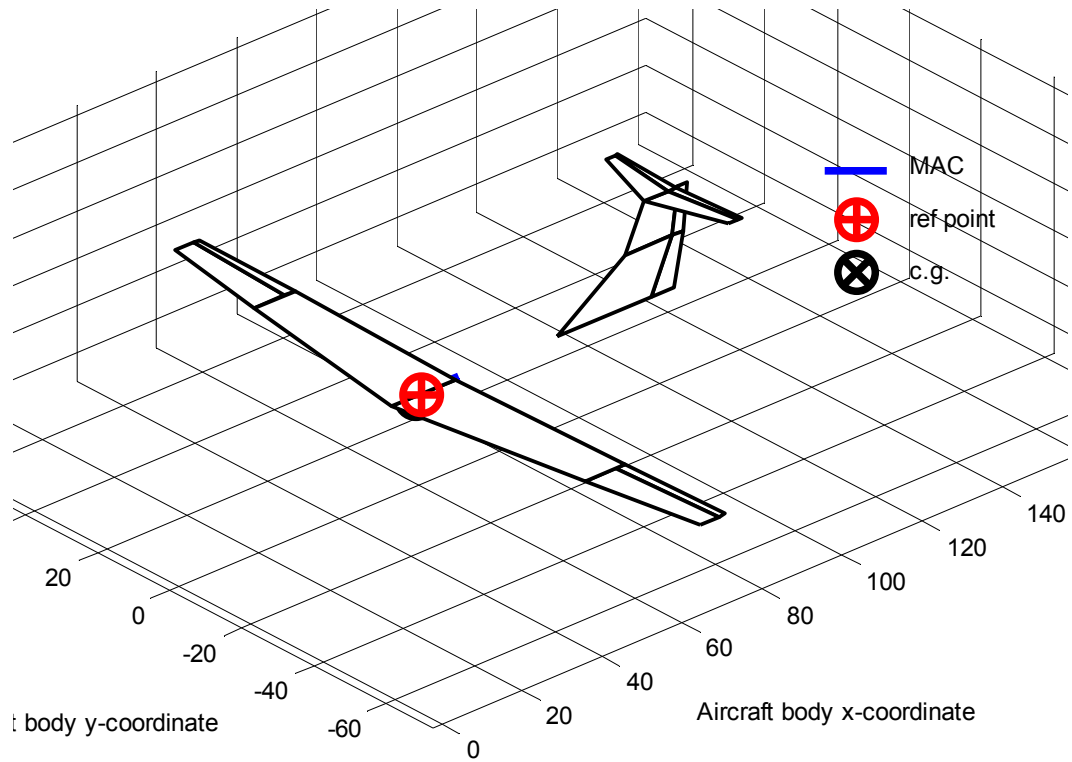


Figure 31 Steady, Vortex-Lattice Method Eco-Strut Model Produced in Tornado

Table 8 Longitudinal Stability Derivatives

Longitudinal Derivatives	
$C_{m_\alpha}$	-0.960
$C_{m_\alpha}$	0.085
$C_{m_q}$	-49.779
$C_{L_\alpha}$	5.704
$C_{L_q}$	12.52
$C_{L_{de}}$	0.605
$C_{D_{de}}$	0.013
$C_{m_{de}}$	-2.819

**Table 9** Lateral-Directional Stability Derivatives

Lateral-Directional Derivatives	
$C_{l_B}$	0.044
$C_{l_p}$	-0.589
$C_{l_r}$	0.063
$C_{n_B}$	-0.180
$C_{n_p}$	0.015
$C_{n_r}$	-0.157
$C_{y_B}$	-0.495
$C_{y_p}$	0.007
$C_{y_r}$	-0.426
$C_{y_{da}}$	0.007
$C_{l_{da}}$	0.228
$C_{n_{da}}$	-0.002
$C_{y_{de}}$	0
$C_{l_{de}}$	0
$C_{n_{de}}$	0
$C_{y_{dr}}$	-0.135
$C_{l_{dr}}$	0.013
$C_{n_{dr}}$	-0.050

## 7.8 Longitudinal Maneuvering

The longitudinal characteristics of aircraft can be broken into two important characteristics. These are the short period, and the phugoid. The requirements for Class 1 flight rating performance in the Short Period mode can be seen in Table 10.

**Table 10** The Short Period Mode Requirements for Level 1 Flight Conditions

Flight Category	Natural Short Period Frequency ( $\omega_{n_{sp}}$ )		Short Period Damping Ratio ( $\zeta_{sp}$ )	
	Eco-Strut Value	Level 1 Requirement	Eco-Strut Value	Level 1 Requirement
A	1.179	$1 < \omega_{n_{sp}} < 2$	1.265	$.35 < \zeta_{sp} < 1.3$
B	0.638	$.2 < \omega_{n_{sp}} < 2$	1.487	$.3 < \zeta_{sp} < 2$
C	1.179	$1 < \omega_{n_{sp}} < 2$	1.265	$.35 < \zeta_{sp} < 1.3$

Flight categories A and C are for takeoff and landing conditions, respectively, while category B is the cruise flight condition. The Eco-Strut is well within the requirements for Level 1 flight over

all flight conditions, meaning the aircraft successfully damps out any short period oscillation quickly, and does not require a control system for this flight phase. The disturbance from the short period oscillation over time can be seen in Figure 32.

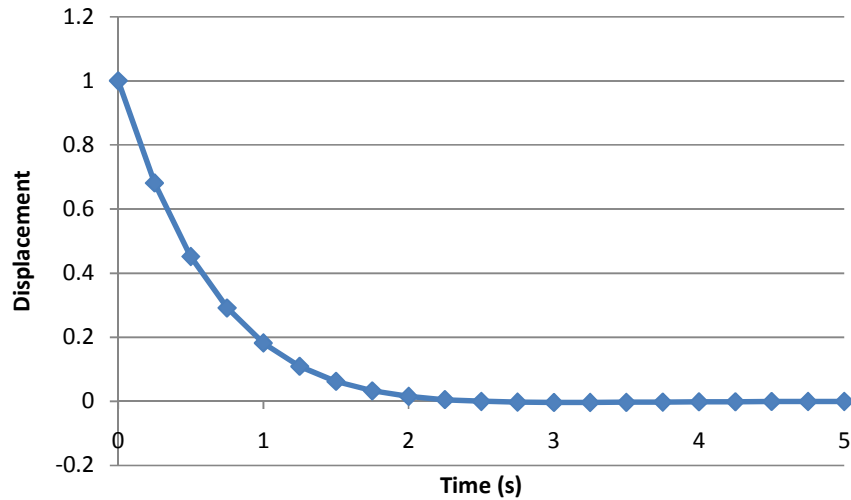


**Figure 32** The Short Period Mode over Time

As can be seen in Figure 32, the pitch displacement and oscillation from the short period mode damp out very quickly without any extra control loop. The Phugoid mode has a longer period, and slower damping, but is also a pitch oscillation. The Level 1 requirements for the Phugoid mode can be seen in Table 11.

**Table 11** The Phugoid Mode Requirements for Level 1 Flight Conditions

	<b>Phugoid Damping</b>
Level 1 Requirement	> .04
Eco-Strut Value	0.023

The Eco-Strut Phugoid is under-damped, so it will have to be stabilized using a proportional feedback control law. A plot of the uncontrolled Phugoid can be seen in Figure 33.

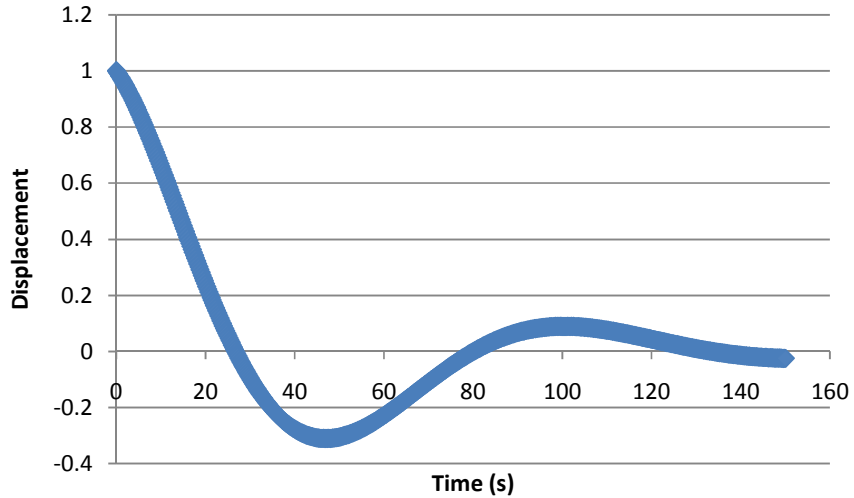


**Figure 33** The Uncontrolled Phugoid Mode Over Time

In order to control the phugoid mode and achieve a suitably high damping ratio, the Eco-Strut’s thrust is setup with a proportional feedback control law. This law uses both the angle of attack, and the speed of the aircraft to modulate the aircraft’s thrust. The gains for the angle of attack modulation and the speed are 7.14 and 0.01, respectively. Using this control law, the Eco-Strut’s new damping ratio becomes .256, well beyond the minimum requirement of 0.04. A plot of the new, damped phugoid displacement over time can be seen in Figure 32.

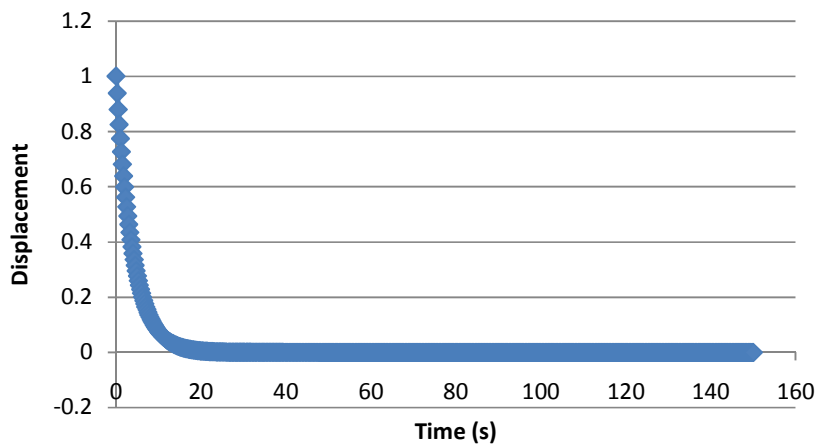


**Figure 34** The Phugoid Mode Over Time When Thrust is Controlled by a Proportional Feedback Control Loop

### 7.9 Departure Criteria

Another effective predictor of aircraft handling and stability characteristics is the comparison between the aircraft lateral control departure parameter (LCDP) and its  $C_{n\beta_{dynamic}}$ . The comparison of these values allows for the determination of the aircraft spin and departure susceptibilities. These values are dependent upon the angle of attack, so it is important to consider a range of the two values and ensure that they are both in a region with no departures. See Table 12 for a table of these two values for the Eco-Strut over various angles of attack.

**Table 12** The Eco-Strut LCDP and  $C_{n\beta_{dynamic}}$  Values Over Angles of Attack

$\alpha$	LCDP	$C_{n\beta_{dynamic}}$
-4	0.00335	0.00331
0	0.00314	0.00314
2	0.00302	0.00303
4	0.00290	0.00291
6	0.00278	0.00279
8	0.00265	0.00266
10	0.00251	0.00252

When these values are plotted on an integrated Bihrl-Weissman Chart, the aircraft’s lateral-directional trends become apparent. See Figure 35 for a plot of this data.

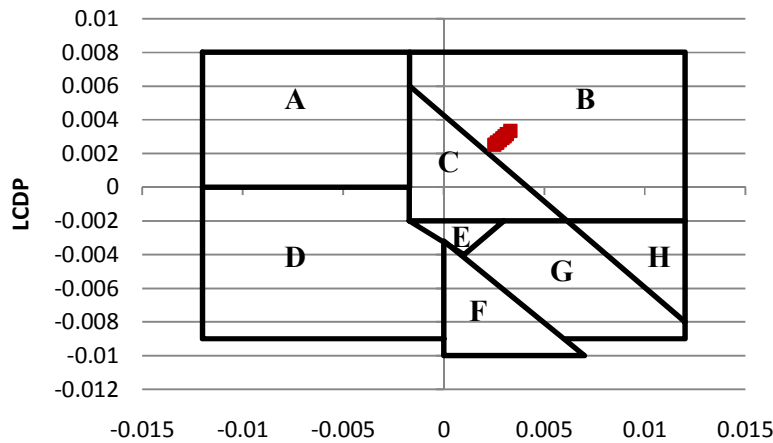


**Figure 35** The Eco-Strut location on the Bihrl-Weissman Chart – see below for a description of the 8 regions

Regions:

- A – High directional instability
- B – Highly departure and spin resistant
- C – Weak departure and spin resistance, no roll reversals, heavily influenced by outside factors
- D – Strong departure, roll reversals, and spin tendencies
- E – Weak spin tendency, moderate departure and roll reversal, affected by secondary factors
- F – Strong departure, roll reversals, and spin tendencies
- G – Weak spin tendency, strong roll reversal, results in control induced departure
- H – Spin resistant, objectionable roll reversals can induce departure and post stall gyrations

As can be seen, across the entire flight envelope, the Cirrus Eco-Strut remains inside the B region of the Bihrl-Weissman Chart, meaning it displays a large resistance to both spins and departures.

## 8 Performance

### 8.1 Requirements

The Eco-Strut is tasked with replacing the current 150 person passenger aircraft in the current aviation industry, and so must have comparable or better performance characteristics to the Boeing 737 and A320. The performance requirements required, as specified in the RFP can be seen in Table 13.

**Table 13 Cirrus Eco-Strut RFP Requirements**

Category	RFP Requirement
Range (max) (nm)	2800
Velocity (cruise)	Mach .78
Takeoff Distance (ft)	7000
Landing Velocity (kts)	135
Operating Altitude (ft)	$35,000 < x < 43,000$
Fuel Burn (lb/pax)	< 41 for a 500 nm mission

### 8.2 Takeoff Performance

The Eco-Strut must function on conventional airstrips used today by the aircraft it is going to replace. This means that it must be able to takeoff in under 7,000 ft, on a hot (86° Fahrenheit) day at sea level. Using the lift parameters determined in Section 6, the takeoff parameters for the Eco-Strut were calculated. The coefficients of lift used can be seen in Table 14, and the takeoff performance of the Cirrus Eco-Strut can be seen in Table 14, the specific quantitative parameters can be obtained.

**Table 14 Cirrus Eco-Strut Parameters**

	Cirrus Eco-Strut
$C_L$	0.47
$C_{L,max}$	1.95
Takeoff Velocity (ft/s)	223.99
Balanced Takeoff Field Length (ft)	3930

The Eco-Strut is well within the maximum takeoff field length, meaning it is a viable option for all airports now utilizing the A320 and/or the B737.

### 8.3 Range

As stated in the RFP, the Eco-Strut missions will be composed of the following ranges:

500 nm	50%
1000 nm	40%
2000 nm	10%

This means that the average, or expected range is 850nm, while the maximum range of the aircraft is 2800nm. Figure 36 shows a plot of the distance the Eco-Strut has flown plotted against the aircraft's weight at that stage in the flight.

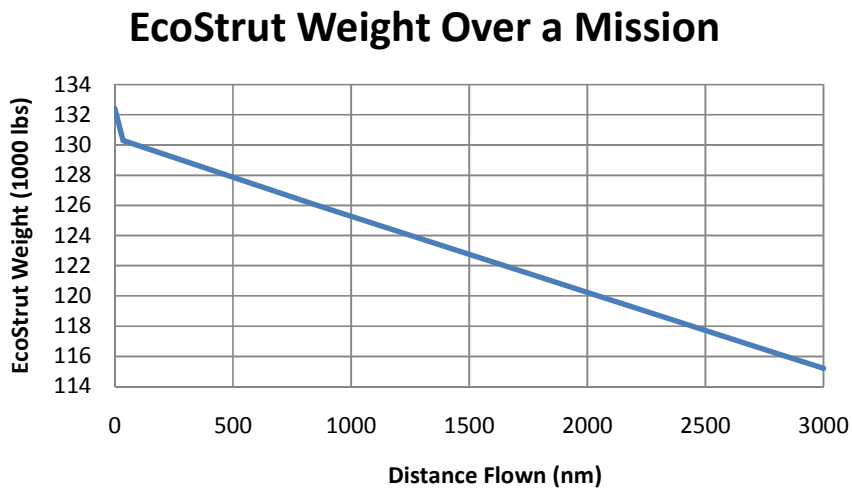


**Figure 36** Cirrus Eco-Strut Range versus Weights

As can be seen, the Eco-Strut is more than capable of making a flight over 2800 nm.

### 8.4 Landing Performance

During landings, it is key to not come in too quickly, or the aircraft will cause large amounts of fatigue and wear to both its own landing gear, and the tarmac. This is why it is extremely important for the Eco-Strut to be able to land at a speed lower than 135 kt (or 227.85 ft/s). See Table 15 for a summary of the Eco-Strut landing characteristics.

**Table 15** Cirrus Eco-Strut Maximum Performance Characteristics

<b>Landing Velocity (ft/s)</b>	226.8
<b>Landing Velocity (kt)</b>	134.4
<b>Balanced Landing Field Length (ft)</b>	2964

This approach velocity is just within the requirement specified for the RFP, which seems troubling at first glance. This, however, is less worrisome when the weight of the vehicle is considered, as the Eco-Strut weighs significantly less than its counterparts, giving it significantly lower momentum in landing situations.

## 8.5 Cruise and Fuel Consumption

One of the most important drivers of the Eco-Strut’s design was the significant reduction fuel burn. In order to achieve this, the cruise Mach number must be determined in order to maximize the specific range of the aircraft. This was done by plotting specific range as a function of Mach number (taking into account the drag rise and compressibility effects). At the mach number of 0.8, and a cruise altitude of 40,000 ft, the specific range is 0.1335 nm/lb, however the highest specific range occurred at a slightly lower mach number. A cruise velocity of Mach 0.8 was still chosen, despite the slightly lower specific range, because it was decided that meeting the desired RFP objectives of a cruise velocity of Mach 0.8 (the required value is 0.78, but 0.8 is desired) was more important than further fuel savings, so long as the 0.1335 nm/lb specific range was sufficient to meet the fuel reduction goals. The plot of specific range against Mach number can be seen in Figure 37.

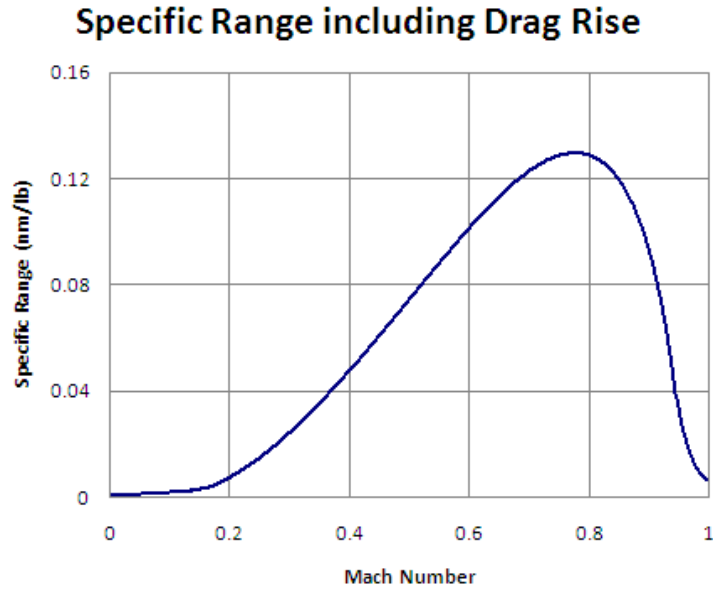


Figure 37 Specific Range including Drag Rise at an Altitude of 40,000 ft

For a 500nm flight, the RFP stipulates that less than 41 lbs of fuel can be burned per seat, and a value under 38 lbs per seat is desired. Each mission can be broken down into 8 distinct categories of flight, and these categories for an 850nm mission can be seen in Figure 38.

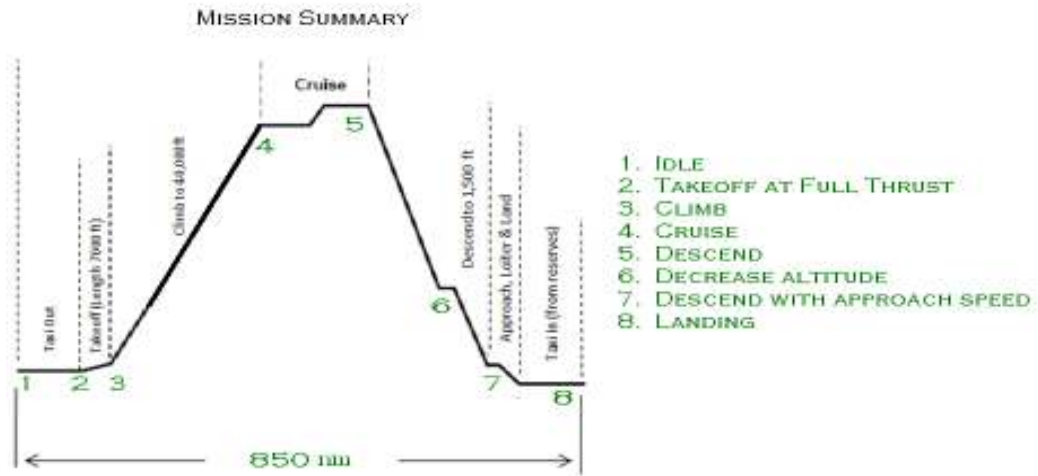


Figure 38 Eco-Strut 850 nm Mission

When flying at Mach 0.8 in cruise for this mission, the Eco-Strut achieves a fuel burn of 30.7 lbs per seat, including fuel spent in takeoff, and climb. To see the fuel burn over various missions, see Table 16.

**Table 16** Eco-Strut Fuel Burn

Climb		Cruise			Total Trip		Per Person	
Time (min)	Fuel Consumed (lb)	Range (nm)	time (sec)	Fuel (lb)	Fuel (lb)	Fuel (gal)	Fuel (lb)	Fuel (gal)
17	2089	500	4134	2518	4607	677.5	<b>30.7</b>	4.5
17	2089	850	7028	4280	6369	936.7	42.5	6.2
17	2089	1000	8269	5036	7125	1047.8	47.5	7.0
17	2089	2000	16537	10071	12160	1788.3	81.1	11.9
17	2089	2800	23152	14100	16189	2380.7	107.9	15.9

Considering the total fuel required as illustrated in Table 16, a detailed schematic of the amount of fuel the Eco-Strut will be able to carry on board is shown in Figure 38. The fuel boxes in the wings are placed at approximately 7% of the chord from the leading edge. The fuel box on top of the fuselage is maintained for reserved fuel. The two small probes on either side of the wings are placed just inboard of the engines for dumping purposes in the event of emergencies. The total fuel capacity the Eco-Strut will be able to hold is approximately 6,396 gallons or 45,912 lbs. This value is significantly more than the amount needed for a 2,800nm mission (16,189 lbs), and the amount needed according to the sizing calculations in Section 3 (35,750 lbs). See Figure 39 for an image of the aircraft with the fuel tanks shown.

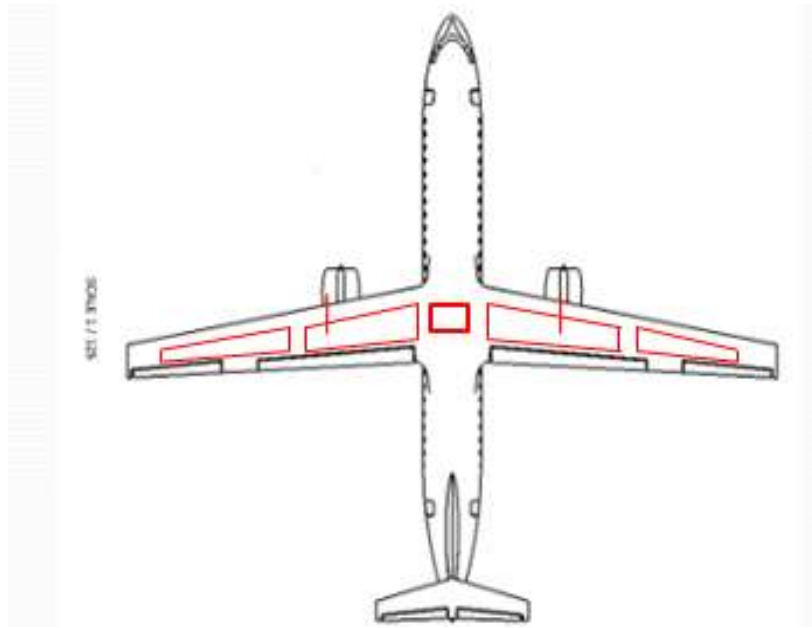


**Figure 39** Eco-Strut Fuel Tanks

## 9 Materials and Structure

### 9.1 Materials

Because a major component of the design is the material selection, possible materials for the components of the strut braced wing concept were investigated based on the materials used in modern aircraft. The main issue with materials selection for aircraft is that the material must be strong for structural integrity and also be light to still be aerodynamic. The three most common materials used in aircraft today are composites, aluminum, and titanium. Aluminum and titanium are used often because they are strong metals but still light enough to be used. Metals are also much cheaper compared to the much stronger and lighter composites. The following two figures, Figure 40 and Figure 41, show the strength and weight for the most common aerospace materials [23].

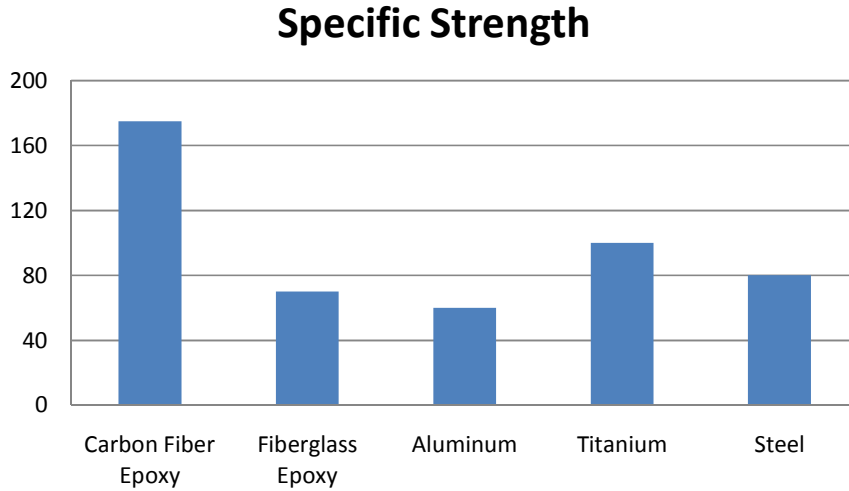


**Figure 40** Specific Strength for Aerospace Materials

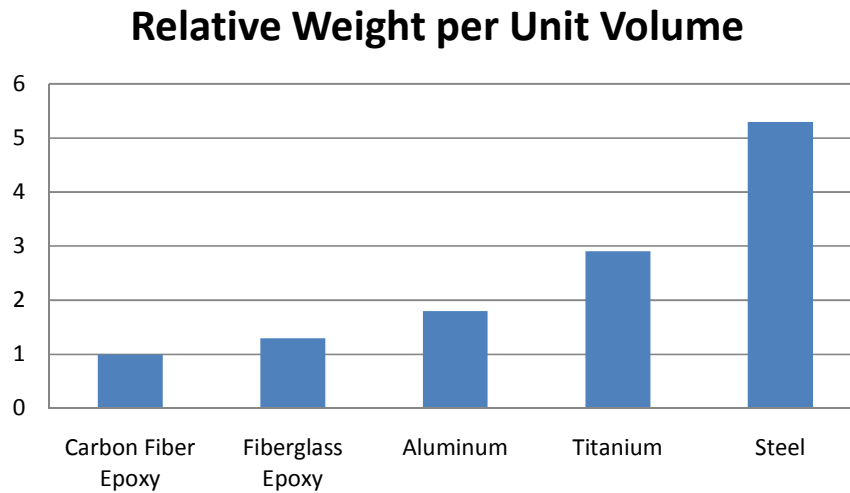


**Figure 41** Specific Strength for Aerospace Materials

To determine if composites are worth the cost, the materials used to make two of the newest and most advanced aircraft were investigated. The Boeing 787 and the Airbus A350 are two of the most anticipated commercial airliners. Both are much bigger than the RFP requires for this particular design project, but the materials can still be used for the SBW design concept. Both the 787 and A350 are composed of at least half composite materials, a fifth Aluminum, about a seventh Titanium,

approximately a tenth Steel, and the remaining parts are a variety of other materials. The two pie charts shown below, Figure 42 show the materials distribution for the 787 and A350 [24].

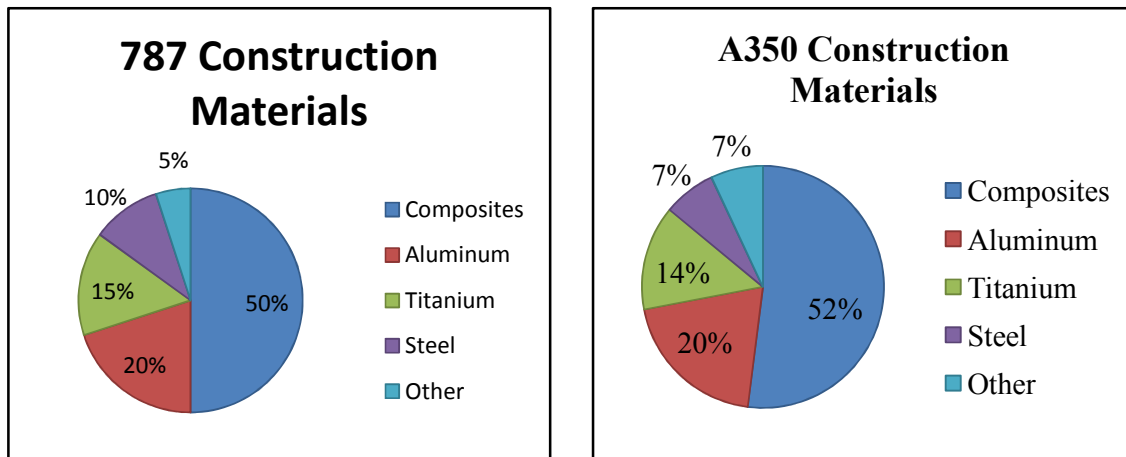


**Figure 42** Materials Distribution for Boeing 787 & Airbus A350

Since at least half of the construction of these new airliners consists of composites, the use of composites must be worth the added cost of the actual material. Composites do not have to be inspected as often as aluminum for corrosion and fatigue due to the physical properties of composites. According to Airbus, the use of composites on the A350 results in a 60% reduction in corrosion and fatigue tests [25]. The other cost savings for composites is that the much lighter weight reduces the amount of fuel required. According to Boeing, the use of composites reduces the weight by 20%, which in turn reduces the amount of fuel used by 20% and reduces the seat mile cost by 10% [23]. Reducing the weight will also reduce the emissions.

Based on this investigation of material selection, the materials of each of the components of the SBW design were chosen. The fuselage skin will be made of carbon laminate and the nose and wing fairings will be made of fiberglass. The wings and horizontal and vertical tail will consist of a combination of Aluminum and composites such as carbon laminate and fiberglass. The engine nacelle and pylon will consist of Aluminum, carbon sandwich, and a variety of stronger and heavier metals due to the huge load of the engine weight and thrust from the engine. A materials breakdown drawing is shown as Figure 43.

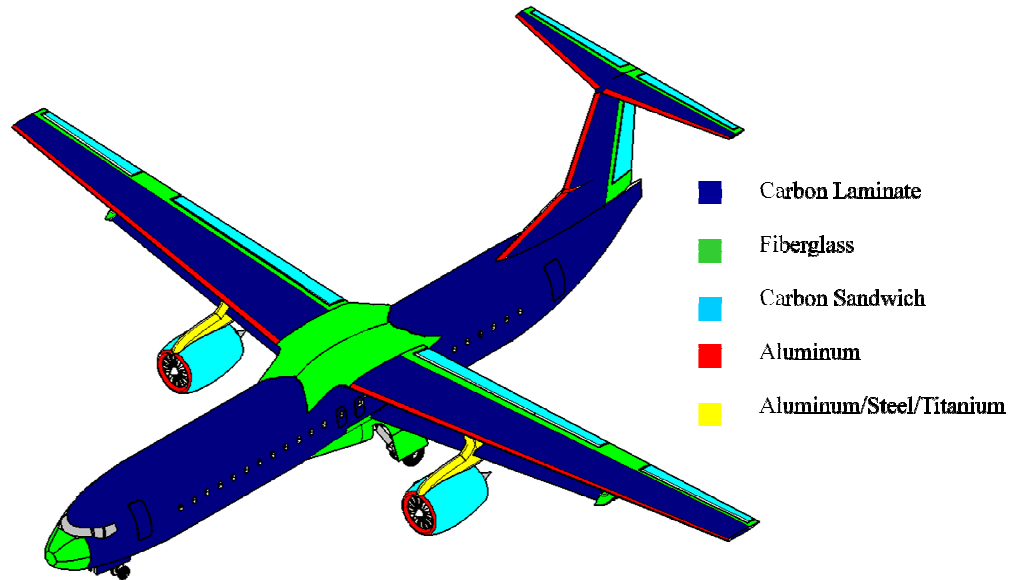


**Figure 43** Materials Breakdown Drawing of Strut Braced Wing

With the material selection complete, the structural analysis was conducted to determine the sizing of the various structural members of the aircraft and to ensure that the materials chosen resulted in a structurally sound aircraft.

## 9.2 Structural Analysis

The first step of the structural analysis was to make the V-n diagram for both gust and maneuver. For most commercial aircraft,  $n = -1$  and  $n = 2.5$  were used for the maneuver plot and gust of 25, 50, and 66 fps were used for the gust plot. Based on the dimensions and performance of the aircraft, the V-n diagram shown below as Figure 44 was developed.

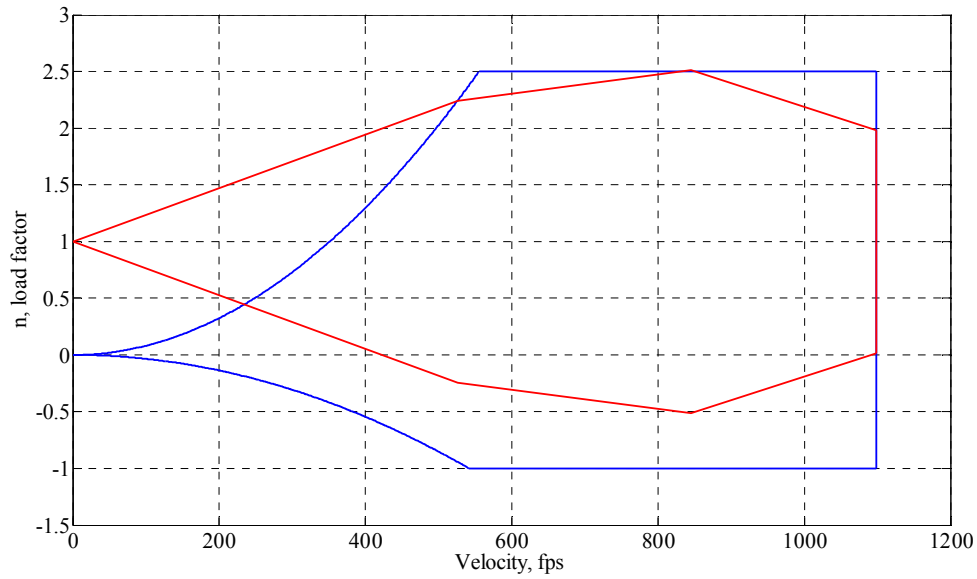


**Figure 44** V-n Diagram for Maneuver and Gust Loads

With the V-n diagram complete, the next step was to determine the shear and bending moment along the span of the wing and checking to see if the aircraft would fail under such loading. A simple flowchart outlining the steps of a program written to do the analysis and design is shown below as Figure 45.

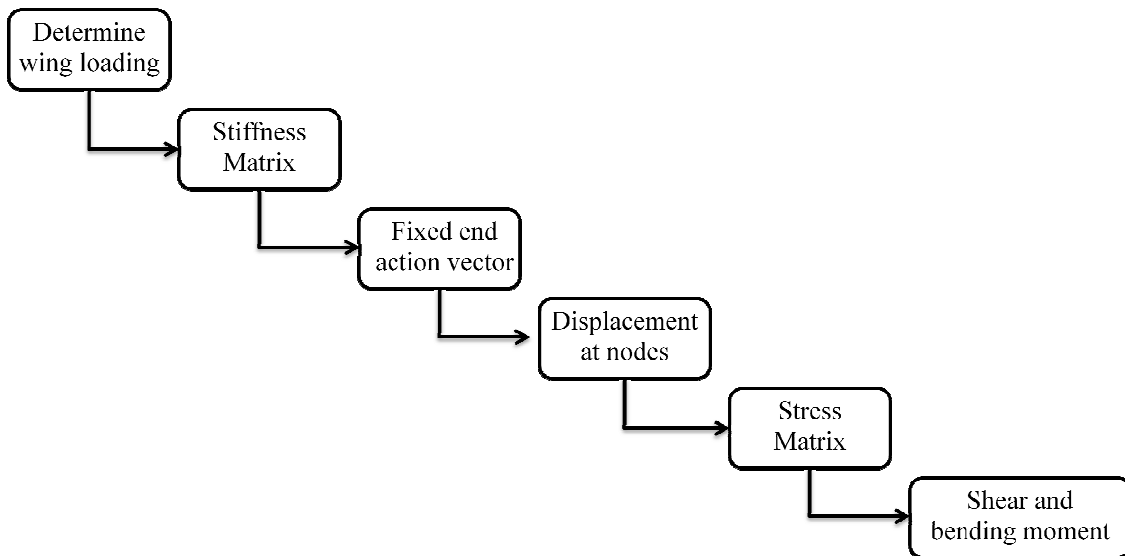


**Figure 45** Outline of Structural Analysis Code

The wing loading was approximated as being elliptic and four points were chosen along the span as the nodes for the structural analysis [26]. The four nodes chosen were the root, jury strut, offset, and tip. Linear loading was assumed between each pair of these four points to make the structural analysis simpler. The wing loading for steady, level flight is shown below as Figure 46.

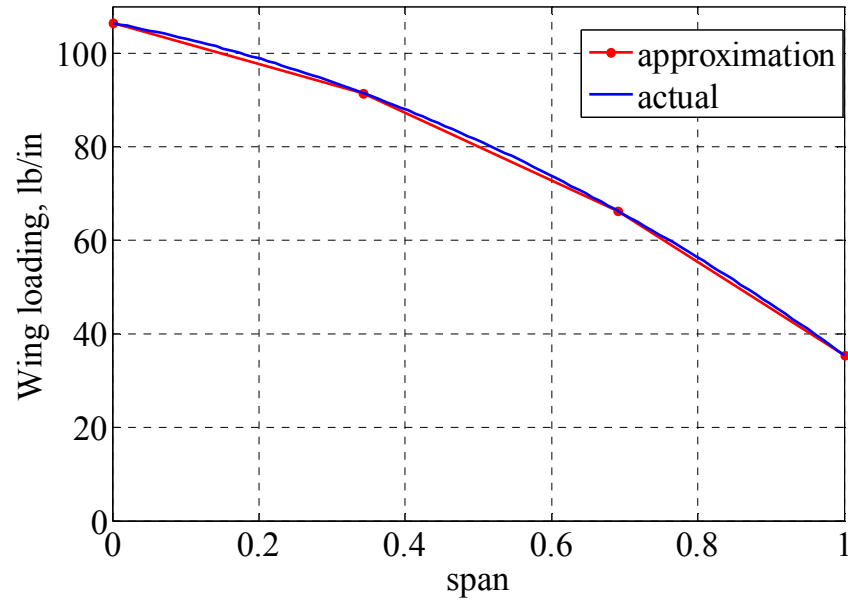


**Figure 46** Wing Loading at Steady, Level Flight for Structural Analysis

Because the structural design of an aircraft is based on pull-up conditions, the wing loading for  $n = 2.5$  was used and a plot is shown below as Figure 47.

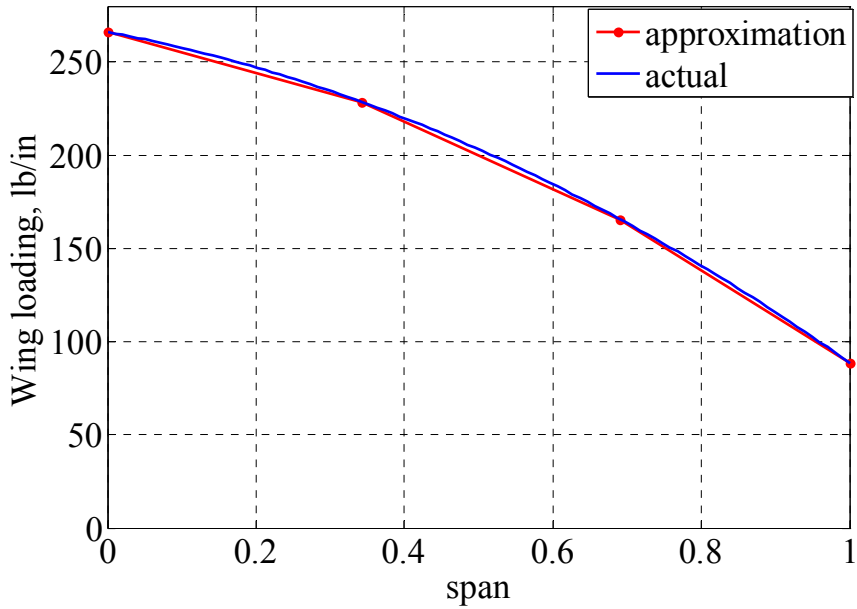


**Figure 47** Wing Loading at  $n = 2.5$  for Structural Analysis

For the rest of the analysis to be completed, nodes and structural components had to be chosen. Figure 48 provides the nomenclature.

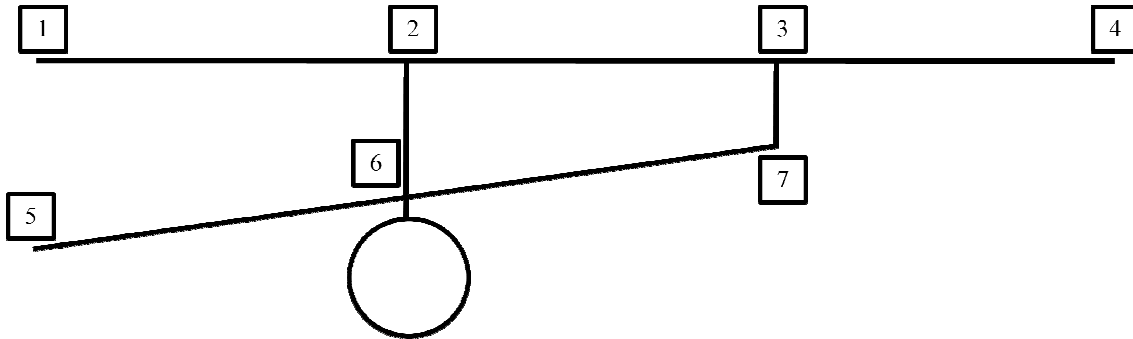


**Figure 48** Nodes of the Wing Structure

Nodes 1 - 4 have already been described, node 5 is where the strut meets the fuselage, node 6 is where the strut meets the jury strut, and node 7 is where the offset meets the strut.

With the nodes chosen, the structural type of the elements between the nodes had to be chosen. The three structural types are trusses, beams, and frames [27]. Elements 1-2, 2-3, 2-6, and 3-

7 are frames, elements 5-6 and 6-7 are trusses, and element 3-4 is a beam. A diagram of the structural elements is shown below as Figure 49.

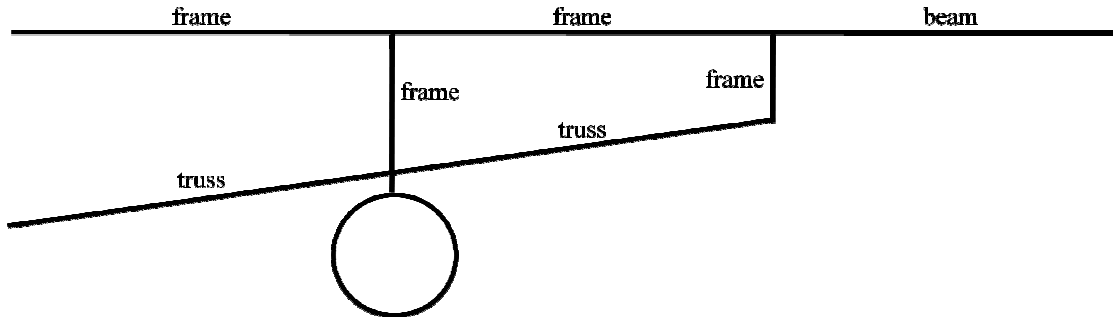


Figure 49 Structural Type of Each Element

Based on the structural type of the seven elements, the degrees of freedom are shown below as Figure 50.

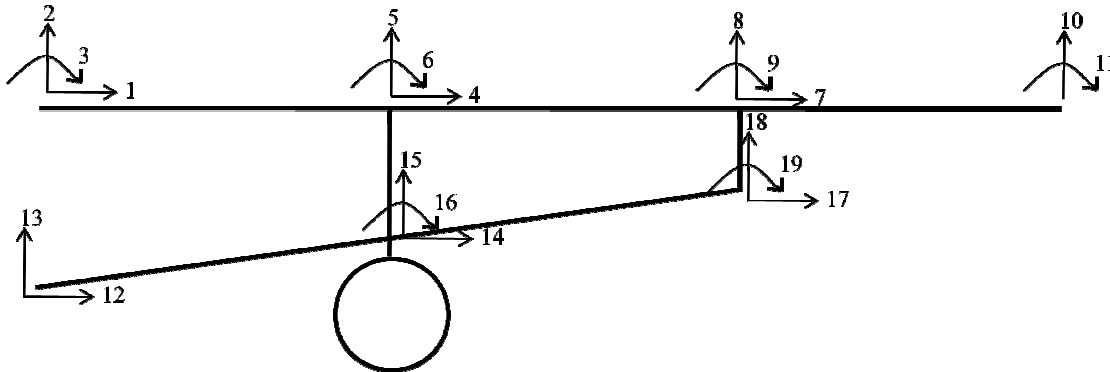
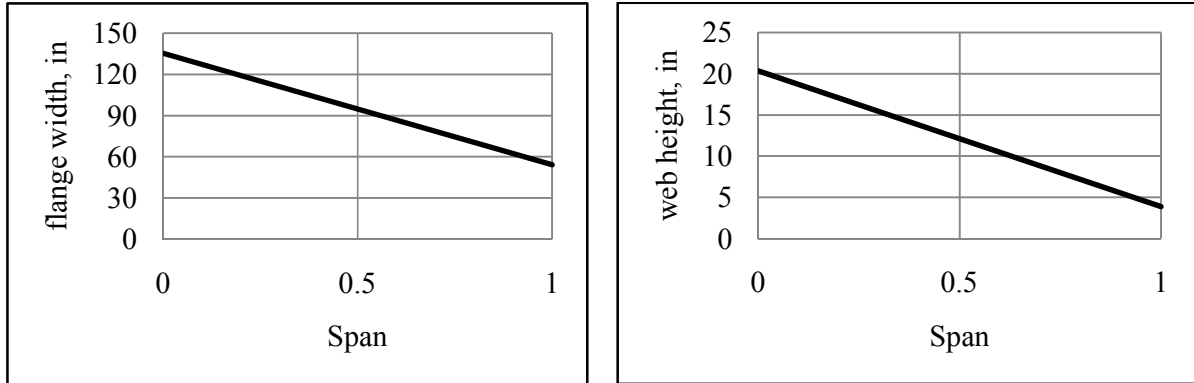


Figure 50 Degrees of Freedom at Each Node of the Structure

To determine the restrained stiffness matrix, cross sections of the individual elements had to be chosen. A rectangular cross section was chosen for elements 1-2, 2-3, 3-4, 5-6, 6-7, and 3-7 but an I cross section was chosen for the jury strut, element 2-6. The height of the web and width of the flange were determined based on the height of the web being the entire height of the airfoil and the

width of the flange being 70% of the chord length of the airfoil. The dimensions are plotted as a function of span in Figure 51.



**Figure 51** The Flange Width and Web Height as a Function of Span

With the wing being tapered, the thickness and chord of the airfoil changes along the span, therefore some approximations had to be made. The height of the web and width of the flange for element 1-2 is the average of the height and width at the root and jury strut, element 2-3 is the average of the height and width at the jury strut and offset, and element 3-4 is the average of the height and width at the offset and tip. The dimensions of the strut, jury strut, and offset are based on a combination of aerodynamics and structures, which will be further investigated for the final report, but are 2/3 the height and width of the wing where the offset is located for all four pieces.

Degrees of freedom 1, 2, 3, 12, and 13 were disregarded in the restrained stiffness matrix because nodes 1 and 5 are attached to the fuselage. Based on the Young's modulus, length, cross sectional area, moment of inertia, and angle of the individual elements, the restrained stiffness matrix was assembled resulting in a 14 x 14 matrix. The fixed end action vector (14 x 1) was then determined with all entries equal to zero except for the ones corresponding to 5, 6, 8, 9, 10, and 11. The applied generalized force vector (14 x 1) was also determined with all entries equal to zero except for the one corresponding to 15, which is the weight of the engine. With these two vectors and the restrained stiffness matrix, the displacements at all the nodes are calculated.

The final shear and bending moment is actually the sum of the shear and bending moment from the fixed end action and the shear and bending moment due to the nodal displacements. The shear and bending moment due to the fixed end action is determined by solving the differential equations for shear and bending moments and using the corresponding boundary conditions. The shear and bending moment due to the nodal displacements is determined by multiplying the stress matrix by the corresponding displacements [27]. The shear and bending moment plots as a function of span are shown below as Figure 52 and Figure 53.

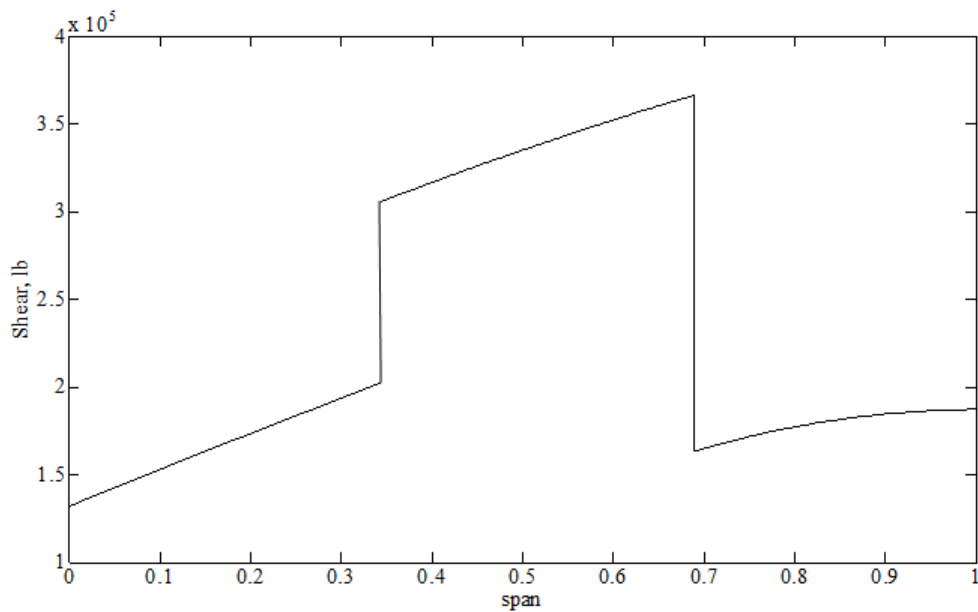


**Figure 52** Shear as a Function of Span

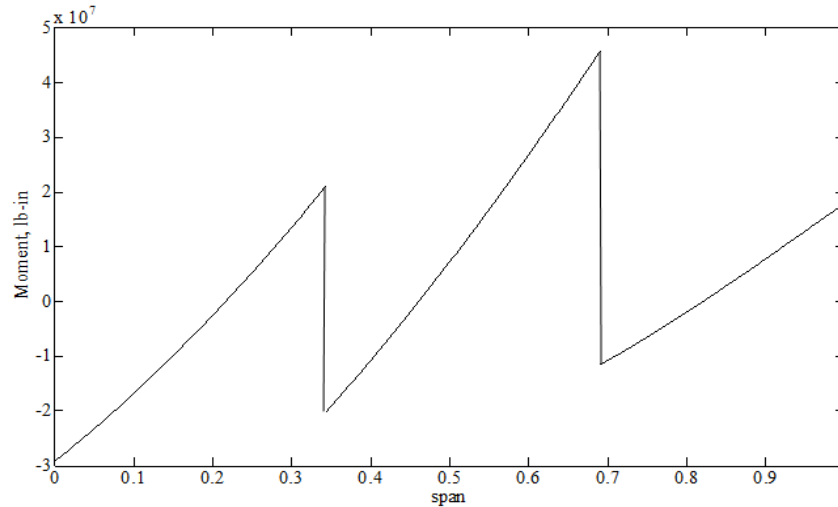
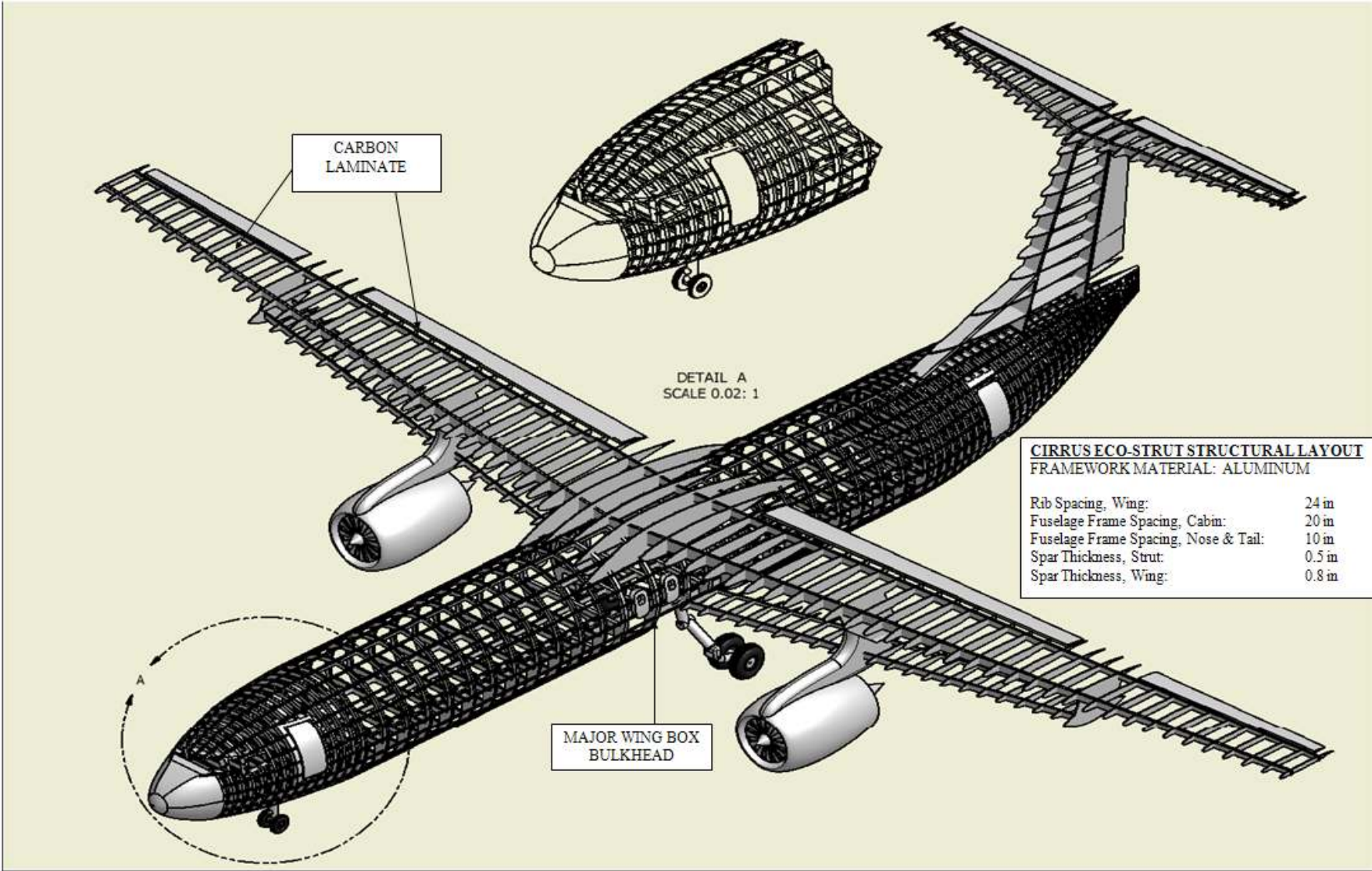


**Figure 53** Bending Moment as a Function of Span

Based on the structural analysis and the materials used, the strut braced wing design was found to not fail within a factor of safety of 1.5 and resulted in a weight savings of 20% compared to an aircraft not using composite materials. The sizing used for the wing was a rib spacing of 24 inches for both the wing and strut, spar locations of 0.2 chord and 0.7 chord for the wing, and spar locations of 0.2 and 0.8 chord for the strut. The maximum thickness for the wing spar was determined to be 0.8 inches and the maximum thickness for the strut to be 0.5 inches. The thickness could be optimized by using an advanced finite element code to show the change in the thickness as a function of span and would result in even more weight savings. The fuselage sizing consisted of frames spaced every 20 inches in the cabin and spaced on average every 10 inches in the nose and tail regions. The bulkheads were placed at the key attachment points such as where the wing and landing gear meet the fuselage, where the tail meets the fuselage, and pressure bulkheads at both ends of the cabin. The structural drawing based on the sizing previously mentioned is located on the following page.



## 10 Systems

### 10.1 Landing Gear Kinematics

The Cirrus Eco-Strut is supported by a standard tricycle landing gear with two tires on the nose gear and two tires for each of the two main gear struts. The landing gear was sized to meet the weight demands of the aircraft, type of runway used, FAR 25, and a 25% growth allowance. Landing gear sizing was performed using the methodology presented in Roskam’s Airplane Design Part IV [5]. Both the Boeing 737 and Airbus A320 operate on Type III runways so the Eco-Strut’s landing gear was also sized to this value. Type III runways require tire pressures between 120 and 200 psi. The Eco-Strut’s tires will be inflated with nitrogen to approximately 170 and 150 psi for the main gear and nose gear respectively. The maximum tire operating speed was also calculated based on previously calculated take off and landing speeds of the Eco-Strut (See Performance 8). The maximum operating speed at take off is 135 mph and 186 mph at landing. A simple static analysis determined that the reaction force at the nose gear was approximately 11,817 pounds and 66,659 pounds at the main gear. Allowing for 25% growth and calculating for the maximum static load per tire results in 41,662 pounds and 7,386 pounds for the main gear and nose gear respectively. A load analysis summary can be viewed in Table 17.

**Table 17** Cirrus Eco-Strut Landing Gear Load Analysis Summary

	Nose Gear	Main Gear
Reaction Force, lbs	11817	66659
Max Static Load (per tire), lbs	7386	41662
Inflation Pressure, psi	150	170

Using the data presented above along with tire data tables readily found on tire manufacturer’s websites, two different tires were selected for the Eco-Strut that meet the inflation pressure requirements and more importantly the maximum static load. Weight per tire was also considered during the selection process. Table 18 shows some of the tires under consideration and the chosen tire. The selections, all Type VII tires and bolded in Table 18, are a 24”x7.7” Goodyear Flight

Leader Series tire is selected for the nose gear while a 46”x16” Goodyear Flight Leader Series tire is selected for the main gear [8]. These two selections adequately met the operating speed requirement, inflation pressure requirement, and the loading requirement.

**Table 18** Cirrus Eco-Strut Selected Tire Data (Design Point Bolded)

Nose Gear -- Type VII Tire					
Tire Size (in)	Ply	Rated Speed (mph)	Rated Load (lbs)	Max. Rated Inflation (psi)	Weight (lbs)
24x7.7	6	190	2950	55	22.8
24x7.7	8	160	4150	75	22.5
24x7.7	10	210	5400	90	26.0
<b>24x7.7</b>	<b>16</b>	<b>225</b>	<b>9725</b>	<b>165</b>	<b>31.9</b>
30x8.8	16	225	14200	170	53.1
Main Gear -- Type VII Tire					
Tire Size (in)	Ply	Rated Speed (mph)	Rated Load (lbs)	Max. Rated Inflation (psi)	Weight (lbs)
44x16	28	174	38400	185	167.7
<b>46x16</b>	<b>28</b>	<b>225</b>	<b>41800</b>	<b>210</b>	<b>198.4</b>
46x16	30	225	44800	225	207.7
46x16	32	225	48000	245	208.0
46x16	30	225	44800	225	206.9

Sizing was also performed for the oleo pneumatic shock absorber length and diameter. On the main gear struts, the shock absorber length is approximately 3.24 feet and has a diameter of 0.69 feet. On the nose gear strut, the shock absorber length is approximately 0.97 feet and has a diameter of 0.39 feet. Landing gear location with respect to the fuselage is shown in Figure 54.

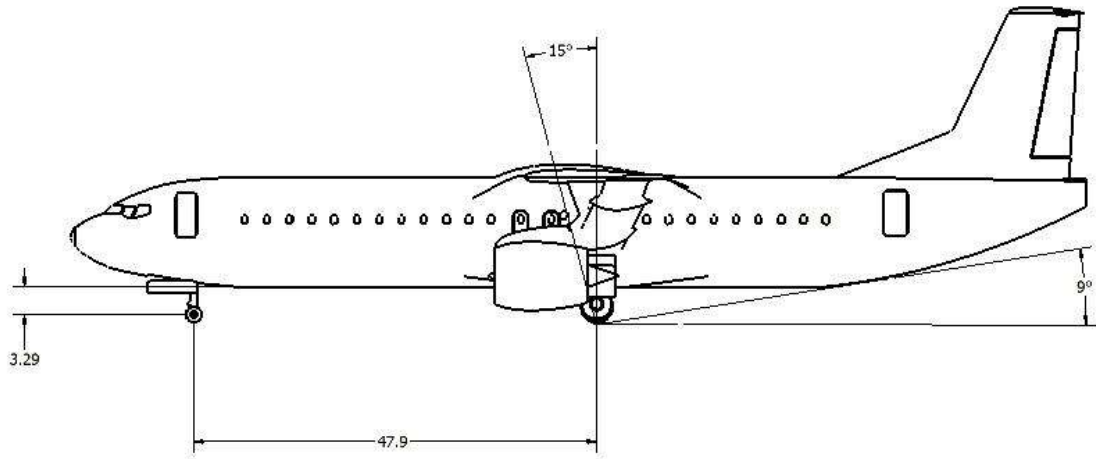


**Figure 54** Eco-Strut Landing Gear Location

The overall landing gear structure and kinematics is modeled off of the BAE 146—a similar high-wing aircraft. Due to the large wingspan of the Eco-Strut, the distance between the two main gear struts had to be large enough to meet the tip-over requirement. When deployed, the BAE 146 landing gear extends outward, away from the fuselage resulting in a distance greater than the width of the fuselage and satisfactory compliant with the tip-over requirement. In Figure 55, the kinematics of the landing gear of the Eco-Strut is illustrated. Braking for the Eco-Strut is performed by an electromechanical brake system developed by Goodrich Corporation [8]. This electric braking technology exhibits several benefits compared to traditional hydraulic brakes including modular actuators for increased reliability and ease of maintenance, onboard automatic braking system health reporting, and increased performance and life [8]. Goodrich Corporation insists that this electromechanical braking system performs at or above the standards of traditional hydraulic systems. The Eco-Strut uses one braking unit per wheel for a total of six units.

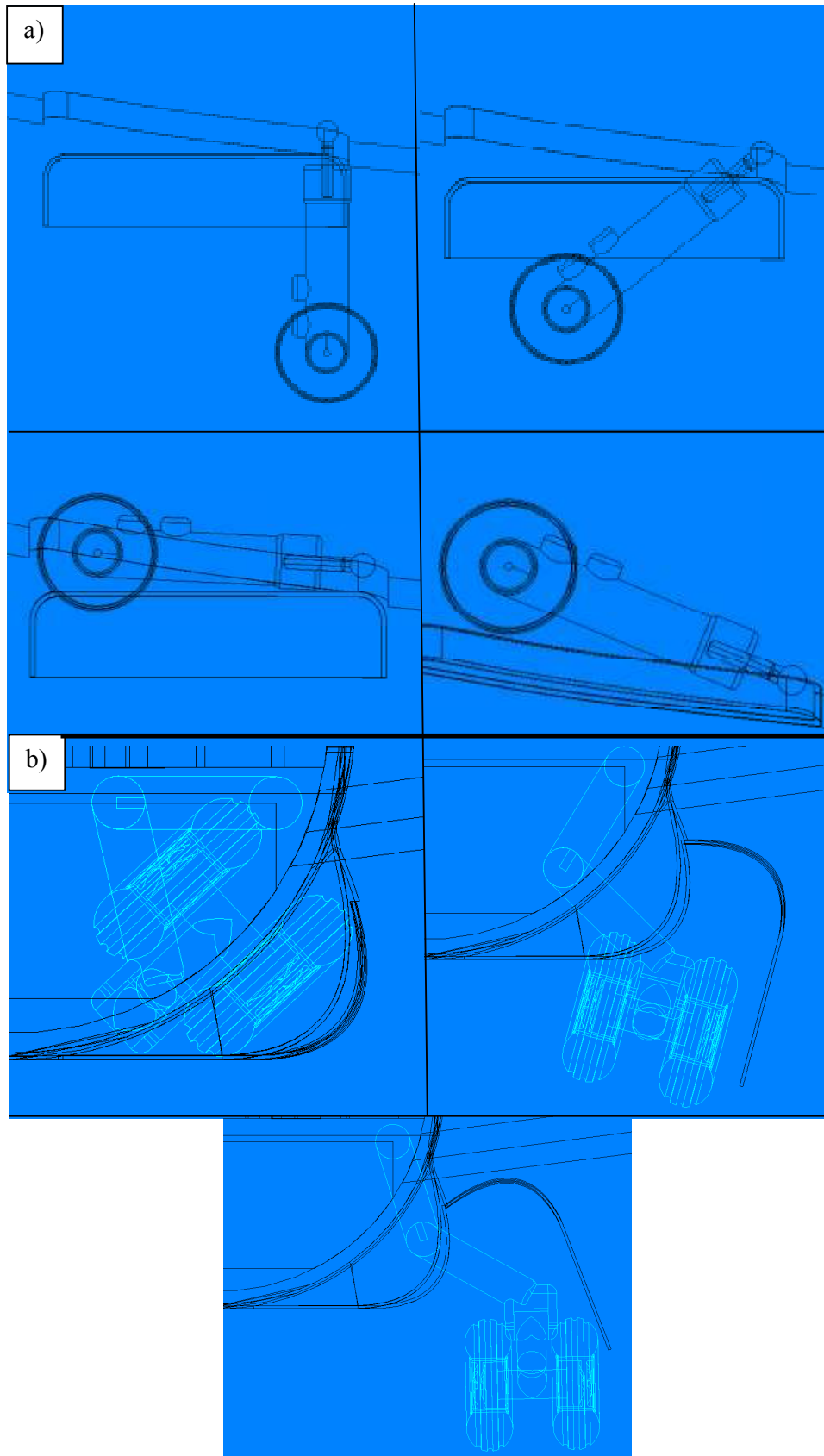


**Figure 55 Eco-Strut a) Nose Landing Gear b) Main Landing Gear Kinematics**

### **10.2 No-Bleed System Architecture**

Recent technological developments in aircraft systems have allowed engineers to develop an efficient alternative to the common system architecture used in many aircraft around the world today. Specifically, a system architecture has been devised which eliminates both the bleed manifold on aircraft engines and maintenance prone pneumatic system and instead electrified all aircraft systems once serviced by these two components [9]. The Boeing 787, due to make its first flight later this year, will employ such a system architecture and promises to yield significant improvements in aircraft system operation. These improvements include improved fuel consumption due to more efficient power management, reduced maintenance costs due to elimination of the previously mentioned bleed system and the use of less parts, improved reliability due to the use of modern electronics, reduced community noise, and increased range due to lower overall weight [9]. Because bleed manifolds have been eliminated on the engines, the engines operate at a much higher efficiency than engines with the bleed manifolds installed. Engineers believe that as much as 35% less power will be extracted from the engines using this system architecture [9]. Weight savings are also high due to the elimination of the bleed manifolds and bleed air piping through the wings.

The no-bleed system architecture is employed on the Cirrus Eco-Strut in an effort to improve overall system efficiencies and allow the Eco-Strut to remain competitive, from a modernization standpoint, upon its introduction into the aviation industry in the year 2018. The no-bleed system architecture exhibits characteristics which parallel the design drivers used throughout the design process; they are improved fuel consumption, reduced costs, and reduced community noise. The no-bleed system architecture is an advantageous choice to the Eco-Strut's design. The remaining system sections will highlight the various components of the no-bleed system architecture.

### **10.3 Electrical System**

As previously mentioned, the no-bleed system architecture powers many system components once serviced by both the bleed manifold and pneumatic system. Consequently, several nontraditional aircraft voltage requirements arise requiring a hybrid electrical system. This hybrid electrical system is employed on the Cirrus Eco-Strut and can be seen in Table 19.

**Table 19** Hybrid Electrical System Voltages and Supplied Services

	Voltage	Services
Traditional	115 VAC	Aircraft Electronics/Avionics Bay, External Power Receptacles
	28 VDC	Aircraft Electronics/Avionics Bay
Nontraditional (No-Bleed Consequence)	235 VAC	Engine and APU Generators, Transformer Units (to convert to $\pm 270$ VDC)
	$\pm 270$ VDC	Cabin Pressurization Motors, Ram Air Fan Motors, Hydraulic Pump Motors, Nitrogen Generation (Fuel Tank Inerting)

To generate this power, six generators—two on each engine and two on the APU—are connected directly to the engine gearbox at a variable frequency proportional to the engine speed [9]. These generators operate at 235 VAC. Power conditioners and transformers convert this voltage to the necessary voltage for each specific electrified service as seen in Table 19. The Eco-Strut also has four, two forward and two aft, external power receptacles for ground vehicles and maintenance. This is convenient for ground personnel as a GPU is not necessarily needed within the gate box. In the event of electrical failure, a ram air turbine located just aft of the main gear can be deployed to generate electricity for flight required systems. If a power failure is detected, the ram air turbine will deploy until the blades of the turbine are in freestream. During normal flight, the ram air turbine is stored within the body of the fuselage. Figure 56 shows a schematic of the electrical system of the Eco-Strut and the services supplied.

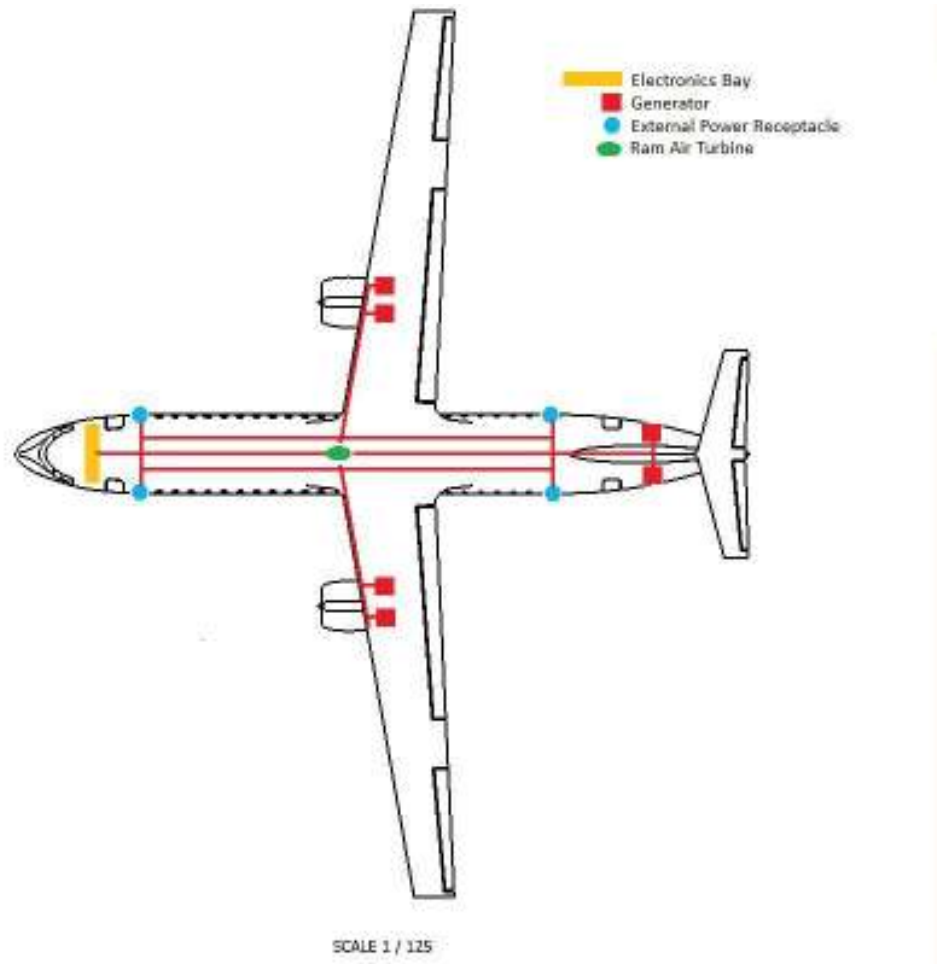


**Figure 56** Cirrus Eco-Strut Electrical System Schematic

Most critical to the electrical system is the regime in which the engines can be started. Typically starting regimes use the generators on the APU in conjunction with the generators on each engine. The Eco-Strut has the ability to start its engines using the APU generators, engine generators, or two 115 VAC GPUs. Similarly the APU is started using the aircraft battery, one GPU, or one engine generator. A similar starting regime is employed on the upcoming Boeing 787 [9].

#### **10.4 Hydraulic System**

The Eco-Strut’s hydraulic system consists of three independent systems—left, center, and right—and is comparable to most aircraft flying today with the exception of the center system. The left and right systems are identical and are powered by engine-driven pumps mounted on the engine gearbox [9]. These two systems service the thrust reversers and flaps. Flight control surface actuation

is performed by electro-hydrostatic actuators rather than typical hydraulic actuators. Redundancy is in place in the event of failure on the primary actuators. The center system is powered by two large electric motors and service landing gear actuation, nose gear steering, and ram air turbine actuation. The major difference between the Eco-Strut's center hydraulic system and traditional aircraft is that one of the large pumps on the center system remains in operation throughout the duration of the flight and the second large pump is only in operation for takeoff and landing. Landing gear actuation is a high demand service that requires the use of both pumps. Table 20 summarizes the roles of each system and the areas they service.

**Table 20** Hydraulic System Summary

<b>System</b>	<b>Services</b>
Left	Thrust Reversers, Flaps
Center	Landing Gear Actuation, Nose Gear Steering, Ram Air Turbine Actuation
Right	Thrust Reversers, Flaps

The hydraulic system on the Eco-Strut will operate at a high pressure of approximately 5,000psi at 30 gpm. A higher than normal operating pressure allows the use of smaller hydraulic components saving both space and weight [9]. Actuation on the Eco-Strut is performed by electro-hydrostatic actuators. A schematic of the hydraulic system of the Eco-Strut can be seen in Figure 57.

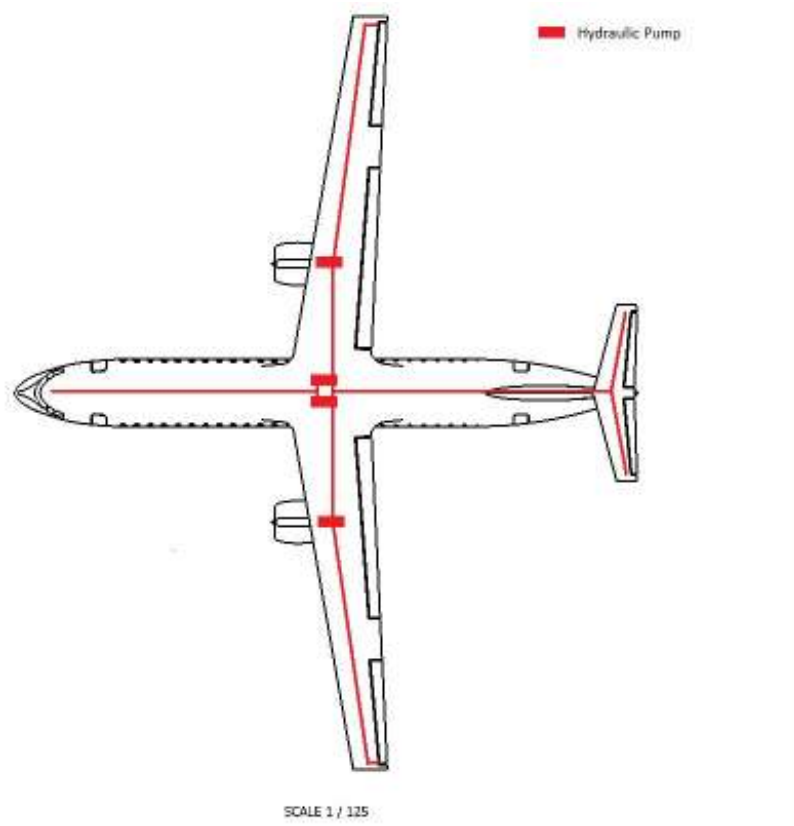


**Figure 57** Cirrus Eco-Strut Hydraulic System

## 10.5 Avionics

The Cirrus Eco-Strut is outfitted with Honeywell’s Primus Epic Integrated Avionics System. This avionics package features advanced flight deck functionality, improved situational awareness, and increased system flexibility [10]. It features large 10”x13” LCD screens displaying integrated navigation and graphical flight planning functionality [10]. The integrated navigation display layers terrain data, weather radar, and GPS all on one screen. Also included in this package are fully digital autopilot and autothrottle, integrated flight management system, integrated EGPWS, integrated communication management, radio altimeter, micro-inertial reference system, air data sensors, GPS sensors, TCAS, AFIS, and a lightning sensor system [10]. HUDs are located on both the pilot and first officer’s side of the cockpit displaying aircraft performance, position, airport and runway orientation, actual flight path, and touchdown point [10]. The HUD eliminates the need for the pilot

to look down at instruments during takeoff and landing thus increasing overall safety of the aircraft and passengers.

Communication and navigation systems are provided by Honeywell's Quantum Line. This is an integrated communications/navigation package which consists of ILS receiver, VOR marker receiver, DME interrogator, VHF data radio, multi-mode receiver, automatic direction finder receiver, HF radio, and VHF AM Transceiver. Also, the Eco-Strut will be outfitted with a Rockwell Collins SAT 2100 SATCOM/HST 2110 high speed transceiver [11]. This device facilitates text messaging, instant messenger, VoIP, cell phone service, virtual private network, secure phone, internet access, and email. Features such as these allow the most up to date information for the cockpit as well as passenger comfort and entertainment.

### **10.6 Cockpit**

The Eco-Strut's cockpit was designed with functionality and ease of access in mind; the layout is seen in Figure 58. Six 10"x13" LCD screens are installed for on-demand access to a vast variety of information. Six 10"x13" LCD screens are installed for on-demand access to a vast variety of information. Engine and radio/communication controls are located in the center console with cabin and fuel controls located in the overhead console. Both the pilot and first officer have a primary flight display and navigation/weather display while each share a multifunction display in the center of the main console and an engine display located in the center console. Two tablet computers, one for the pilot and one for the first officer, are connected to the flight management system onboard and can be removed from the cockpit before and after flight. Pilots can create flight plans before entering the aircraft and automatically synchronize their tablet to the aircraft onboard computers during preflight checks.

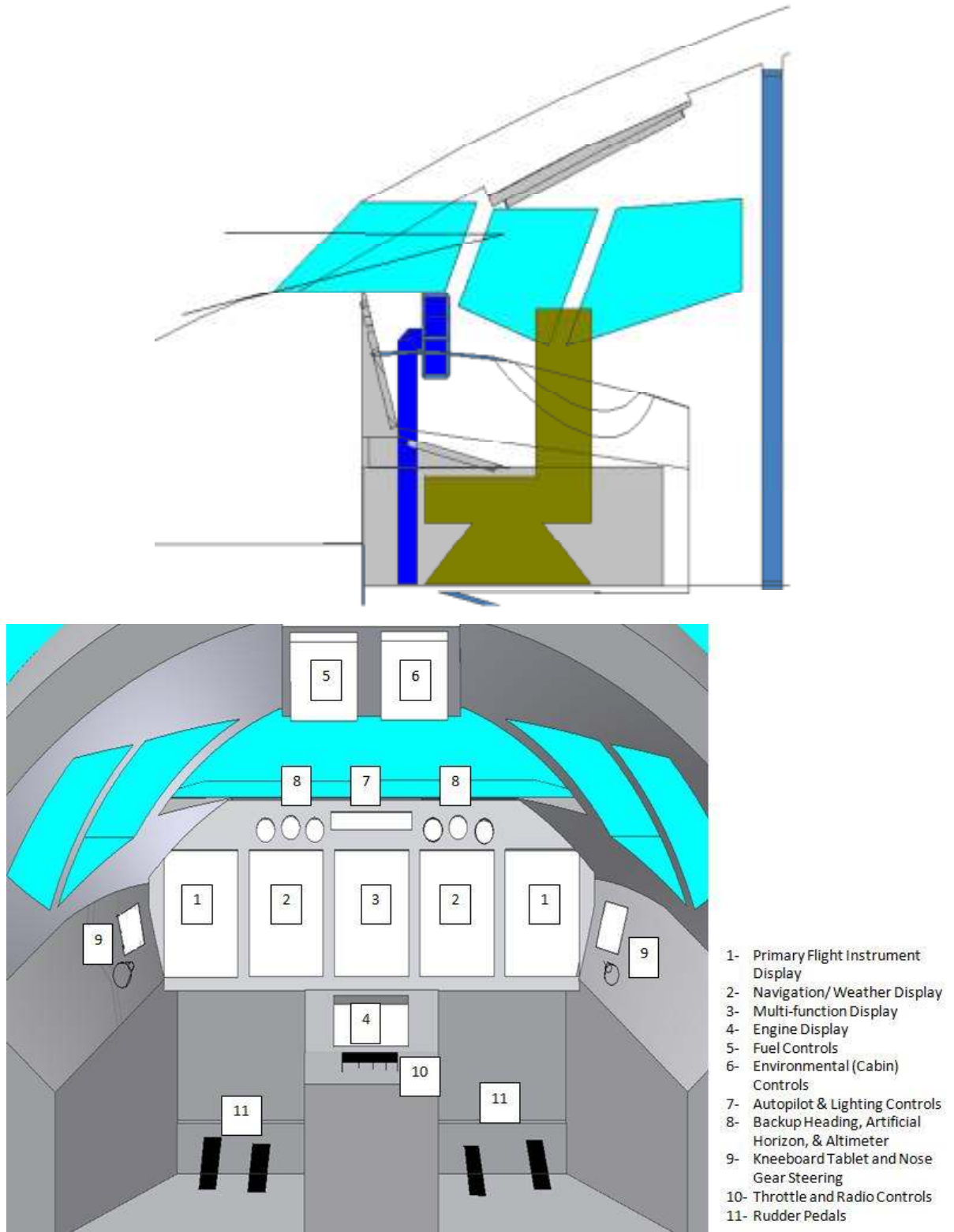


Figure 58 Cirrus Eco-Strut Cockpit Layout

### 10.7 Wing Ice Protection

With the elimination of a bleed air system, a new type of deicing system is used. GKN Aerospace has developed a heater mat that can be molded to fit in any area where ice accretion is of concern. The mat, as seen in Figure 59, is manufactured of multiple layers of carbon and glass, sprayed with a conductive metal which acts as a heating element when electrified [12]. These mats are currently in use by the V-22 Osprey, the F-35, and the Boeing 787 [12]. The heater mats operate at a temperature range of 45°F to 70°F and consume approximately 45 to 75 kW of electricity. Also, venting ports once located on the underside of the wing to exhaust bleed air from the wing are no longer needed with the use of heater mats, thus noise and drag are completely eliminated from any deicing services [9]. The Eco-Strut employs this technology under the leading edges of the wings, leading edge of the horizontal and vertical tail, as well as around the cowling of each engine. The heater mat is used only as a deicing device and not an anti-icing device in effort to conserve energy.



**Figure 59** Leading Edge Heater Mat [11]

### 10.8 Environmental Control System

Another unique feature of the Cirrus Eco-Strut is the cabin pressurization level. Many aircraft made of aluminum have high interior cabin pressurizations equivalent to 8,000 feet so that at high altitudes structural deformation is not of concern. However, due to the Eco-Strut's use of composite materials, the cabin pressurization is equivalent to 6,000 feet. Lower interior cabin pressure and higher humidity levels are beneficial to passengers for both comfort and health.

Traditional cabin temperature control is employed throughout the Eco-Strut. Control is made available through the environmental control panel in the cockpit. Both air conditioning and heating are available depending on ambient air conditions.

## 10.9 Emergency Systems

The Cirrus Eco-Strut has approximately six emergency exit doors—two forward, two aft, and two in the middle of the fuselage. Emergency escape slides are installed on all six doors which can be activated just after departure and deactivated immediately after landing. When opened while activated, the slides will deploy away from the side of the fuselage. Figure 60 shows the emergency exit locations on the Cirrus Eco-Strut. Also, in the event of rapid cabin depressurization, emergency oxygen masks fall at each passenger seat from the ceiling. Bottled medical oxygen is available in the forward and aft crew stations along with a complete first aid kit.

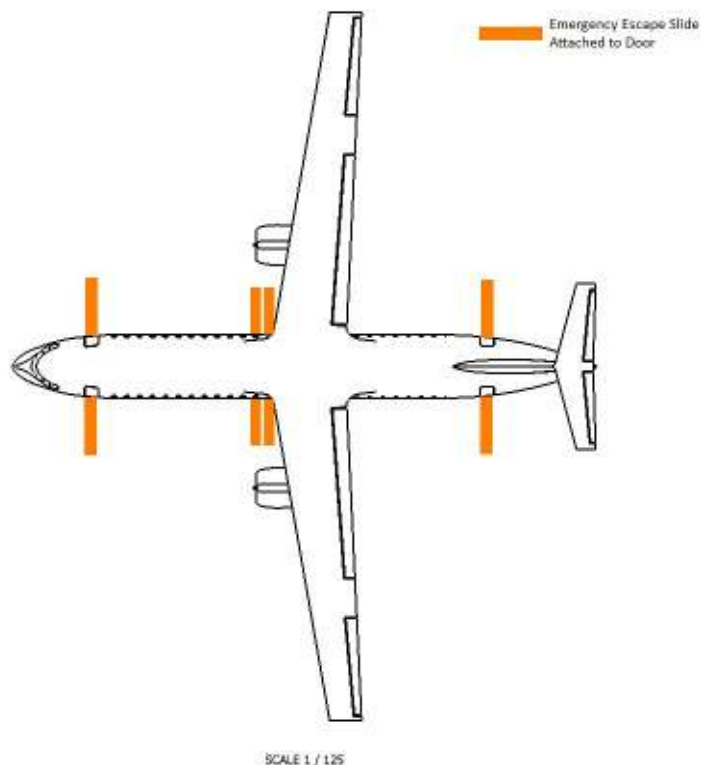


**Figure 60** Eco-Strut Emergency Exit Locations

## 10.10 Fire Prevention

Fire prevention is of great concern to airline operators, so the Cirrus Eco-Strut is outfitted with a comprehensive fire protection system developed by the industry leader in fire prevention, Kidde Aerospace [13]. The fire protection system includes engine and APU thermal fire detection and extinguishing, cargo compartment smoke detection and extinguishing, lavatory smoke detection and extinguishing, and cockpit panel smoke detection and extinguishing. Also, fire extinguishers are located within the cabin at the forward and aft crew stations as well as one in the cockpit and one in the cargo hold.

## 10.11 Lighting

The Cirrus Eco-Strut is outfitted with all required aircraft lighting as mandated by FAR 25. These lights, furnished by Honeywell's Astreon Exterior Lighting Series, includes navigation lights, anti-collision beacons, strobe lights, taxi lights, landing lights, and logo lights [33]. Figure 61 details the lighting configuration on the Eco-Strut.

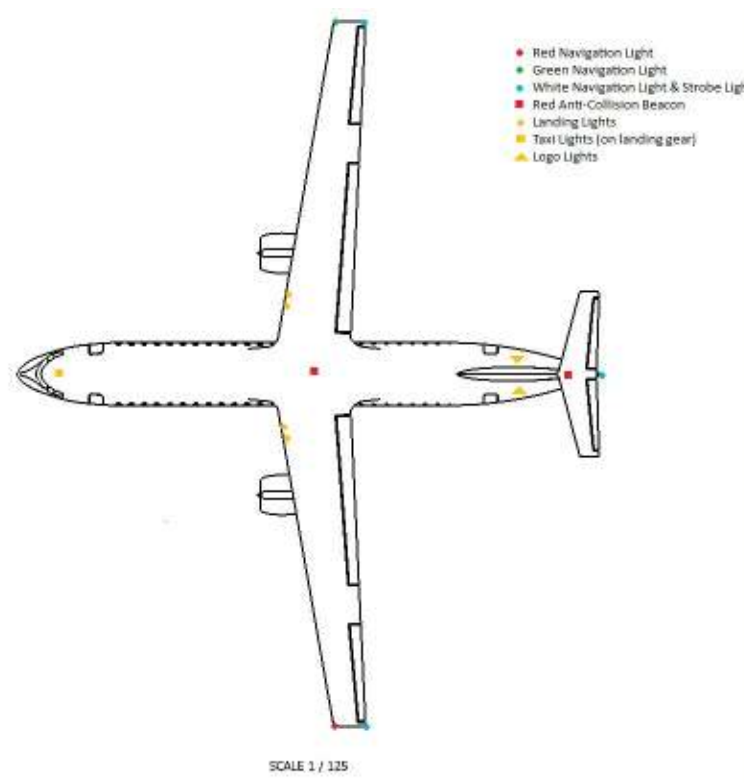


**Figure 61** Cirrus Eco-Strut Exterior Lighting Configuration

## **10.12 Water, Galley, and Lavatory Systems**

Approximately 50 gallons of water is carried on the Eco-Strut equivalent to about 0.3 gallons of water per passenger including crew. Water is stored in five small 10 gallon water tanks located within the cargo hold. Traditional aircraft use the pneumatic system to pressurize the water tanks so water can be circulated throughout the aircraft. Instead the Eco-Strut uses an electric air compressor to pressurize the tanks. All water tanks are flushed and sanitized regularly in accordance with EPA regulations.

Two galleys—one forward and one aft—are on the Eco-Strut for in-flight beverage and meal service. The galleys are complete with food coolers, warmers, coffee makers, and a small sink with infrared faucet. Galley components are furnished by Jamco aircraft interiors known for their low weight design, durability, and vast presence in the aircraft industry [34].

Three lavatories—one forward and two aft—are onboard the Eco-Strut. Each lavatory is 3'x3'x7' and is vacuum flush. Small sinks with infrared faucets are also located within the lavatory for passenger convenience [35]. Pumping service is required immediately following each flight.

# **11 Cost Analysis**

The affordability and cost efficiency of the Cirrus Eco-Strut is a key requirement and design consideration. By focusing on existing technologies and components, and more efficient configurations, aircraft lifecycle costs, and particularly operating costs, have been significantly reduced.

## **11.1 Cost Reduction Methods**

Aircraft costs are heavily dependent upon several factors. These are aircraft weight (or TOGW), and aircraft technology. Aircraft cost increases logarithmically with TOGW, so any reductions in aircraft weight can result in dramatic savings over the lifecycle of the aircraft. Aircraft technology includes factors such as advanced materials costs, and the usage of revolutionary configurations or systems. These costs are sometimes harder to quantify, as they often save weight, or reduce costs in other

aspects of the aircraft; however, relying on proven technologies can significantly reduce aircraft costs, as less engineering is required to overcome new problems. See Sections 4, 7, 9.1, and 10 for details regarding technologies utilized in this design. See Figure 62 for an illustration of general trends in aircraft pricing.

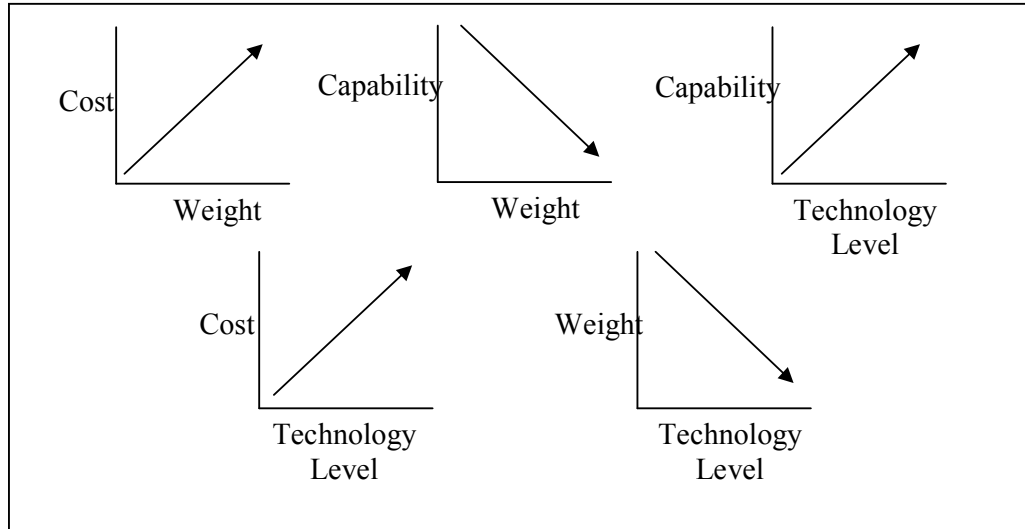


**Figure 62** General Trends for Aircraft Pricing [4]

### 11.2 Cost Analysis Assumptions

Several key values were assumed in the prediction of the Eco-Strut's cost. The most important of these values are listed below.

- Quantity Produced: 500, 1500
- Fuel Price: \$2.50/gal
- Quantity Test Aircraft Produced: 4
- Annual Flight Hours: 3,000
- Profit from RDTE and ACQ Phases: 10%
- Financing Costs for RDTE and ACQ Phases: 13%
- Production Rate: 3/month for the 500 run, and 12/month for the 1500 run

The two quantities to be produced and the fuel price were specified in the requirements. The quantity of test aircraft produced was selected based upon the number deemed adequate, as two will be equipped with instrumentation for testing and analysis. The 3,000 annual flight hours per plane were estimated based upon commercial passenger aircraft of this size. This prediction method can be seen in Roskam Part VIII [21]. The production rates of 3 aircraft per month for the 500 unit production run, and 12 aircraft per month for the 1500 aircraft production run were deemed feasible based upon the Boeing 737 production rate, which peaked at over 20 aircraft per month.

### 11.3 Life Cycle Costs

Life cycle costs are the costs accrued by the aircraft over its design (Research, Design, Testing, and Evaluation), production (or Acquisition), flight (or Operations), and retirement (or Disposal). The life cycle cost for the entire run of aircraft was calculated for production runs of both 500 and 1,500 aircraft.

### 11.4 Research, Development, Testing and Evaluation

**Table 21** Design and Testing Cost of Eco-Strut (in 2009 U.S. Dollars)

	500 Aircraft Production Run	1500 Aircraft Production Run
Costs for Development, Support and Testing	\$423 million	\$423 million
Engineering and Design Costs	\$849 million	\$849 million
Flight Test Aircraft Costs	\$1.23 billion	\$1.28 billion
Flight Test Operations Costs	\$109 million	\$109 million
Profit from RDTE Phase	\$339 million	\$346 million
Finance cost for RDTE Phase	\$441 million	\$450 million
<b>Total RDTE Cost</b>	<b>\$3.39 billion</b>	<b>\$3.46 billion</b>

Obviously, the research and development for both production runs are relatively the same, as the number that will eventually be produced has very little impact on the difficulties inherent in the design. The rates at which the aircraft are to be produced does somewhat impact the tooling costs, as more tools are needed to speed the production along.

**Table 22** Average RDTE Aircraft Cost

	500 Aircraft Production Run	1500 Aircraft Production Run
<b>Average RDTE/aircraft</b>	<b>\$6,780,000</b>	<b>\$2,310,000</b>

The average cost of research and development per plane is significantly different. This is because while the RDTE costs are relatively similar for the two runs, the fact that three times as many aircraft are produced in the 1500 production run, which drives down the average significantly.

### 11.5 Acquisition Cost

**Table 23** Cost to Requisition 500 or 1500 Eco-Strut Aircrafts (in U.S. Dollars)

	500 Aircraft Production Run	1500 Aircraft Production Run
Engineering and Design Costs	\$1.21 billion	\$1.66 billion
Airplane Production Costs	\$25.3 billion	\$54.8 billion
Acquisition Phase Profits	\$2.59 billion	\$6.27 billion
<b>Total Acquisition Phase Cost</b>	<b>\$29.5 billion</b>	<b>\$62.7 billion</b>

When total acquisition phase costs are combined with research and development costs, and then divided by the total number of aircraft produced, the price at which each plane will be sold to airlines can be determined. This can be seen in Table 24.

**Table 24** Cirrus Eco-Strut Price (in U.S. Dollars)

	500 Aircraft Production Run	1500 Aircraft Production Run
Total RDTE Cost	\$3.39 billion	\$3.46 billion
Total Acquisition Phase Cost	\$29.5 billion	\$62.7 billion
<b>Aircraft Price</b>	<b>\$65.73 million</b>	<b>\$44.12 million</b>

These aircraft prices are extremely competitive when compared to other comparable 150 passenger aircraft. A Boeing 737 costs anywhere between \$50-\$85 million, depending on its configuration and capabilities. According to Boeing’s website, a 737-800 variant costs approximately \$76.75 million, and this aircraft is the most current 150 passenger variant, so it makes sense to use it as a baseline comparison. Obviously, the Eco-Strut is more than competitive with its rival aircraft in

terms of initial cost, with savings as high as 18% for a 500 aircraft production run, and 45.6% for a 1500 aircraft production run.

### 11.6 Operational Cost

**Table 25** Cost of Operating Eco-Strut with 30 year Lifespan (in U.S. Dollars)

	500 Aircraft Production Run	1500 Aircraft Production Run
Direct Crew Costs	\$19.0 billion	\$57.0 billion
Fuel, Oil and Lubricants Cost	\$6.15 billion	\$18.4 billion
Insurance Cost	\$13.9 billion	\$28.0 billion
Direct Operating Maintenance Cost	\$123.8 billion	\$334.7 billion
Losses to Depreciation	\$127.3 billion	\$296.5 billion
Landing Fees, Navigation Fees, and Registry Taxes	\$4.71 billion	\$14.1 billion
Indirect Operating Cost (passenger meals, attendants, etc)	\$5.86 billion	\$15.5 billion
<b>Total Operating Phase Cost</b>	<b>\$301 billion</b>	<b>\$764 billion</b>

These operating costs were developed assuming a thirty-year operational lifetime for each aircraft, with each aircraft flying 3,000 hours per year. An important consideration when analyzing this cost is the cost per passenger of the aircraft. Due to the strut-braced wing design of the Cirrus Eco-Strut, and the weight savings inherent in such a design, the cost per passenger of the Eco-Strut is extremely low when compared to its competitors. See the Table 26 below for these numbers for an 850 nautical mile flight.

**Table 26** Operational Costs Comparison (in U.S. Dollars) [14]

	Average 737	Eco-Strut 500 Aircraft Production Run	Eco-Strut 1500 Aircraft Production Run
Cost per seat	\$131.07	\$117.83	\$99.80
<b>% savings over 737</b>	<b>0.00%</b>	<b>10.10%</b>	<b>23.86%</b>

With only 500 aircraft produced, the operating cost per seat of the Eco-Strut still was nearly 12% below the operating cost per seat of the Boeing 737. These savings per seat can be more than

doubled by increasing the production run to 1500. Obviously, some airlines are capable of operating below the \$131.07 per passenger price listed above by cutting services, however the same practices would work for the Eco-Strut, and both aircraft would see similar savings under such circumstances. An 850 nautical mile flight was used for this analysis, as it is the expected flight distance given in the RFP (50% of flights are 500nm, 40% are 1000nm, and 10% are 2000nm).

**11.7 Disposal Phase**

The Cirrus Eco-Strut is designed to be lightweight and economical, and utilizes no new or revolutionary materials that would require excessive disposal costs. For this reason, its disposal cost should remain relatively low.

**Table 27** Disposal Cost of all Requisitioned Aircraft (in U.S. Dollars)

	500 Aircraft Production Run	1500 Aircraft Production Run
<b>Disposal Phase</b>	<b>\$4.77 billion</b>	<b>\$10.19 billion</b>

**11.8 Total Life Cycle Costs**

The use of a strut-braced wing configuration and proven technologies has made the Cirrus Eco-Strut extremely economical to both produce and fly. It offers significant savings when compared to the Boeing 737, and has the potential to dramatically reduce commercial aircraft operating costs.

**Table 28** Total Cost to Design, Test, and Manufacture, Utilize and Dispose of the Cirrus Eco-Strut (in U.S. Dollars)

	500 Aircraft Production Run	1500 Aircraft Production Run
Life Cycle Costs	\$47.66 billion	\$101.84 billion
<b>Life Cycle Costs Per Aircraft</b>	<b>\$95.32 million</b>	<b>\$67.90 million</b>

## 12 Conclusion

The 2008-2009 American Institute of Aeronautics and Astronautics Foundation Team Aircraft Design Competition presented us with a challenge to design a new 150 passenger commercial transport with reduced fuel burn, reduced community noise, and competitive acquisition and operational costs. Cirrus Technologies accepted this challenge and has designed an aircraft which meets and/or exceeds all requirements explicitly stated in the RFP. Table 29 details the major technical requirements specified in the RFP and the Eco-Strut’s compliance. The previous sections of this report provided insight into our design methodology, iterative optimization, and component selection. The Eco-Strut employs several advanced technologies which promise to improve overall performance. In the event of a delay in development of these advanced technologies, risk mitigation has been addressed and alternative technologies described. Cirrus Technologies has shown how the Eco-Strut is a competitive aircraft design and an excellent candidate for future consideration by airline companies. We expect that airline companies will find our design a viable solution to improve future profitability.

**Table 29 RFP Compliance Summary**

<b>Criterion</b>	<b>RFP Requirement (Objective)</b>	<b>Eco-Strut Capability</b>	<b>Compliance</b>
Passenger Capacity	150 dual class	150 dual class	Yes
Fuel Burn (500 nm mission)	41 lbs/seat (38 lbs/seat)	37 lbs/seat	Yes
Community Noise	ICAO Chapter 4 minus 20 dB	ICAO Chapter 4 minus 20 dB	Yes
Maximum Range	2800 nm	3273 nm	Yes
Cruise Speed	Mach 0.78 (Mach 0.80)	Mach 0.80	Yes
Maximum Landing Speed	135 knots	133 knots	Yes
Maximum Takeoff Field Length	7000 feet	3930 feet	Yes
Operating Costs (reduction)	8% or better (10% or better)	12%	Yes

## References

- [1] Gundlach, J. F., et al. *Multidisciplinary Design Optimization and Industry Review of a 2010 Strut-Braced Wing Transonic Transport*. MS Thesis, Virginia Tech. 2000.
- [2] Ko, Y.-Y. *The Role of Constraints and Vehicle Concepts in Transport Design: A Comparison of Cantilever and Strut-Braced Wing Airplane Concepts*. MS Thesis, Virginia Tech. May 2000.
- [3] Ko, Y.-Y. *The Multidisciplinary Design Optimization of a Distributed Propulsion Blended-Wing-Body Aircraft*. Ph.D. Thesis, Virginia Tech. April 2003.
- [4] Raymer, Daniel P. *Aircraft Design: A Conceptual Approach Fourth Edition*. AIAA Educational Series. 4th edition. Reston, VA. 2006.
- [5] Roskam, Jan. *Airplane Design Part IV: Layout Design of Landing Gear & Systems*. Lawrence, Kansas: Design Analysis & Research, 2007.
- [6] Roskam, Jan. *Airplane Design Part V: Weights*. Lawrence, Kansas: Design Analysis & Research, 2007.
- [7] *Electro-Mechanical Braking System*. <<http://www.goodrich.com>>
- [8] *Aviation Tires*. <<http://www.goodyearaviation.com/resources/pdf/datatires.pdf>>.
- [9] Sinnett, Mike. *787 No-Bleed Systems*. <[http://www.boeing.com/commercial/aeromagazine/articles/qtr\\_4\\_07/AERO\\_Q407\\_article2.pdf](http://www.boeing.com/commercial/aeromagazine/articles/qtr_4_07/AERO_Q407_article2.pdf)>
- [10] *Primus Epic Integrated Avionics*. <<http://www.honeywell.com/sites/aero/PrimusEpic.htm>>
- [11] *Rockwell Collins SAT-2100/HST-2110*. <[http://www.rockwellcollins.com/content/pdf/pdf\\_3188.pdf](http://www.rockwellcollins.com/content/pdf/pdf_3188.pdf)>
- [12] *787 integrates new composite wing deicing system*. <<http://www.compositesworld.com/articles/787-integrates-new-composite-wing-deicing-system.aspx>>
- [13] *Kidde Aerospace Fire Systems*. <<http://www.kidde-aerospace.com/>>.
- [14] Smallen, Dave. *First Quarter 2006 Airline Financial Data: Regional and Low-Cost Passenger Airlines Report Domestic Profit; Network Carriers Report Smaller Loss*. <[http://www.bts.gov/press\\_releases/2006/bts029\\_06/html/bts029\\_06.html](http://www.bts.gov/press_releases/2006/bts029_06/html/bts029_06.html)>.
- [15] *ICAO Engine Exhaust Emissions Data Bank Subsonic Engines*. <[http://www.caa.co.uk/docs/702/1CM005\\_01102004.pdf](http://www.caa.co.uk/docs/702/1CM005_01102004.pdf)>.
- [16] *PurePower PW1000G*. <[http://www.pw.utc.com/vgn-ext-templating/v/index.jsp?vnextoid=59ab4d845c37a110V\\_gnVCM10000c45a529fRCRD](http://www.pw.utc.com/vgn-ext-templating/v/index.jsp?vnextoid=59ab4d845c37a110V_gnVCM10000c45a529fRCRD)> Dec 2008.>
- [17] Depitre, Alain. *Noise Certification Workshop for ICAO*. August 2005.
- [18] Remillieux, Marcel C., Camargo, Hugo E., Ravetta, Patricio A., Burdisso, Ricardo A., and Ng, Wing F., *Noise Reduction of a Model-Scale Landing Gear Measured in the Virginia Tech Aeroacoustic Wind Tunnel*. 14th AIAA/CEAS Aeroacoustics Conference, Vancouver, British Columbia, May 5-7, 2008. AIAA-2008-2818.
- [19] Hreinsson, Guobjorn S., Faculty Advisor, W.H. Mason. *Aircraft Noise*. December 1993.
- [20] Roskam, Jan. *Airplane Design Part VII: Determination of Stability, Control and Performance Characteristics: FAR and Military Requirements*. Lawrence, Kansas: Design Analysis & Research, 2007.
- [21] Roskam, Jan. *Airplane Design Part VIII: Airplane Cost Estimation: Design, Development, Manufacturing and Operating*. Lawrence, Kansas: Design Analysis & Research, 2007.
- [22] Melin, Tomas and Adriene Berard. *Tornado Vortex Lattice Version 134 Beta*. <<http://www.redhammer.se/tornado>>.
- [23] Thomas, Geoffrey; Norris, Guy; Wagner, Mark; Smith, Christine Forbes. *Boeing 787 Dreamliner - Flying Redefined*. 1st edition. 2005.
- [24] Kingsley-Jones, Max. *Airbus's A350 vision takes shape*. <<http://www.flightglobal.com/articles/2006/12/12/211028/airbuss-a350-vision-takes-shape-flight-takes-an-in-depth-look-at-the-new.html>>.
- [25] *A350 XWB*. <<http://www.airbus.com/en/aircraftfamilies/a350/efficiency/wing.html>>.
- [26] Corke, Thomas C. *Design of Aircraft*. South Bend, IN. 2002.

- [27] Johnson, Eric R. *AOE 3214 Aerospace Structures*. Virginia Tech.
- [28] Mason, W.H., *Configuration Aerodynamics*, 2006  
<[http://www.aoe.vt.edu/~mason/Mason\\_f/ConfigAero.html](http://www.aoe.vt.edu/~mason/Mason_f/ConfigAero.html)>
- [29] Braslow, A.,L., Maddalon, D.,V., Bartlett, D.,W., Wagner, R.,D., Collier, F.,S., *Applied Aspects of Laminar-Flow Technology, Appears in Viscous Drag Reduction in Boundary Layers*, AIAA Progress in Astronautics and Aeronautics, Volume 123, Washington D.C. 1990.
- [30] Virginia Tech Aerospace Engineering Aerodynamics and Design Software Collection, *VLMpc.exe*, <[http://www.aoe.vt.edu/~mason/Mason\\_f/MRsoft.html#VLMpc](http://www.aoe.vt.edu/~mason/Mason_f/MRsoft.html#VLMpc)>
- [31] Virginia Tech Aerospace Engineering Aerodynamics and Design Software Collection, *friction.exe*, <[http://www.aoe.vt.edu/~mason/Mason\\_f/MRsoft.html#SkinFriction](http://www.aoe.vt.edu/~mason/Mason_f/MRsoft.html#SkinFriction)>.
- [32] Roskam, J., *Methods For Estimating Drag Polars Of Subsonic Airplanes*, University of Kansas. Lawrence, Kansas. 1973.
- [33] *Honeywell Exterior Aircraft Lighting*.  
<[http://www.honeywell.com/sites/aero/Aircraft\\_Lighting3\\_C3B8B3C2A-554A-D1A0-67E4-5EE3C63767BA\\_H00119971-50AA-125A-6492-2483986B0536.htm](http://www.honeywell.com/sites/aero/Aircraft_Lighting3_C3B8B3C2A-554A-D1A0-67E4-5EE3C63767BA_H00119971-50AA-125A-6492-2483986B0536.htm)>.
- [34] *Jamco Aircraft Galley Products*.  
<<http://www.jamco.co.jp/e/e-interiors/e-galley/galley-index.html>>.
- [35] *Jamco Aircraft Lavatory Products*.  
<<http://www.jamco.co.jp/e/e-interiors/e-lavatory/lav-index.html>>.